NASA SP-5117

TECHNOLOGY UTILIZATION

SOME NASA CONTRIBUTIONS TO HUMAN FACTORS ENGINEERING

A SURVEY

NATIONAL AERONAUTICS AND SPACE ADMINISTRATION

NASA SP-5117

SOME NASA CONTRIBUTIONS TO HUMAN FACTORS ENGINEERING

A SURVEY

By R. A. Behan and H. W. Wendhausen

The Mentoris Company
555 Capitol Mall
Sacramento, California

Prepared under contract NASw-2173
for
Computer Sciences Corporation
Falls Church, Virginia

Technology Utilization Office 1973
NATIONAL AERONAUTICS AND SPACE ADMINISTRATION
Washington, D.C.

For sale by the Superintendent of Documents,
U.S. Government Printing Office, Washington, D.C. 20402
Price $1.15 Stock No. 3300-00563
Library of Congress Catalog Card Number 73-600328

Foreword

This is one of a series of special publications issued to help persons outside of the aerospace field benefit from the results of the programs of the National Aeronautics and Space Administration.

Human factors research can help engineers match the capabilities and limitations of machines with those of human beings. Impressive progress in doing this has been made since World War II. Further use of recent advances such as those described here can reduce hazards and increase efficiency in many activities on the surface of the Earth as well as in the exploration of space.

Interested persons will find additional information in the references cited and in the bibliography prepared by the authors.

Director,
Technology Utilization Office

Acknowledgments

Many individuals provided information, guidance, and constructive criticism that contributed materially to the value of this survey. Shortcomings are to be attributed to the authors. We were aided generously by Mary Conners, Richard Haines, Charles Kubokawa, R. Patton, Robert Randle, M. Sadoff, and John Stewart of Ames Research Center; Gary Beasley, Randolph Chambers, Bruce Conway, Henry Elkins, Jack Hatfield, Paul Kurbjan, Amos Spady, and Ralph Stone of Langley Research Center; and William Huffstetler of Johnson Space Center.

Contents

CHAPTER 1

Human Factors Engineering

At Springer, N. Mex., a switchman mistakenly set a switch causing a passenger train and a mail train to collide, killing 20 persons and injuring 35 others. In 1965, two airliners collided in midair over the Grand Canyon—poor pilot visibility was blamed for this tragedy. In 1962, six infants died in a hospital from a formula prepared with salt instead of sugar—the storage bins for the sugar and the salt had been incorrectly labeled. Possibly these disasters could have been avoided by the effective application of human factors engineering. Alphonse Chapanis (ref. 1) defines such engineering as follows:

> Human factors engineering, or human engineering, is concerned with ways of designing machines, operations, and work environments so that they match human capacities and limitations.

As early as 1898, Frederick Taylor conducted studies to determine the best design of shovels and the optimum weight per shovel load for handling sand, slag, rice-coal, and iron ore. Frank B. Gilbreth made a classic study of bricklaying in 1911. He then designed a scaffold that could be lowered or raised quickly and a shelf that held all the bricks and mortar at their most convenient positions. By making changes in the transportation and inspection of bricks as well as in their arrangement on this scaffold, Gilbreth was able to increase the rate of bricklaying from 120 to 350 bricks per hour. Time and motion studies were developed to a fine technique in the years that followed. However, their main emphasis was on man as a source of mechanical power.

It was not until World War II, with the advent of machines that made demands on man's sensory, perceptual, judgmental, and decisionmaking capabilities, that modern human factors engineering was developed. The new machines raised some intricate and unusual questions about human abilities: How much information can a man absorb from a radar screen? How much optical distortion is tolerable in the windscreen of a high-speed aircraft flying low-level strafing missions? What happens if a human operator is suddenly decompressed when the walls of a pressurized aircraft rupture? What are the optimum time constants to build into a rate-aided gunnery tracking system? Can a man withstand an acceleration 12 times the force of gravity for 15 sec? How many sizes of oxygen mask are required to fit the full range of male faces?

These questions could not be answered adequately by common sense or by

the time-and-motion engineers' principles of motion economy. Thus, during World War II, a group of scientists turned its efforts to integrating man into the new and complicated machine systems that were the products of the war effort. These experts were not engineers but behavioral scientists—psychologists, physiologists, anthropometrists, and physicians. As a result of their influence, human factors engineering emerged as a special discipline. It developed in response to the need to consider the human contribution to the performance of complex machines, because failure to consider man's capabilities resulted in performance errors that were at best expensive and at worst lethal.

COMMERCIAL UTILITY

The advantages of using human factors engineering for general industry are accident reduction, increased productivity, and extended equipment life.

Accident Reduction

Good human factors engineering will reduce accidents. For example, in a human factors study of fire department equipment, it was discovered that collisions of fire trucks with cars while firemen were answering a call were all too frequent. Further investigation revealed that the accidents usually occurred at corners or curves in the road because the siren button (which must be kept depressed to sound the siren) was installed on the floor for foot operation. When turning a corner or rounding a curve, the driver had to remove his foot from the siren button to use the brake, the clutch, and the accelerator; consequently, cars were not being warned of the high-speed cornering of the fire engine.

Increased Productivity

The purpose of equipment is to increase man's capability and thereby accomplish more than man can by himself. It follows that the better the equipment is designed to fit man, the more smoothly and effectively it will be used, and, consequently, the more the man/machine unit will produce. Poorly human-engineered equipment that man finds difficult or uncomfortable to use will cause him to tire more quickly and make more mistakes. For example, pilots flying helicopters are subject to low-frequency vibrations that tend to shake their internal organs out of position. A device such as the vibration isolation seat system (see ch. 5) could reduce the effects of such vibrations and the pilot could expect a longer, healthier life.

Equipment Life

Well-designed equipment will last longer than poorly designed equipment because if it fits man's needs it is prized by workers and receives better care.

Equipment that is difficult to use is frustrating–it is not unusual for any of us to vent our frustrations on an annoying piece of equipment. Companies frequently cut corners on costs by putting makeshift labels on equipment. These labels are ripped off by workers who become disgusted with them, resulting in equipment without labels and an increase of contrary actions and preventable accidents.

RECOGNITION OF A HUMAN FACTORS PROBLEM

A problem may arise whenever man comes into contact with any type of equipment. This is known as the man/equipment interface. However, the connotation of the word "equipment" is quite broad. It includes all conventional military equipment, to which human factors engineering was first applied, and conventional means of transportation: automobiles, commercial aircraft, buses, and trains. In addition, there is a large class of man-operated earth-moving equipment that has not yet been designed according to principles of human factors engineering. Bulldozers, tractors, dredges, and earth movers are examples. Finally, there are other common areas just beginning to be influenced by human factors engineering. These include houses, home appliances, recreational equipment, recreational vehicles, and children's toys. The man/equipment interface is broad indeed.

Two examples of a human factors design problem are shown in figure 1. When the wheels of a car are set for straightaway driving, one spoke of the steering wheel may hide the part of the speedometer that registers rates of speed used for city driving. The driver then may see the speedometer best only when the automobile is turning, a time when he does not observe the speedometer. If two cars of the same model line are placed side-by-side, only one of them may have this defect. This would suggest that the problem arose on the assembly line, and the solution would be for the engineers to design the steering wheel and steering column parts so that they could be mated only in a way that would not block one's view of the speedometer.

The main goals in human factors engineering are to–

(1) Consider any man/machine combination as a total system to insure that the equipment operational requirements do not exceed human abilities

(2) Consider the human performance tolerance, thereby insuring optimal speed, accuracy, and quality of performance; eliminating hazards to operating personnel; and maximizing the comfort of the operator

When evaluating any equipment design, one should ask the following questions about the human operator:

(1) What sensory inputs does the operator use to monitor operations of

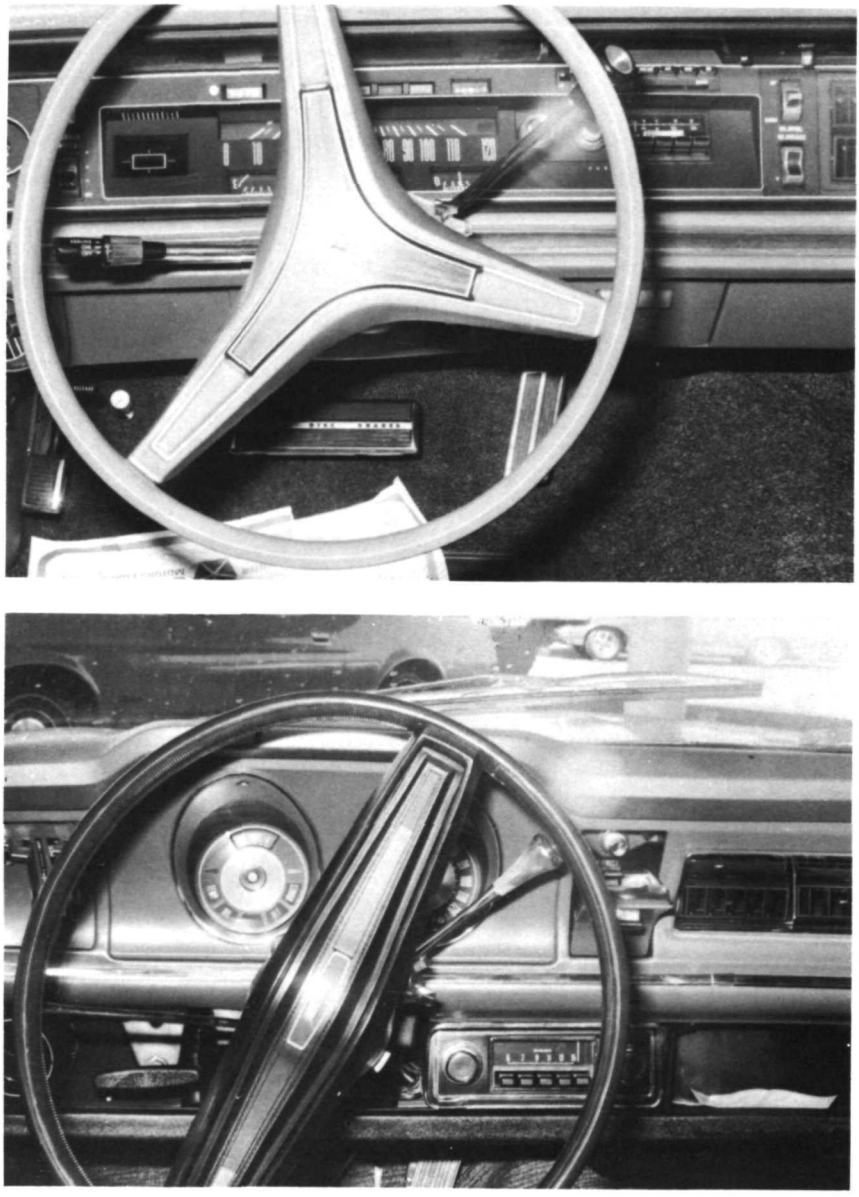

FIGURE 1.–Two examples of a human factors engineering problem.

the equipment? (Hearing, seeing, smelling, or feeling pressure, temperature, or pain?)

(2) What discriminations is the operator required to make during the performance of his job? (Differences between tones, colors, dial indicators?)

(3) What responses will the operator have to make while operating the equipment? (Lever pulling-pushing, knob twisting, button pushing, wheel turning, pedal pushing?)
(4) What movements will the operator make to operate the equipment? (Can he reach all controls? Will he be able to effect all control movements? Can he see, hear, or feel all feedback to be provided by the equipment? Will the operation be fatiguing?)
(5) What are the speed and accuracy requirements for operation? (Is speed or accuracy more important? Can the operator sustain performance?)
(6) What work-rest cycles are required? (What are the effects of fatigue? What are the proper break intervals?)
(7) What hazards are inherent in operating the equipment?

When tackling a human factors engineering problem, one should consider that the man may be required to do all or any combination of the following tasks: operate, monitor, evaluate performance, set up equipment, initiate operation, troubleshoot, remove/disassemble, install/assemble.

As new types of equipment are developed, new tasks will be required, but this list is a good starting point for any human factors engineering analysis and design review.

NASA'S ROLE IN HUMAN FACTORS ENGINEERING

NASA encountered a set of human factors engineering problems that were approximated only by those of the Air Force. Fortunately, a large amount of work on solving such problems was already done. NASA capitalized on these data in developing its own program, but found it inadequate because the entire subject of man's living and working in space was virtually unexplored.

NASA then set about to acquire the missing information as well as to create the necessary knowledge and hardware. Besides putting man on the Moon, it assembled the largest group of technicians and greatest body of knowledge ever used to define man's performance on the ground and in space environments. This technology can now be directed toward the human factors problems on Earth.

Considering the nature of the problems to be solved, the NASA-developed contributions to human factors engineering are characterized by one or more of the following qualities:

(1) A consistent multidisciplinary approach to system problems with human factors an integral part of the project
(2) Development of data on human performance in unusual environments through simulation techniques
(3) Highly specific applications

A multidisciplinary approach to system problems was required by the

nature of the problems involving man. Each discipline made its contribution to the solutions as part of an overall effort; consequently, the solutions cut across the several academic specialties involved. Specific human factors engineering contributions by NASA are difficult to isolate from the total effort. However, an extremely large amount of information was generated in the Earth environment for planning and developing the means to put man into space as well as to sustain him there while he did his work. It is from these latter studies that NASA contributions to human factors engineering are most evident.

Data on human performance in unusual environments were obtained by simulating the conditions of outer space in the Earth environment. NASA had to obtain information that would approximate the human performance envelope in space. The applicability of the data acquired depends almost entirely upon the similarity between the simulation environment and the environment being simulated. NASA data on human performance underwater have direct application to the design of equipment for man to use and the design of tasks for man to perform in the oceans.

Highly specific applications are characteristic of most of the equipment designed for space missions, which involve small numbers of persons in the space flight. Emphasis was placed on the safe return of the astronauts, and survival equipment was designed to support only those tasks to be performed during specific missions. The spacesuits for projects Mercury, Gemini, and Apollo consequently were quite different. They were designed specifically to allow the astronauts to perform their assigned tasks in relationship to the equipment layout and work space afforded by the immediate environment. Dr. William Feddersen, former Director of Human Factors at the Manned Spacecraft Center, commented regarding spacesuit structure that "the fact that he [an astronaut] could reach out and manipulate a knob 20 in. away does not imply that he could reach out and manipulate a knob 10 in. away." The implication of this statement from a human factors engineering standpoint is that equipment should always be designed for the specific tasks that a man is expected to perform.

NASA APPLICATIONS OF HUMAN FACTORS ENGINEERING

The applications of NASA-developed technology that are reported in this survey are not the only useful human factors applications from the NASA program. Six have been used already in other than aerospace settings:

(1) Physiological measurements without the use of attached sensors
(2) Exoskeleton (limb-motion sensors)
(3) Langley Research Center complex coordinator
(4) Shock-absorbing temper foam
(5) Visual sensitivity tester
(6) Coaxial cable cutter

SCOPE OF SURVEY

This survey presents the NASA contributions to the state of the art of human factors engineering, and indicates that these contributions have a variety of applications to nonaerospace activities. Emphasis is placed on contributions relative to man's sensory, motor, decisionmaking, and cognitive behavior and on applications that advance human factors technology.

Contributions relative to man's sensory, motor, cognitive, and decision-making behavior are emphasized to distinguish between human factors applications and those applications from related areas pertaining to the human being, particularly medicine.

Applications that advance human factors technology also are emphasized, thereby excluding applications of conventional human engineering techniques, data, and principles (i.e., anthropometric data, design of dials and controls, and layout of work spaces).

The remainder of the document consists of descriptions of NASA human factors engineering contributions in the areas of measurement of physiological parameters (ch. 2), display techniques (ch. 3), underwater work (ch. 4), vibration and impact research (ch. 5), vision testing (ch. 6), and tools (ch. 7). In each instance the application is described, typical application areas are listed, constraints that limit the applicability of the product or data are discussed, and supporting data that would be required in making a valid application are presented.

CHAPTER 2

Measurement of Physiological Parameters

Human physiological parameters now can be measured in ways that do not require sensors to be implanted.

TECHNIQUE USING UNATTACHED SENSORS

A technique for physiological monitoring using unattached sensors was developed at Philco-Ford Corp. (ref. 2).

Future space vehicles will be relatively large and crewmembers will have to move about within them. Therefore, it would be a decided advantage if there is no need to wear a body harness, and the work described in this chapter was done to find ways to obtain physiological monitoring information with unattached sensors, palm-to-palm, under the following constraints:

(1) No attachments, straps, or adhesives
(2) Information to be taken from the body without any special preparation or procedures (for example, no paste or electrolytes or no abrasion of body surfaces)

System for Physiological Monitors and Unattached Sensors

Figure 2 is a block diagram of a system for monitoring with unattached sensors. It has three components:

(1) Two Palmar dry electrodes and a microphone, which act as sensors
(2) A set of solid-state modular signal conditioners designed to separate, filter, and amplify each channel of physiological information
(3) A stripchart recorder

Fitzwater et al. mounted the sensors and the signal-conditioning package on a conventional office chair to demonstrate the feasibility of the system. Physiological data sensed by the transducers fall into the following categories:

(1) Biopotential: electrocardiogram (ECG)
(2) Bioresistance: galvanic skin response (GSR); low-frequency changes of skin resistance; baseline skin resistance (BSR), direct current.
(3) Bioimpedance: impedance pneumograph (ZPG); low-frequency changes in impedance respiration at 100 kHz; impedance cardio-

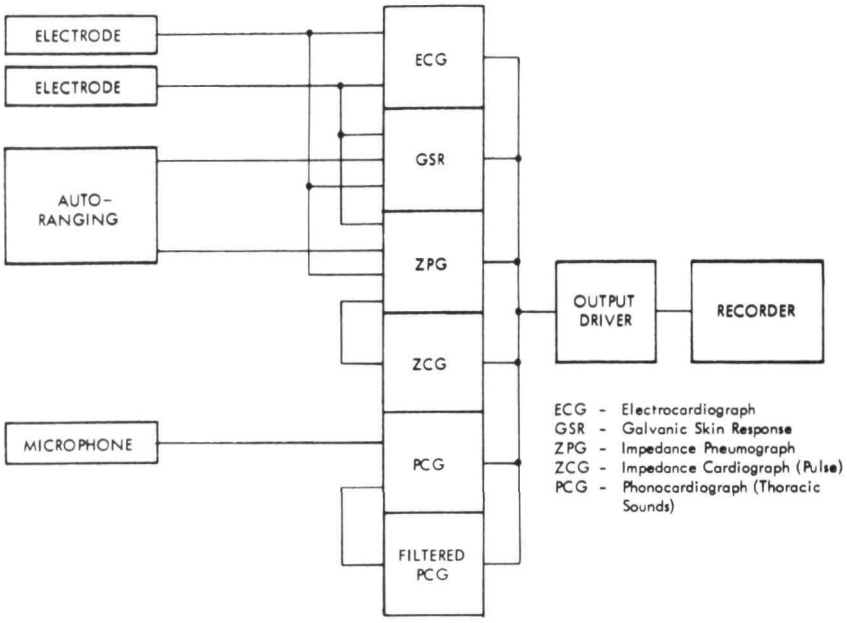

FIGURE 2.–System block diagram for the measurement of physiological parameters without attached electrodes.

graph (ZCG), 0.8 to 5.0 Hz; changes in impedance caused by central blood pulse measured at 100 kHz.

(4) Thoracic sounds: phonocardiograph (PCG); sounds in the 20- to 2000-Hz range, and filtered PCG sounds below 20 Hz.

Common sensors are used to detect the data separated in multiple signal conditioners. Therefore, some caution is necessary in describing the system specifications, particularly the input characteristics. The minimum input impedance on any given channel affects the operation of all other signal-conditioning channels. This minimum input impedance for the system described is differentially 8 kΩ and has a common mode input impedance of approximately 44 MΩ.

Application Areas

Except for certain limitations, the total system fabricated in this study can be used by a technician to collect screening data rapidly from individuals who may be predisposed toward heart disease. It is feasible to install the system in a van and produce a mobile heart-problem screening clinic. (Heart disease is now the second most prevalent killer in the United States.) Mobile screening clinics have been used successfully for many years with chest X-rays.

Technicians can be trained without difficulty to use this system because all

data can be put into computer storage. Also a program can be easily written to evaluate the data on the spot. The evaluation need not be a clinical one but may be only a recommendation to see a physician.

The basic drawback to the system is the limited applicability of the chest (thoracic) sounds channel. To use data collected on this channel, considerable work must be done in the areas of transducer selection and location. Studies must also be conducted to define the significance of thoracic sounds.

In a previous study by Philco-Ford, a number of materials were compared to determine the best dry electrode material for this project:

Material	*Rating*
Aluminum, braid	Fair
Aluminum, smooth	Unusable
Chrome-plated copper	Unusable
Conductive plastic	Unusable
Copper, braid	Most desirable
Copper, smooth	Good
Gold-plated copper	Good
Gold-plated copper braid	Most desirable
Nickel-plated copper	Unusable
Silver-bearing epoxy	Poor
Silver-plated copper	Good
Silver-plated copper braid	Most desirable
Stainless steel	Unusable
Wire bristles, steel	Fair

These materials were tested free of corrosion, oil, or surface dirt. Gold-plated copper was selected for use in the described system because of its relatively high signal-to-noise ratio, relatively low baseline drift (polarization), and immunity to corrosion.

Anthropometric considerations dictated mechanical placement of the electrodes. These electrodes were placed within a comfortable reach of adults and most children. They also were kept short to minimize radiofrequency interference. The electrodes used in the system provided at least 38.7 cm^2 (6 in^2) of surface area per palm to insure that casual resting of the hands on the electrodes would exceed the minimum contact requirements of 6.5 cm^2 (1 in^2) per palm. Figure 3 shows the gold-plated electrodes mounted on an office chair along with the signal-conditioning electronics.

The system was constructed from commercially available equipment and components. Although a design engineer could construct a physiological monitoring system similar to the one used by NASA, new baseline and calibration data would have to be generated for each new system. The signal-conditioner specifications are presented in table 1.

550-754 O - 74 - 2

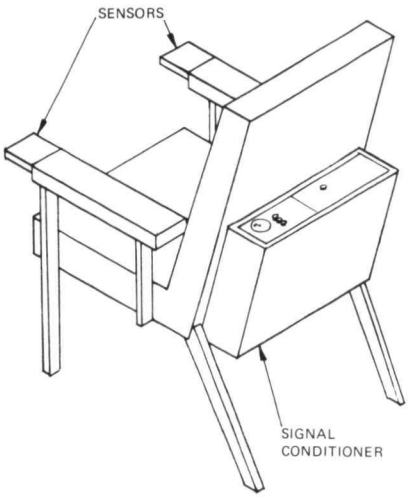

FIGURE 3.–Medical monitoring chair with gold-plated electrodes.

TECHNIQUES FOR DETECTING MOTION AND LIMB POSITION

The techniques and hardware described in this section were developed by Bruce A. Conway of Langley Research Center (ref. 3), principal investigator for the Skylab crew/vehicle disturbances experiment, and by the Martin Marietta Corp., experiment flight hardware contractors, to determine detailed characteristics of crew-motion disturbances (including both discrete and random models of crew-motion forces and torques) to permit effective design of future spacecraft and experiment control systems.

Force Measuring System

An array of load cells was selected as being the easiest to fabricate and maintain, as well as having the capability to survive the launch environment. A laboratory model of a force measurement unit (FMU) was used in simulation studies to verify its measurement capability. Figure 4 shows the flight hardware FMU.

Limb-Motion Sensors

The limb-motion sensor system (LIMS) selected was an external framework similar to an exoskeleton (such as the shell of crustaceans). Potentiometers were used at principal rotation points such as at the elbow and knee.

The exoskeleton LIMS offers advantages of ease of data reduction and resultant savings in experiment weight. Its major disadvantage is that body movement is somewhat restricted, but this effect is minimized if the exoskeleton is properly designed and fits the wearer.

Optimum design concepts for a lightweight exoskeleton LIMS were developed. The exoskeleton is attached to a one-piece form-fitting garment

TABLE 1.–*Signal-Conditioner Specifications*

Signal conditioner[a]	Frequency response (signal conditioner outputs), Hz	Data lag, msec	Maximum recovery time (+5 percent of time from instant of contact), sec	Input range with autoranging, kHz	Output range, V	Output impedance, Ω	Calibration (manual pushbutton switch)
ECG	0.15 to 100		20		±10	600	1 mV in series with electrode
GSR	0 to 50		.5	1 to 60 (baseline)	±10	600	100 in series with electrode
ZPG with 100-kHz carrier	0 to 0.8	9	.5	330 to 760	±10	600	3 in series with electrode
ZCG with 100-kHz carrier	0.8 to 5	150	.5	330 to 760	±10	600	
PCG	20 to 2000		.5		±10	600	
Filtered PCG	20-Hz maximum		.5		±10	600	

[a]Power requirements: 115 V, 60 Hz, 50 W (maximum).

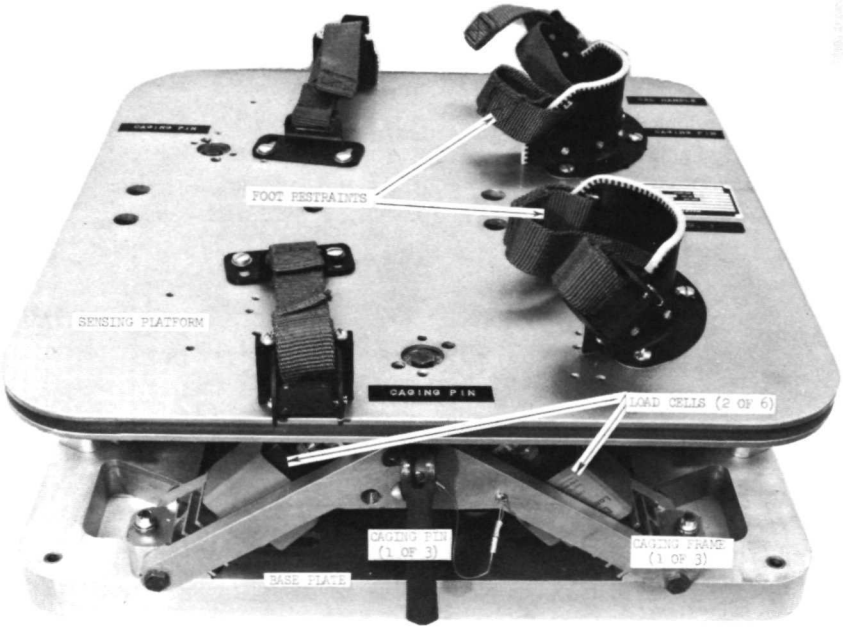

FIGURE 4.–Flight hardware FMU.

(coverall) which provides proper limb alinement and simplifies attachment and removal.

The LIMS consists of an aluminum exoskeleton with 16 potentiometers to measure rotations at the principal body joints. An electrical umbilical is attached between the LIMS and a data system. It provides 5-V direct current power to the potentiometers and carries the data signals back to the data system. The exoskeleton is adjustable to fit astronauts of different sizes. Expansion panels are added to the one-piece suit, increasing its versatility.

Anthropometric/Mathematical Model

A mathematical model of the human body was formulated (app. A of ref. 3) to compute human body segment inertial properties and other biomechanical data. Several major anthropometric points of the skeleton were used in devising this model. These, along with the locations of the body reference planes, appear in figure 5. The remaining points and planes are shown in figure 6.

Right-angle (orthogonal) coordinates are used as a body reference system. This system is defined by the intersection of the three principal body planes shown in figures 5 and 6. The X-axis is formed by the intersection of the sagittal (front to back) and transverse planes, with $+X$ directed toward the front; the Y-axis is defined by the intersection of the frontal and transverse planes, with $+Y$ directed toward the right side; the Z-axis is formed by the

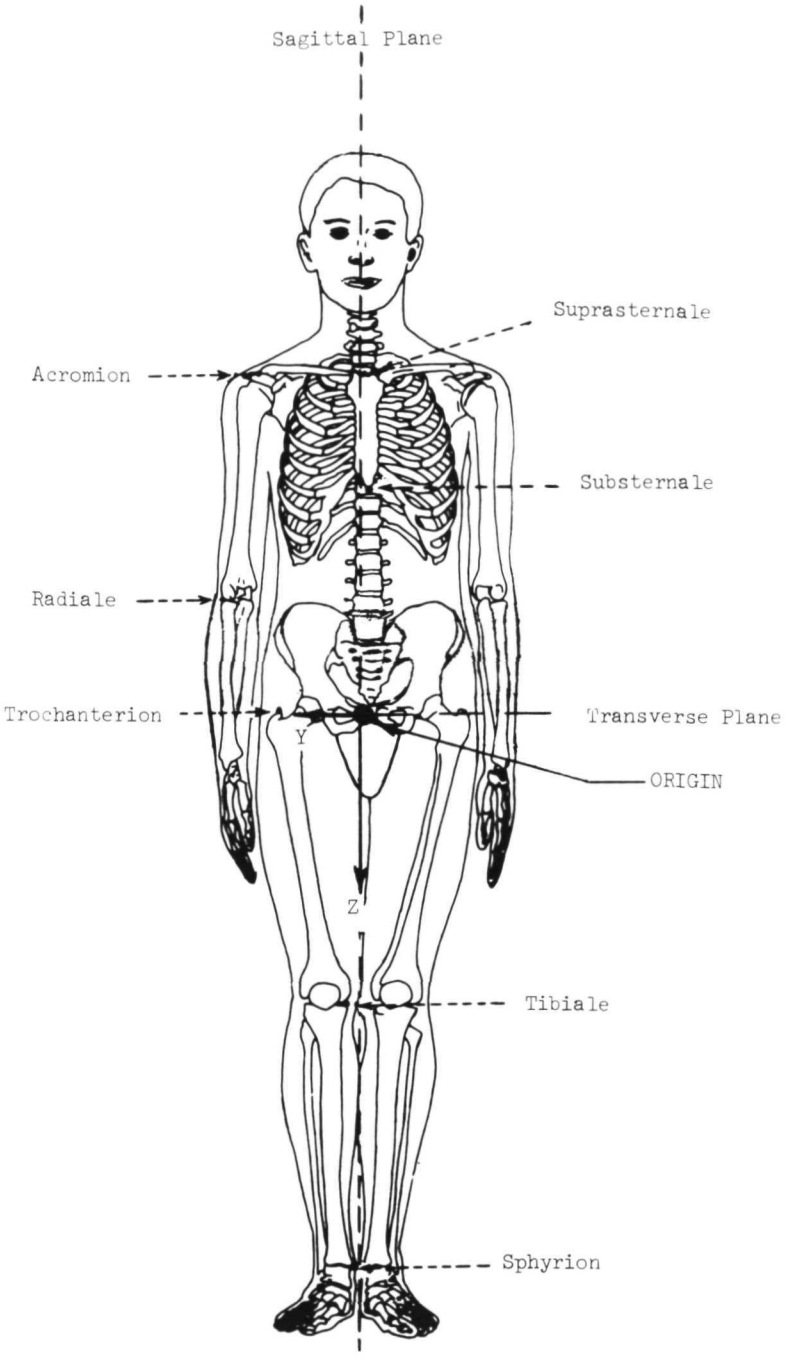

FIGURE 5.–Frontal view of human skeleton.

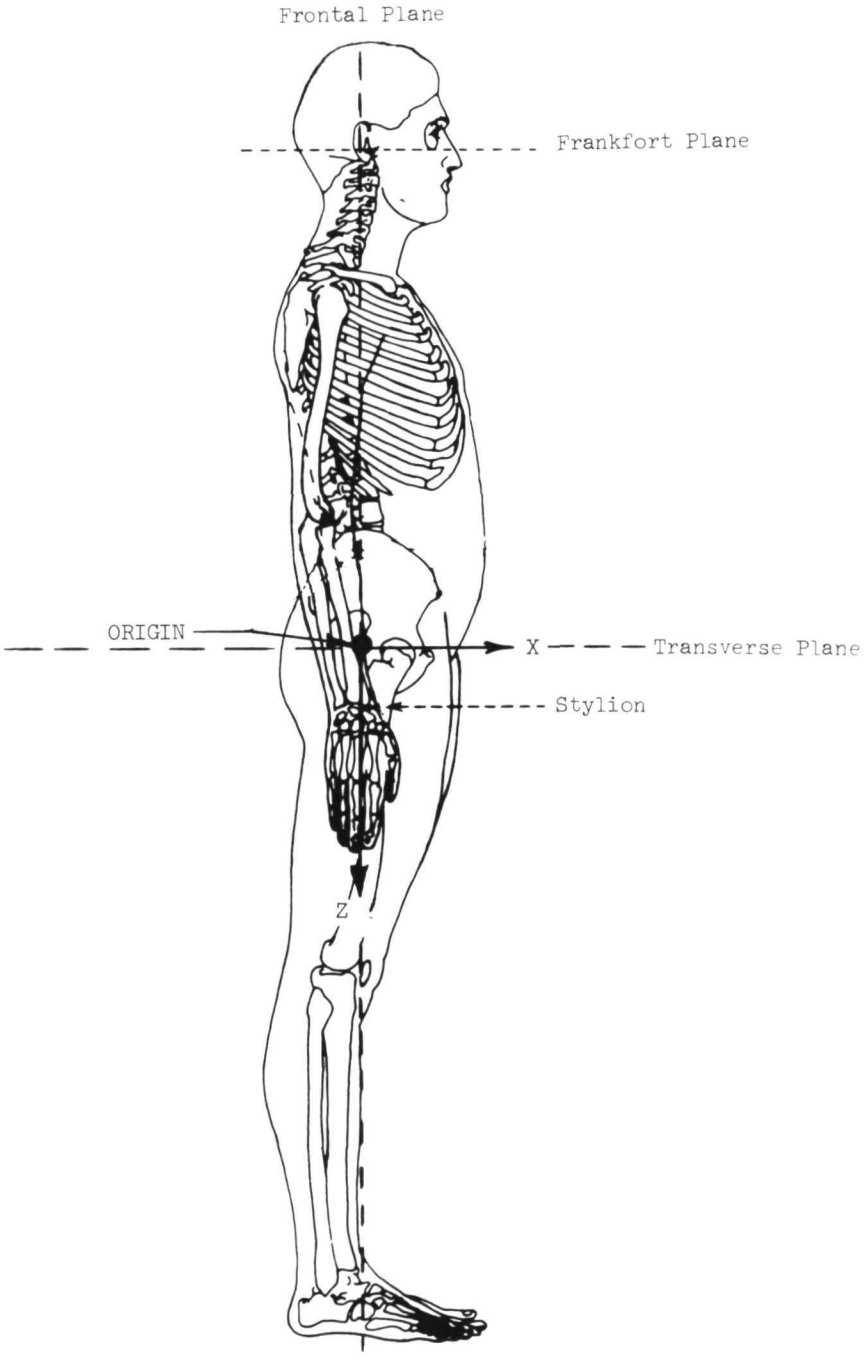

FIGURE 6.–Lateral view of human skeleton.

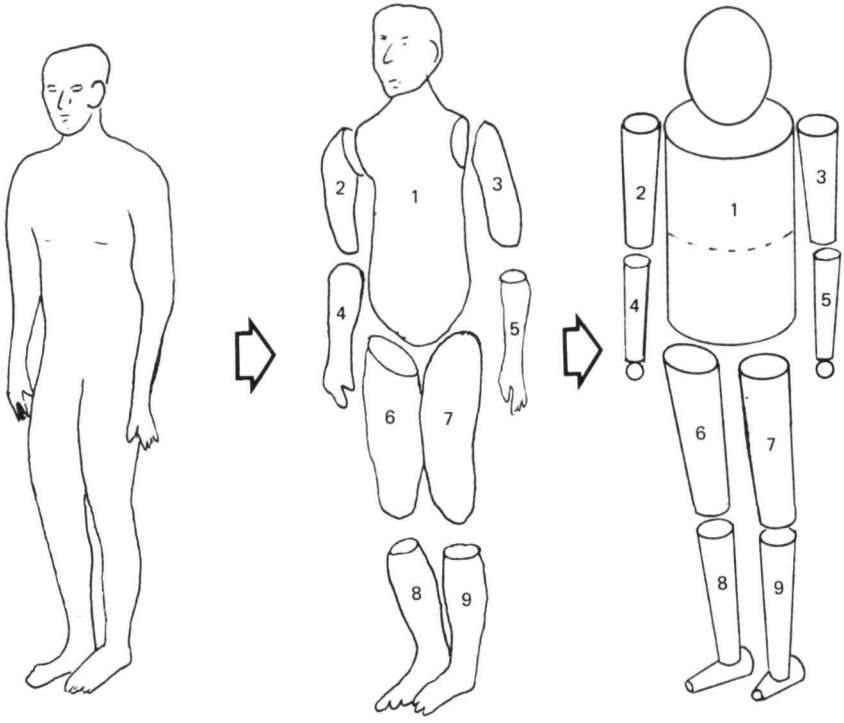

FIGURE 7.–Nine segment model of man.

intersection of the sagittal and frontal planes, with $+Z$ directed toward the feet. The origin of the coordinate system is located at the intersection of the three body reference planes as shown in figures 5 and 6.

Figure 7 illustrates the relationship of the body segments. Segment 1 is treated as a rigid member and results from the combination of three solids: the head is represented by an ellipsoid while the upper and lower torso are represented by right elliptic cylinders. A lower arm segment (segments 4 and 5) is a combination of a sphere for the hand and a frustum of a right circular cone for the lower arm. Another compound segment is the lower leg (segments 8 and 9), which is a combination of two frustrums of cones, one representing the lower leg and the other representing the foot. All other body parts are approximated by simple frustums of right circular cones.

The relative locations of the segment centers of mass and the segment hinge points must be specified to use the mathematical model. Figure 8 shows these locations, along with the orientation of the coordinate axes.

Application Areas

Initially, the application of these techniques appears limited to space-flight

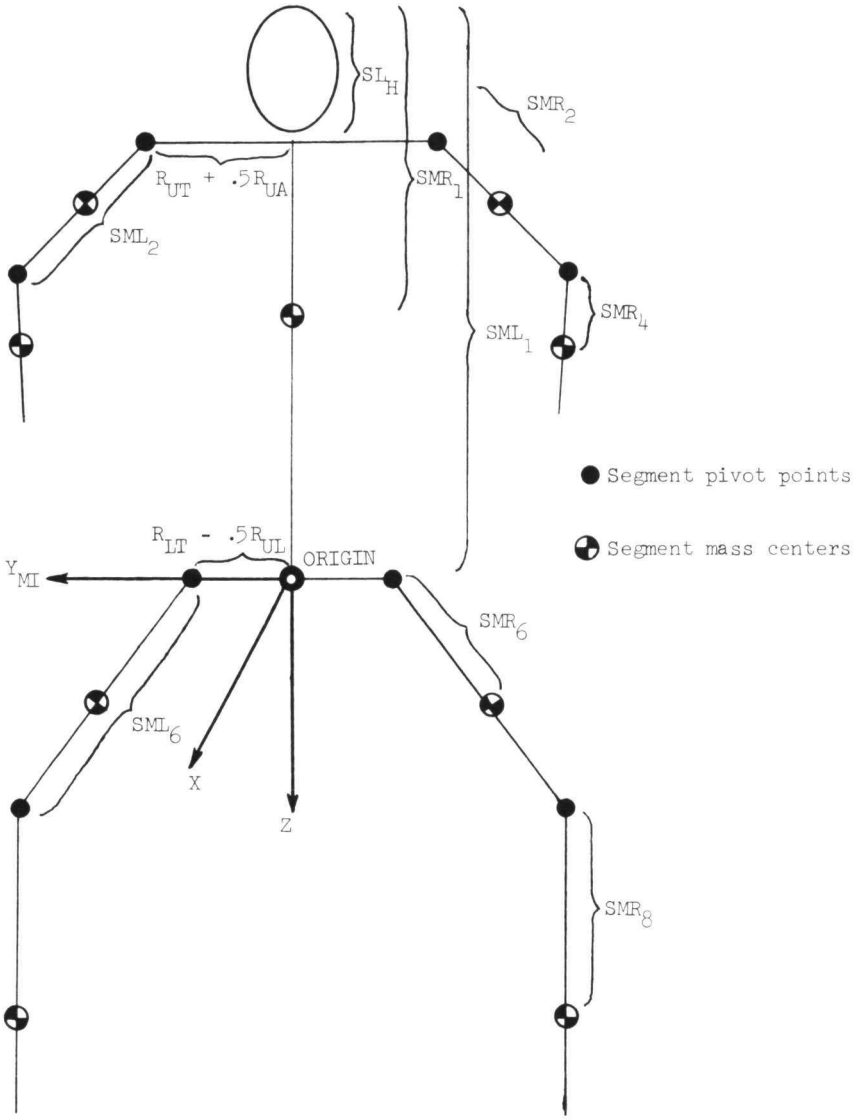

FIGURE 8.–Locations of segment hinge points and centers of mass and coordinate axis orientation.

use. Actually, both the techniques and the equipment can be modified to define the following aspects of human performance:

(1) Total body motions during task performance (duration, direction, and magnitude)
(2) Total forces exerted on the body by equipment used during task performance (direction, duration, and magnitude)

(3) Total forces required of the body during task performance (direction, duration, and magnitude)
(4) Total work space required of the body during task performance (dimensions and duration)

Modification of the equipment and techniques described permits task descriptions to be formulated for the total body at the real-time level of analysis. Classical psychophysical methods provide task analysis at segmented or fragmented levels of approach, examining behavior at the subtask level.

The techniques described herein could be used to evaluate or define performance and work space requirements in the following examples:

(1) Escape hatches and doors in aircraft, boats, automobiles, and buses for such possible contingencies as fire or submergence in water
(2) Devices needed by man to survive in hostile environments, such as fire-fighting equipment, emergency flotation gear, and diving gear
(3) Performance and training methods for physical tasks involving complex coordination, such as golf, tennis, or bowling
(4) Performance envelopes in reduced-friction environments, such as under water

The equipment and techniques were specifically designed to validate an anthropometric model of man to be used in performing simulation studies of man's performance at zero gravity.

The model itself also has possible limitations in use. No consideration is given to motions of the wrist, ankle, or head or to bending of the spine. The hands and feet are small masses in comparison with other body segments and would provide minimal disturbance effects if moved vigorously; however, the head and spinal motions involve larger masses and their omission could affect the collected data.

Twenty-four standard anthropometric measurements are used to dimension the model segments. Table 2 presents a listing of these measurements, their abbreviations, and brief descriptions.

The man's total body mass m_T must be distributed over each of the body segments. A set of regression equations distributes the total body mass over the body segments:

$$\text{Head, neck, and trunk} = \text{HNT} = 0.47m'_T + 5.44 \text{ kg} \quad (1a)$$
$$\text{Both upper arms} = \text{BUA} = 0.08m'_T - 1.32 \text{ kg} \quad (1b)$$
$$\text{Both forearms} = \text{BFO} = 0.04m'_T - 0.23 \text{ kg} \quad (1c)$$
$$\text{Both hands} = \text{BH} = 0.01m'_T + 0.32 \text{ kg} \quad (1d)$$
$$\text{Both upper legs} = \text{BUL} = 0.18m'_T + 1.45 \text{ kg} \quad (1e)$$
$$\text{Both lower legs} = \text{BLL} = 0.11m'_T - 0.86 \text{ kg} \quad (1f)$$
$$\text{Both feet} = \text{BF} = 0.02m'_T + 0.68 \text{ kg} \quad (1g)$$

where

$$m'_T = \frac{m_T - 5.48}{0.91}$$

The corrected total mass of model man m'_T distributes mass proportionally to the segment masses.

Development of the nine segment model of man, including appropriate dynamic equations, is presented in appendixes A and B of reference 3.

TABLE 2.–*Anthropometric Measurements*

Measurement	Abbreviation	Brief description
Ankle circumference	ANKC	Minimum circumference of right ankle
Axillary arm circumference	AXILC	Horizontal circumference of upper arm at armpit
Buttock depth	BUTTD	Front-to-rear dimension of body at buttocks
Chest breadth	CHESB	Width of body (less arms) at level of nipples
Chest depth	CHESD	Front-to-rear dimension of chest at level of nipples
Elbow circumference	ELBC	Circumference of arm at elbow (arms extended)
Fist circumference	FISTC	Circumference of fist measured over thumb and knuckles
Forearm length	FOARL	Length of extended lower arm between elbow and wrist
Foot length	FOOTL	Maximum length of foot from heel to toe
Knee circumference	GKNEC	Circumference of right knee at kneecap (standing)
Head circumference	HEADC	Maximum circumference of head above eyebrows
Hip breadth	HIPB	Maximum width of body at hips
Shoulder height	SHLDH	Distance from floor to right shoulder (acromion), standing
Sitting height	SITH	Height from seat to top of head, subject sitting erect with knees bent 90°
Sphyrion height	SPHYH	Distance from floor to sphyrion (ankle), subject standing
Stature	STAT	Distance from floor to top of head, subject standing erect
Substernale height	SUBH	Distance from floor to substernale (lower breastbone), subject standing
Thigh circumference	THIHC	Horizontal circumference of upper right thigh, standing
Tibiale height	TIBH	Distance from floor to tibiale (knee), subject standing
Trochanteric height	TROCH	Distance from floor to trochanterion (hip), subject standing
Upper arm length	UPARL	Distance from shoulder to elbow (acromion to radiale), arm at side
Waist breadth	WAISB	Minimum width of waist, standing
Waist depth	WAISD	Front-to-rear dimension of body at waist
Wrist circumference	WRISC	Minimum circumference of wrist, arm extended

TECHNIQUES FOR DETERMINING EFFECTS OF WEIGHTLESSNESS

The hardware and techniques described in this section were developed by the Denver Division of Martin Marietta Corp. and the NASA Marshall Space Flight Center for the NASA Manned Spacecraft Center (ref. 4) to assess the time and course of cardiovascular deconditioning as well as the degree of orthostatic intolerance and impairment of physical capacity that is induced by zero gravity during space flight.

Lower Body Negative Pressure Device

The lower body negative pressure device (LBNPD) can maintain a pressure differential between cabin ambient and the LBNPD interior over a range from 0 to 7.3 kN/m^2 (0 to 55 mm Hg) below cabin ambient. The device has an adjustable waist seal to fit the subject properly and supports to keep his trunk centered. Restraints inside the LBNPD prevent the subject's feet from contacting any surface of the device. Two connectors inside the device allow the limb volume measuring system (LVMS) plethysmographs to be connected. Controls are provided at the LBNPD for operation by the observer. An emergency pressure release is located within easy reach of both the subject and the observer. A pressure relief device limits the pressure differential to a maximum of 7.3 kN/m^2 (55 mm Hg). An interior light allows the observer to view the plethysmograph positions during experiment operation. A vacuum selector valve selects 4.0, 5.3, and 6.7 kN/m^2 (30, 40, and 50 mm Hg) at 5-min intervals. The pneumatics of the device are illustrated in figure 9 and a block diagram of the LBNPD is shown in figure 10.

Limb Volume Measuring System

The LVMS is used to measure the percentage of change in volume of the lower legs before, during, and after the application of negative pressure. Measurement is made by using plethysmographs installed on the upper calves of the legs. Variable capacitance is measured using the skin of the leg as one plate of the capacitor. The other plate is contained in the transducer, which is held rigidly in place by the plethysmograph structure. Variations in the percentage of leg volume result from blood being pulled into the veins of the leg by the action of the negative pressure. The percentage of change is determined from the distance between the skin and the fixed plate.

Blood Pressure Measuring System

The blood pressure measuring system (BPMS) measures blood pressure by an occlusion cuff installed on the left arm above the elbow and over the brachial artery. Workshop nitrogen pressure is supplied to the cuff by a pressurization programer. This pressure is monitored by the BPMS electronics

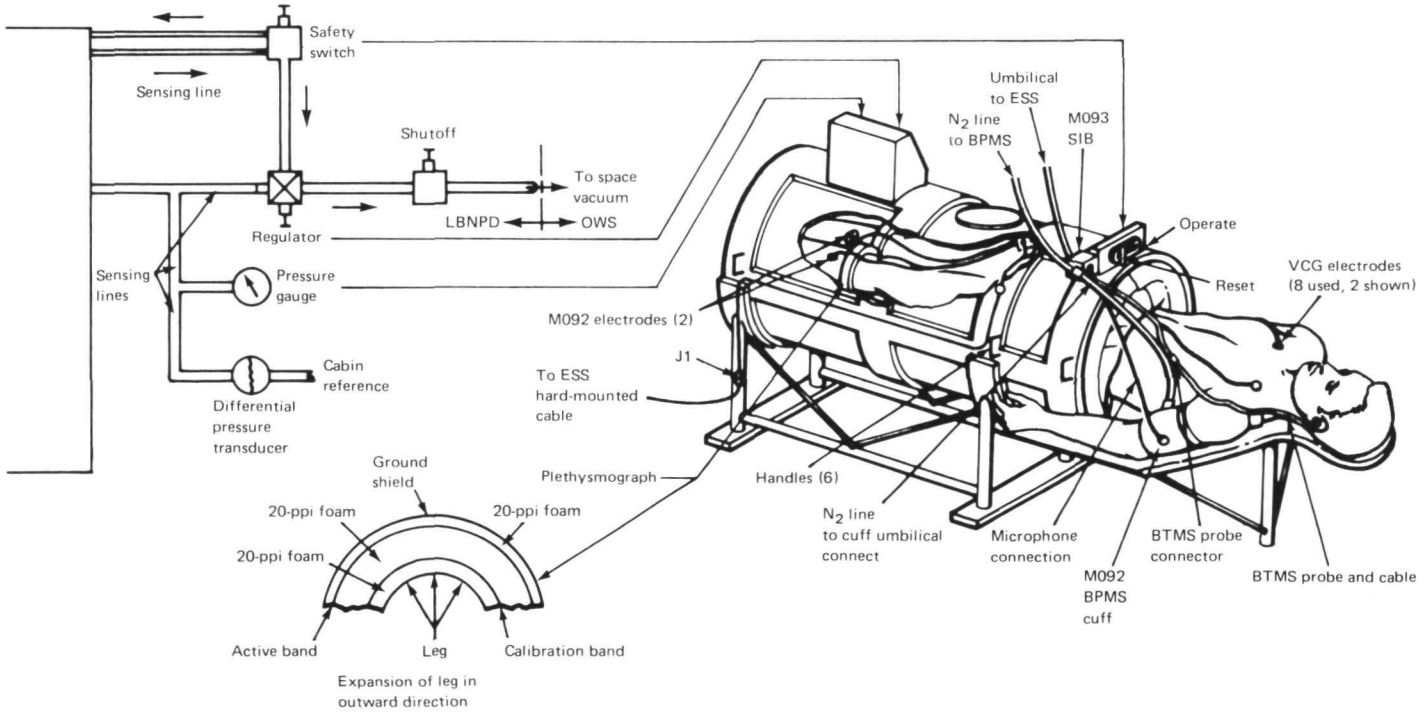

FIGURE 9.–LBNPD pneumatics (BPMS = blood pressure measuring system; BTMS = body temperature measuring system; ESS = experiment support system; SIB = subject interface box; VCG = vectorcardiogram.)

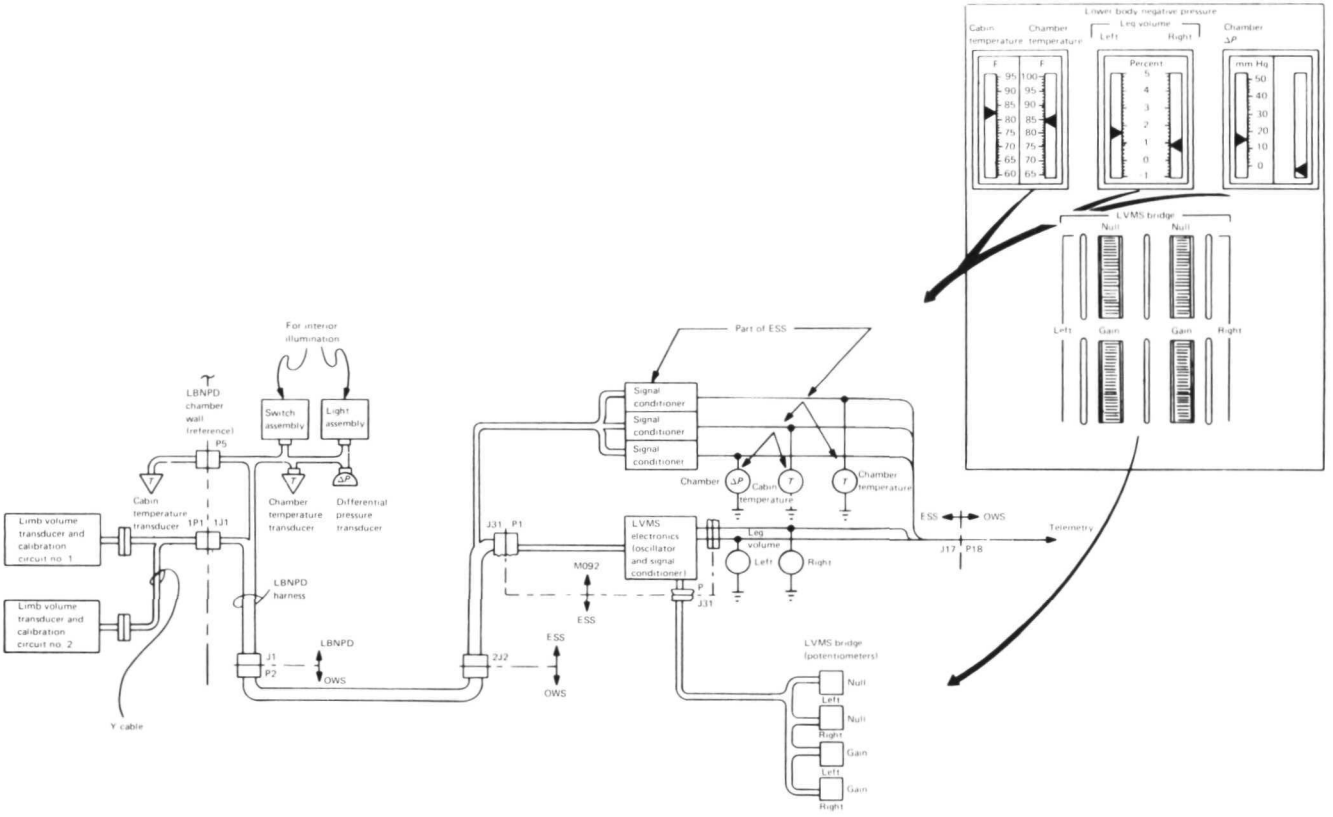

FIGURE 10.–LBNPD block diagram.

module located in the experiment support system (ESS) and by an aneroid clipped to the subject interface box (SIB). The cuff contains a microphone for monitoring Korotkoff sounds as well as a transducer for monitoring pressure. Sufficient pressure is applied to the cuff to stop the flow of blood in the brachial artery. The pressure is then reduced at a constant rate while the microphone monitors Korotkoff sounds.

Cuff Assembly

The occlusion cuff is a flaccid band that is readily adjustable to fit either arm. The cuff has an integral pulse sensor and is designed to insure that the pulse sensor is automatically placed over the brachial artery when placed on the arm.

A cuff pressurization programer is used. It incorporates valving, control circuitry, and logic to permit automatic fill, bleed-down, and evacuation of air pressure. The programer is designed so that cycling can be set at the option of the observer to take place for 30 sec at 22 kN/m^2 (160 mm Hg) or 60 sec at 27 and 33 kN/m^2 (200 and 250 mm Hg). A fourth option allows the cuff pressurization cycle to be started manually. A pneumatic line connects the pressurization unit to the occlusion cuff. This line has quick-disconnect fittings near the cuff and at the pressurization unit. A relief valve is provided to prevent cuff pressure from exceeding 35 kN/m^2 (260 mm Hg) differential with respect to ambient. Figure 11 is a block diagram of the system.

Blood Pressure Measuring System Module

The cuff pressurization programer cycling is controlled by switches on the ESS panel. The blood pressure programer switch selects either an automatic (30 or 60 sec) or a manual position. When the "initiate" switch is turned on, a solenoid-operated valve allows nitrogen to pressurize the cuff to 22 ± 0.7 kN/m^2 (160 ±5 mm Hg) for a 30-sec selection or to 27 ± 0.7 kN/m^2 (200 ±5 mm Hg) in the manual or 60-sec mode. When the desired level is reached, the system automatically stops the nitrogen and allows the pressure to bleed off through a fixed orifice down to 7 kN/m^2 (50 mm Hg) or less. During this bleed-down, Korotkoff sounds are monitored to establish systolic and diastolic pressure values. When either diastolic pressure is determined or the pressure decreases to 5 kN/m^2 (40 mm Hg), the pressure is reduced as quickly as feasible to ambient.

Korotkoff sounds monitored by the blood pressure measuring system are limited in the signal conditioner to a 200-msec timespan following the heartbeat. This timespan begins 130 msec after the heartbeat and continues for 200 msec. Any sound occurring outside this timespan will not be used to determine systolic or diastolic pressure values.

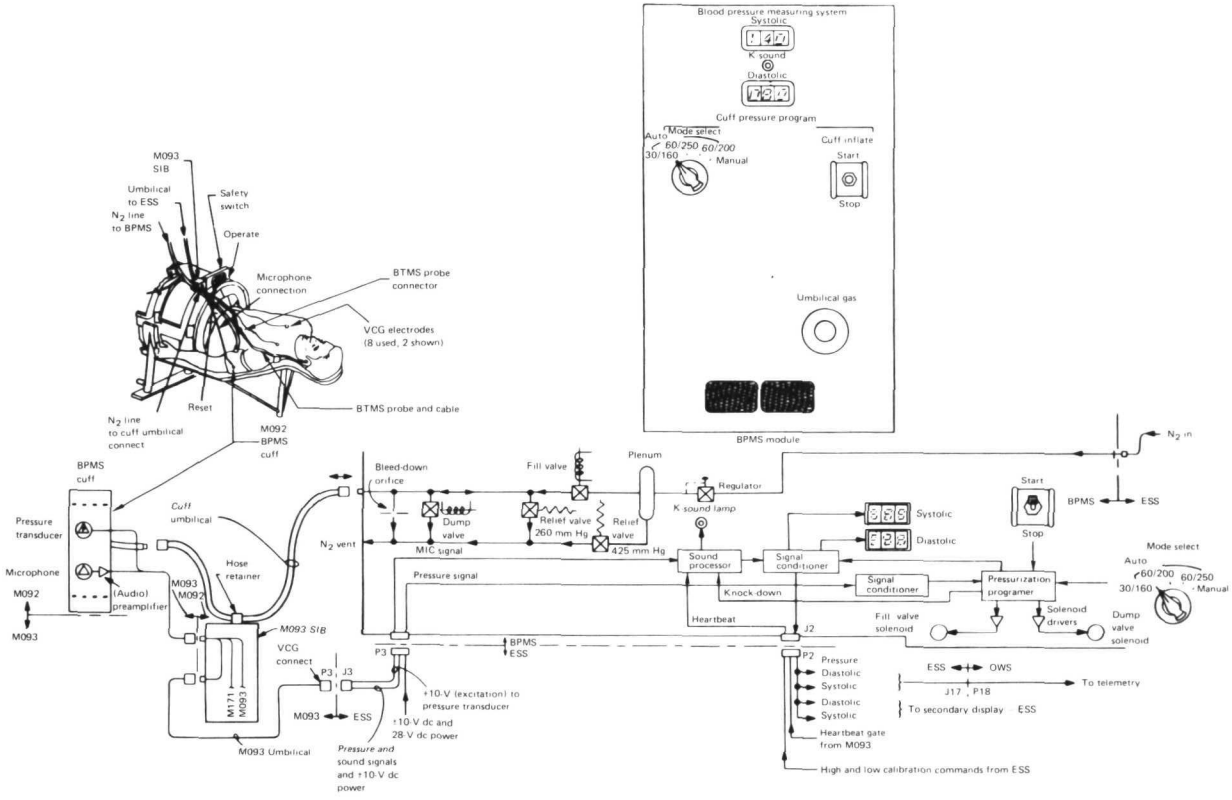

FIGURE 11.–BPMS block diagram.

Body Temperature Measuring System

The body temperature measuring system (BTMS) monitors the body temperature. This system consists of two units: an ear temperature probe and a signal-conditioner assembly that is contained in the SIB. Figure 12 is a block diagram of the BTMS.

Oral Temperature Probe

The oral temperature probe consists of a thermistor extended through a metallic tube that is used orally. The thermistor leads are extended through a cord that connects to the BTMS signal conditioner. Bridge resistors, which match the particular thermistor to the signal conditioner, are contained in the probe assembly connector shell. When used with the signal conditioner, the probe provides a measurement range of 35° to 40.5° C (95° to 105° F).

Signal Conditioner

The BTMS signal conditioner supplies excitation voltage to the oral temperature probe and conditions the probe output to a form that will operate the body temperature indicator on the ESS panel and provide an input to the instrumentation system. In use, the signal conditioner is mounted in the SIB, and the oral temperature probe plugs into this box. The signal conditioner is electrically connected to the SIB, and its power and output signals are transmitted through the vectorcardiogram (VCG) umbilical connected to the ESS.

Interfaces

Figure 13 is an interface block diagram illustrating the operation of the signal conditioner in relationship to the probe. The signal conditioner uses +10- and −10-V power from the ESS. A regulated-bridge excitation voltage is developed from these voltages. The bridge circuit contained in the oral temperature probe assembly consists of four fixed resistors and the thermistor. The thermistor resistance varies with the subject's oral temperature, thereby providing a variable output voltage that is amplified by the signal conditioner. Balance and gain controls are used for ground calibration. A calibration command from the ESS energizes a relay in the signal conditioner that produces a predetermined BTMS output.

Vectorcardiogram System

The VCG system harness is 107 cm (42 in.) long with a connector on one end. It has four color-coded branches with electrodes attached.

VCG Electronics Module

The VCG electronic equipment consists of the following components:

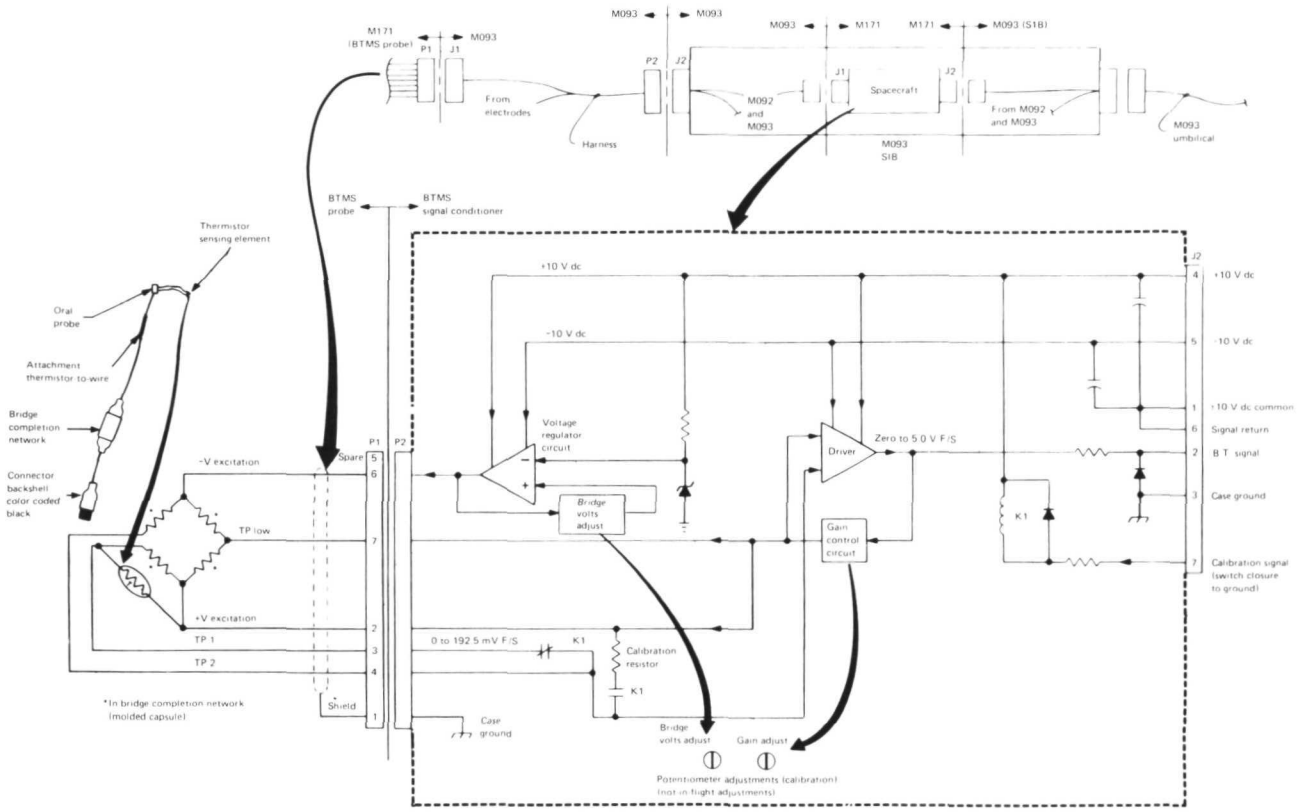

FIGURE 12.–BTMS.

550-754 O - 74 - 3

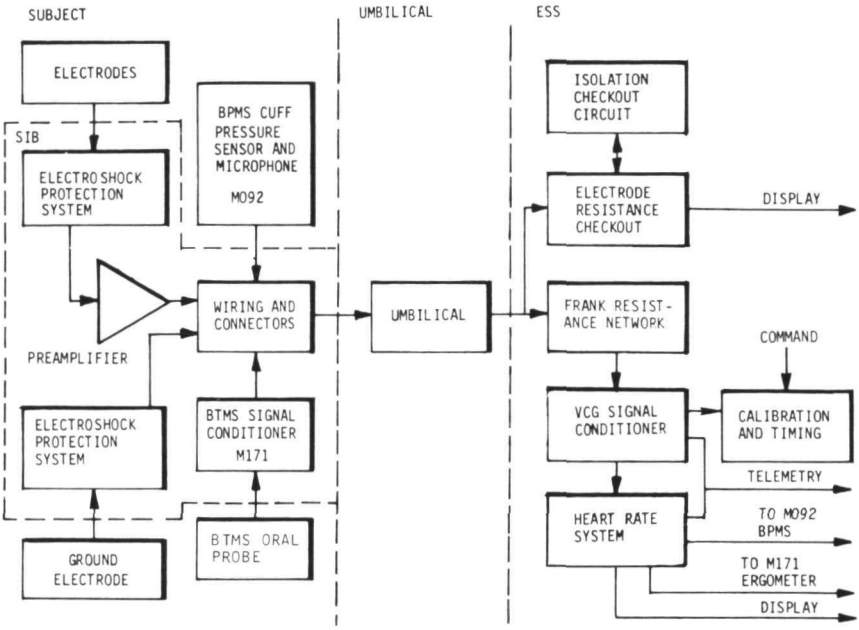

FIGURE 13.–VCG interface block diagram.

(1) Frank VCG resistor network–serves to normalize ECG signals taken on the body into the three orthogonal ECG signals required for VCG analysis
(2) ECG signal conditioner–filters and amplifies the three channels from the VCG resistor network for recording and telemetry
(3) Electrode checkout device–permits measurement of the contact resistance between each electrode and the skin
(4) Heart rate system–measures the average heart rate for each heartbeat period. (Input can be from any one of the three VCG outputs or from the operational bioinstrumentation system ECG output; heart rate is displayed on the ESS panel and transmitted via telemetry.)

Electrodes

The electrodes are sensors that detect the electrical potential at the body's surface. There are eight electrodes including the reference electrode. Electrode positions are shown in figure 14.

Umbilical

From the preamplifiers, the signals are carried to the VCG electronics module by the umbilical, which interconnects the SIB with the ESS.

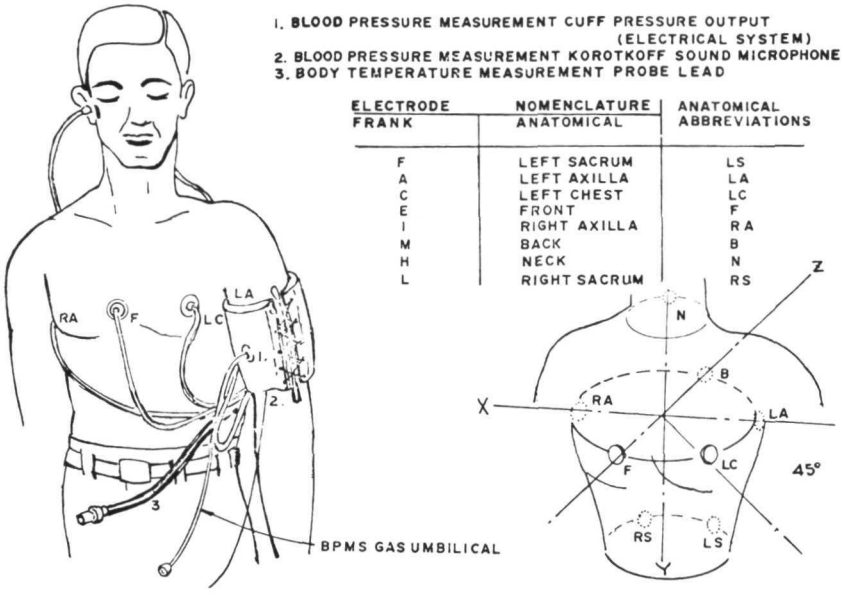

FIGURE 14.–VCG electrode positions.

Metabolic Analyzer

The metabolic analyzer (MA) is an electromechanical device that measures as well as analyzes inhaled and exhaled air. The MA measures the metabolic rate (oxygen consumption, carbon dioxide production, respiration volume per minute, and respiratory quotient) of the subject while resting and during calibrated exercise. Data are presented as a display on the electronic panel. Data are also provided to the ESS panel secondary display and to telemetry.

Mechanical Process

Inhaled air is measured by the inspiration spirometer; exhaled air by the expiration spirometer. As the expiration spirometer is vented, the discharging gas is sampled by the mass spectrometer and the content is analyzed. To calibrate the equipment, a known mixture of gas is introduced into the mass spectrometer.

Electronics

The MA electronic system processes inputs from the mass spectrometer and the MA mechanical system and provides data for display or telemetry. Input signals include partial pressures of oxygen, nitrogen, carbon dioxide, and water from the mass spectrometer and position potentiometer limit switch. Pressure

and temperature transducer signals come from each of the two spirometers. Output signals include oxygen consumed, respiratory quotient, carbon dioxide produced, minute volume, vital capacity, and solenoid drive signals to the valves of the mechanical system.

Mass Spectrometer

The mass spectrometer is a self-contained portion of the MA that measures the partial pressures of water vapor, nitrogen, oxygen, and carbon dioxide in the sample air. It consists of the control circuitry vacuum envelope that encloses the ion source, the magnetic sector, and the ion pump. The control circuitry includes the various power supplies, amplifiers, and control circuitry required for mass spectrometer operation.

Application Areas

The total system is designed to collect data pertaining to the physiological functioning of healthy individuals (astronauts) in two environments: namely, at 1*g* under standard atmospheric conditions and at zero gravity under 3.04 N/cm^2 (5 psi) pure oxygen conditions.

These data are valuable both in medicine and human factors engineering because they help describe the range of "normal" physiological functioning. Most of the clinical data available in the past have been collected from the unhealthy segment of the population. Therefore, little has been known about the undefined area separating abnormal body functioning from that previously defined as "normal." If studies were conducted to refine these data, they would be valuable to both physicians and psychologists. The refined data would allow more realistic interpretations of clinical test results as well as laboratory reports.

The transferable products of this program are—

(1) Baseline data pertaining to the normal range of body functioning to be used by physicians, laboratory (clinical) technicians, and psychologists
(2) A mobile van to allow rapid medical screening of many people who could not normally afford such a diagnostic program (The total system could be computer augmented for operation by technicians and could be used as a referral service for those exhibiting questionable physiological profiles.)
(3) Data for human factors engineering professionals to develop more refined life-support systems
(4) Test equipment used to assess the physical condition of patients confined to bed for long periods of time

The basic drawback to the indicated transfer is the amount of data that must be collected to establish the range of normal physiological functioning. The hardware and techniques were developed for space use because no good data existed for either orbit or Earth. The data gathered from the space study define the body functioning of a small and very special population in space. Most of the data are not transferrable to an Earth population.

CHAPTER 3

Display Techniques

Transferable techniques and products pertaining to flight simulators, aircraft, and display development include a synthetic display technique for computer-controlled simulator and airborne displays developed by Jack J. Hatfield of NASA Langley Research Center (ref. 5). It consists of individual elements of instrumentation that are simulated in the cockpit using a programable electronic display system. The synthetic display concept is based upon an electronic animation technique that allows the cockpit display designer to proceed directly from static (cardboard) instrument mockups to operational displays simulated in the cockpit by high resolution closed-circuit black-and-white television.

SYNTHETIC DISPLAY CONCEPT

Figure 15 is a conceptual system diagram showing the components required to produce an electronic animation display. The dynamic pattern store, which holds the animation characters, is searched by a random access flying spot film scanner. This scanner is, in turn, monitored by a video pickup device that transfers the animation characters to a video mixer via a scan converter. A random access slide projector provides a static pattern store, which is also fed into the video mixer.

A stored program control system accepts flight dynamics inputs and programed instructions. It then determines how data are retrieved from the two storage data banks. The output from the video mixer goes to a 1203-line, 60-field, two-to-one interlace television display.

The synthetic display technique can be used to program a portion of a display rapidly and to present it via closed-circuit television. In addition, the system can be used as a man/machine communication research tool for a systems engineering approach to flight display panel design. This technique is transferable to displays associated with ships, automobiles, trucks, buses, trains, boats, airplanes, and helicopters. It could be used also in any closed-circuit television programed for instructional, advertising, or recreational purposes.

At this stage of development of the electronic animation technique, resolution in the static portions of displays is quite good, but resolution in the dynamic portions of displays requires some improvement. Some distortion is produced in dynamic portions by digital noise and a skewing of dynamic pickup rasters (pattern of scanning lines). Some flicker also has been evident in

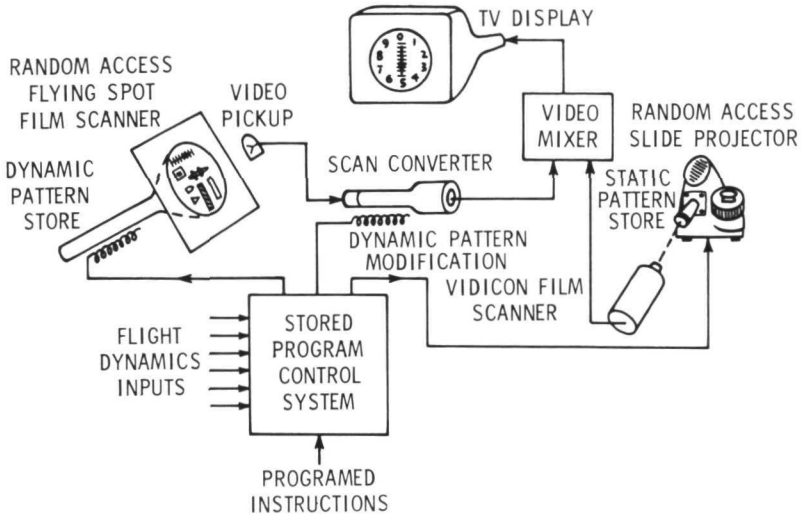

FIGURE 15.–Conceptual system diagram for electronic animation (Television display: 1203 lines, 60 fields, and two-to-one interlace.)

dynamic portions of the synthesized display because a two-tube scan conversion system is used; however, this flicker has been eliminated now through the use of a cathode ray tube to TV camera scan conversion technique. These limitations are being minimized and capabilities have been incorporated for the synthesis of digital displays and displays having rotational dynamics.

When this survey was prepared, the animation functions available for synthetic display generation were translational, rotational, and oscilloscope mode dynamics. However, additional animation functions were being incorporated.

The bar, pointer, and tape, three types of vertical indicators that have been synthetically generated using translational electronic animation dynamics, are shown in figures 16, 17, and 18, respectively. These displays were photographed directly from a display system monitor. They show the static and dynamic portions of the composite display as well as the composite display produced by the video mixing of the static and dynamic pattern mockup. Three static pattern mockups and one dynamic pattern mockup are shown in figure 19. The displays in figures 16 through 19 are fully animated with no ambiguities or discontinuities. For instance, in the three-window vertical tape display (fig. 18), the static pattern is a window with a lubber line (reference mark). The dynamic pattern is a vertically oriented tape that appears to move up or down within the confines of the window according to the dynamics of a flight control parameter. Short-term stability (over a 1-hr period) for the dynamic elements of typical displays, such as those shown in figures 16 through 18, is such that changes in position are less than 0.5 percent of full-scale value.

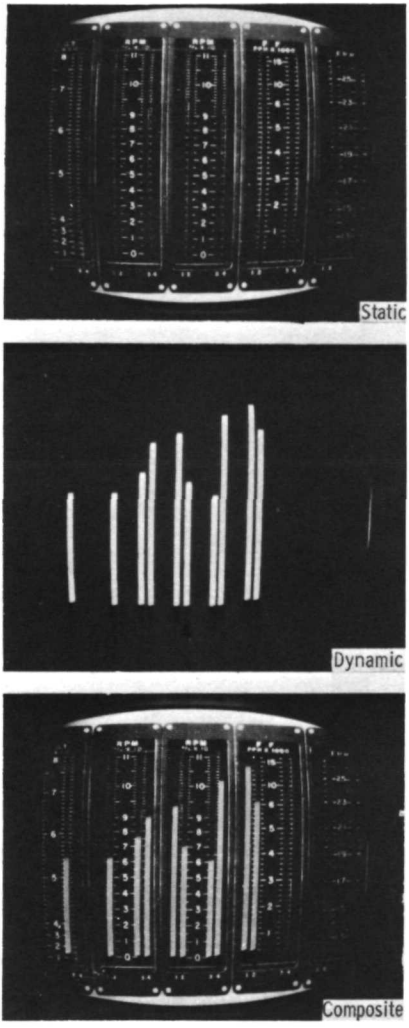

FIGURE 16.–Vertical bar indicator display.

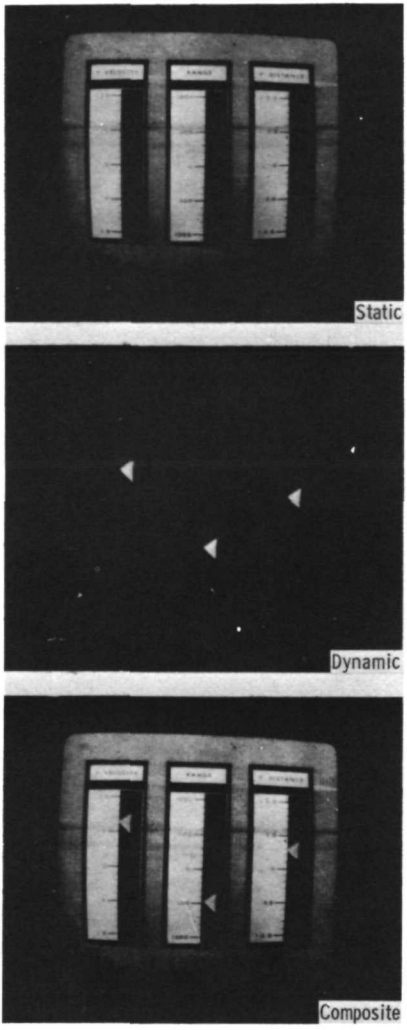

FIGURE 17.–Vertical pointer indicator display.

System performance in the area of programing complexity is indicated by the program length, or number of digital words, required for the generation of specific displays. For those displays shown in figures 16 through 18, the program lengths are 36, 18, and 18 digital words, respectively. These program lengths are shorter than those required with conventional computer cathode ray tube stylized displays; specifically, more than a factor of 10 shorter in the instance of the vertical tape display. The shorter program length of many displays will ease the burden on the programer.

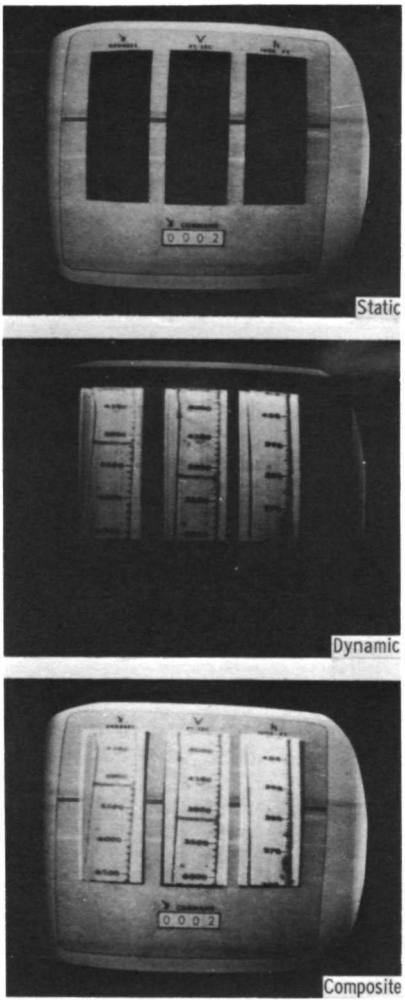

FIGURE 18.–Vertical tape indicator display.

Figure 20 illustrates simulator signal flow while figure 21 portrays the display synthesis principle of electronic animation. Four closed-circuit television display techniques are shown in figure 22.

TELEVISED GRAPHIC DISPLAYS FOR STEEP APPROACHES TO LANDING

Techniques developed by Henry C. Elkins and Jack J. Hatfield of NASA Langley Research Center (ref. 6) for an integrated flight display system can be used to study problems associated with flying steeper than normal Instrument

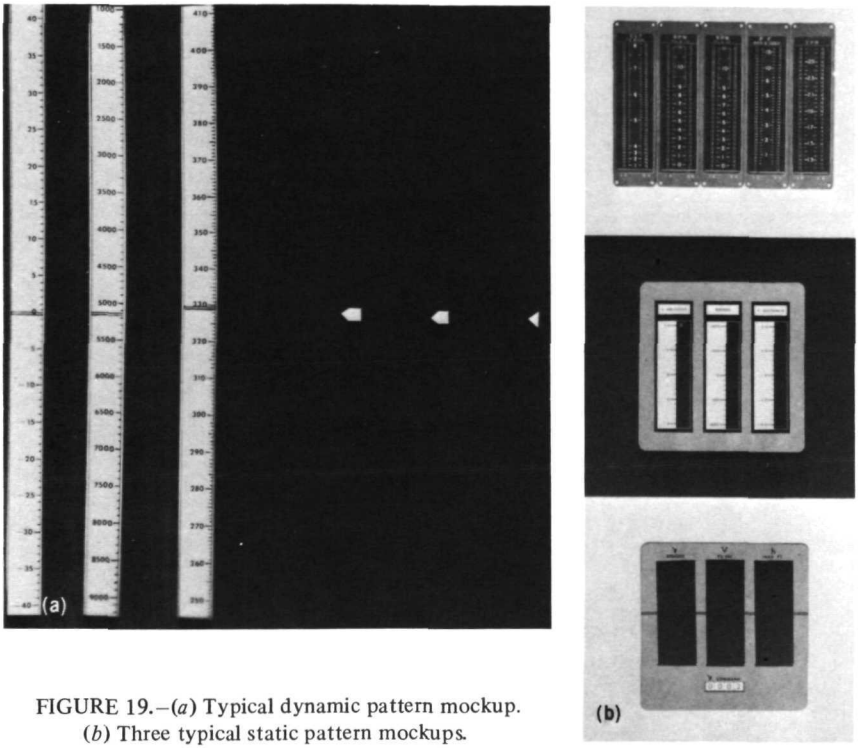

FIGURE 19.–(*a*) Typical dynamic pattern mockup. (*b*) Three typical static pattern mockups.

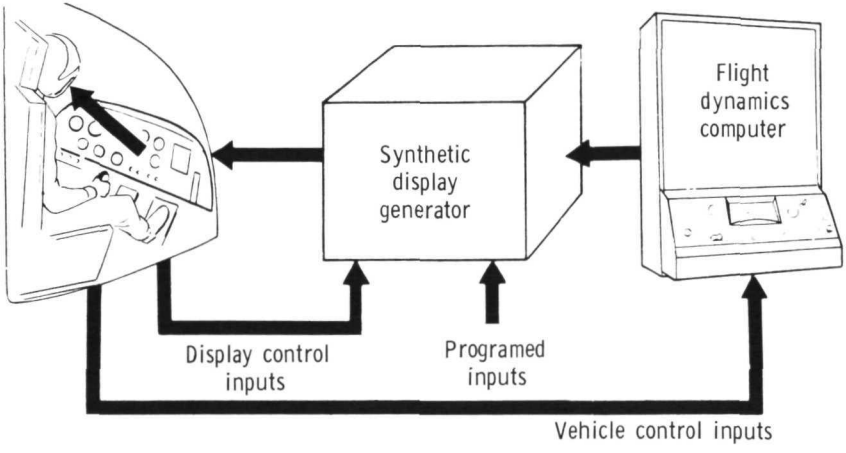

FIGURE 20.–Pictorial diagram showing simulator signal flow using programed synthetic display generation.

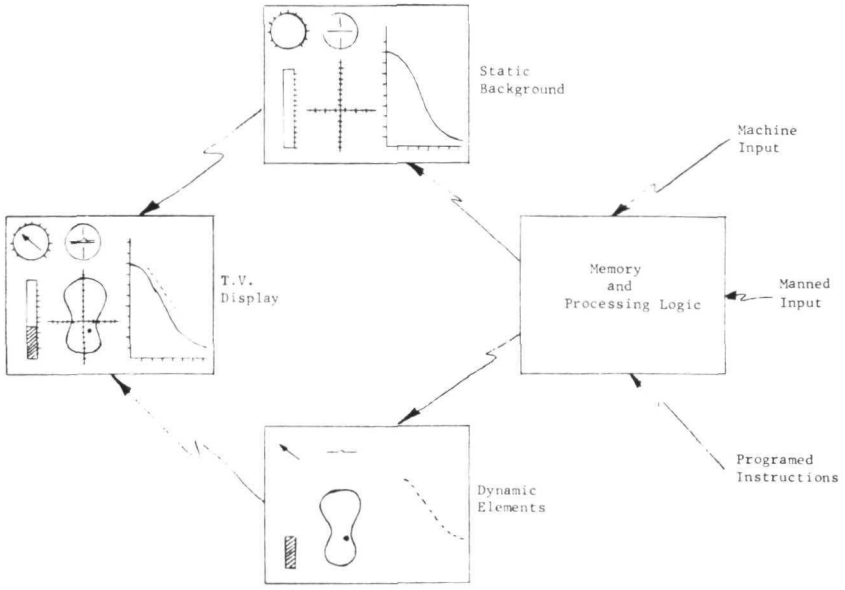

FIGURE 21.–Display synthesis principle of electronic animation.

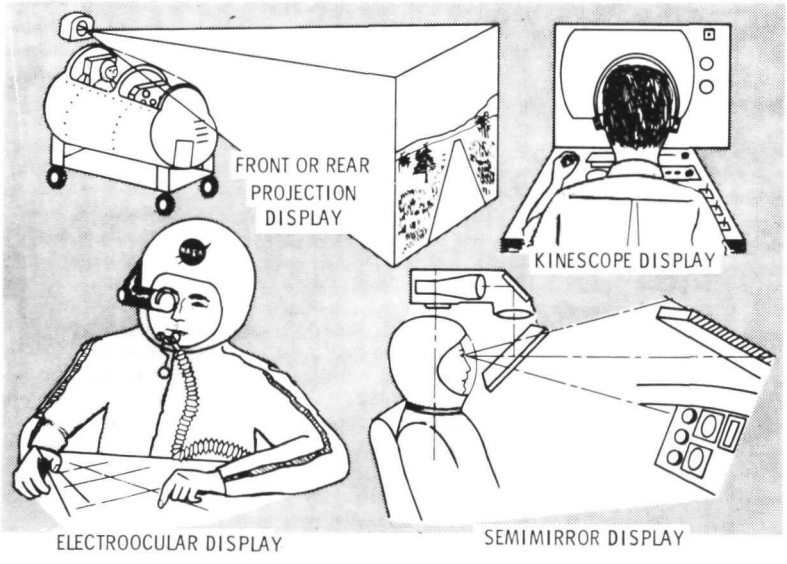

FIGURE 22.–Closed-circuit television display techniques.

Flight Rule landing approaches. Such approaches reduce engine noise encountered along the ground track.

The graphic situation display concept presents information in the form of an "outside-in" profile view of the fixed flightpath and a dynamic aircraft

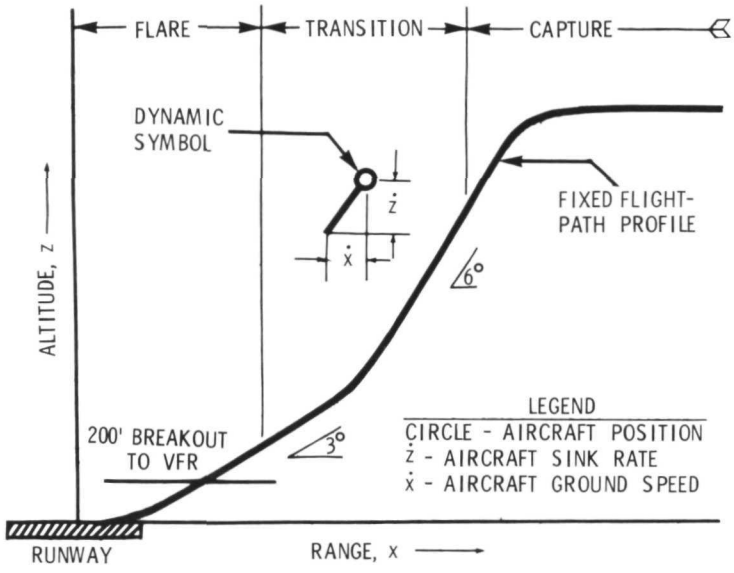

FIGURE 23.–Graphic situation display concept.

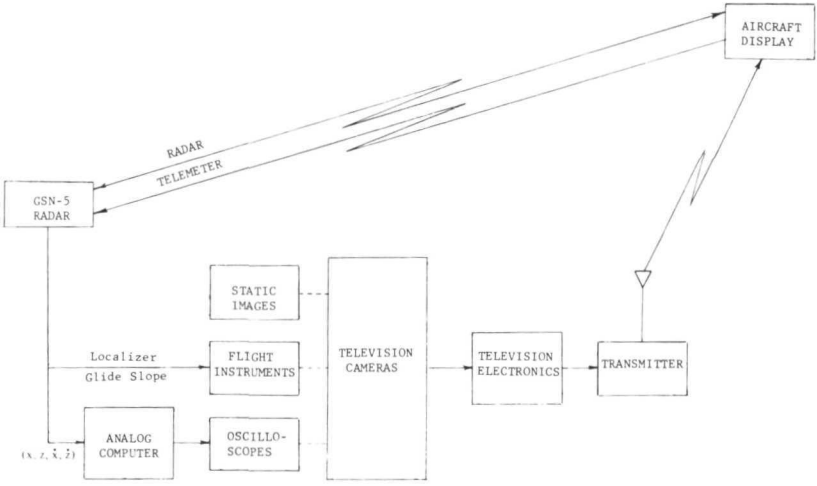

FIGURE 24.–Conceptual display system diagram.

symbol with attached velocity vector. This concept is illustrated in figure 23. The position of the aircraft symbol provides an indication of flightpath deviation, altitude, and range to touchdown. The aircraft velocity vector provides lead guidance information for control of thrust and pitch.

Figure 24 is the conceptual display system diagram. This system is made up of a precision ground-based landing radar, a flexible ground-based television

subsystem, and interchangeable airborne receiver-monitors. Such a system provides several advantages. There are few restrictions on display content, and display format can be changed rapidly. Additionally, the airborne portion of the system is compact, light, easily installed, and inexpensive. It can be operated on board many types of aircraft.

This display system is designed with compatible building blocks and a signal-patching capability. Figure 24 illustrates the basic system operation and shows the origin of the aircraft position (x, z) and velocity $(\dot{x}, \dot{z})$ data, as well as localizer and guide slope deviation information derived by the precision landing radar. Symbols, which are functions of the radar source, are generated on storage and/or nonstorage oscilloscopes by an analog computer. Graphic images, which describe the desired flightpath, are generated by back-lighted photographic transparencies. Television cameras, which view these static and dynamic scenes, convert the image into a 525-line, 60-field, two-to-one interlace television signal for using video insert keying, wiping, additive, and/or nonadditive mixing techniques. The composite video signal is monitored and transmitted to the aircraft for display.

Initial flight tests were made with a two-engine, propeller-driven Aero Commander aircraft with a 6°/3° glide slope. The graphic display technique was supplemented by standard aircraft instrumentation. Pilot performance was

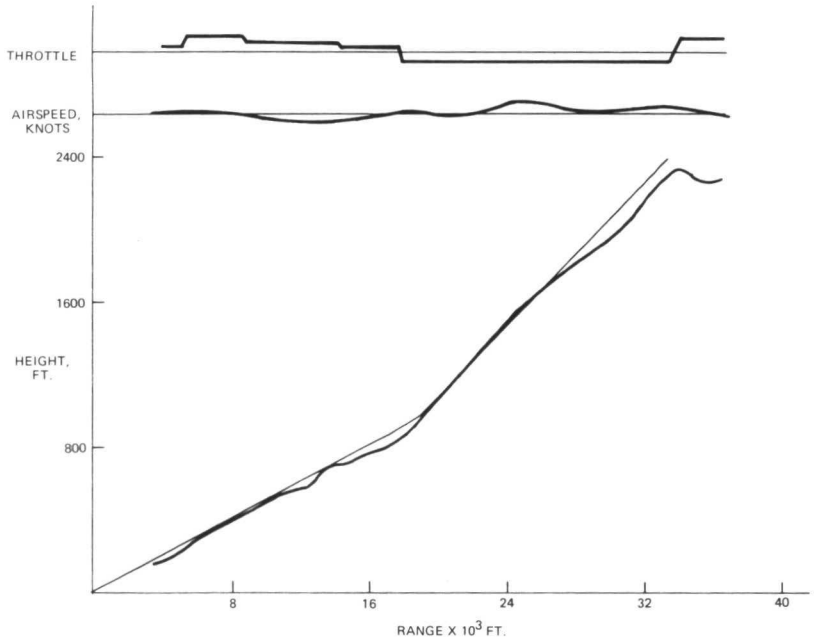

FIGURE 25.–Typical landing approach using CDI display.

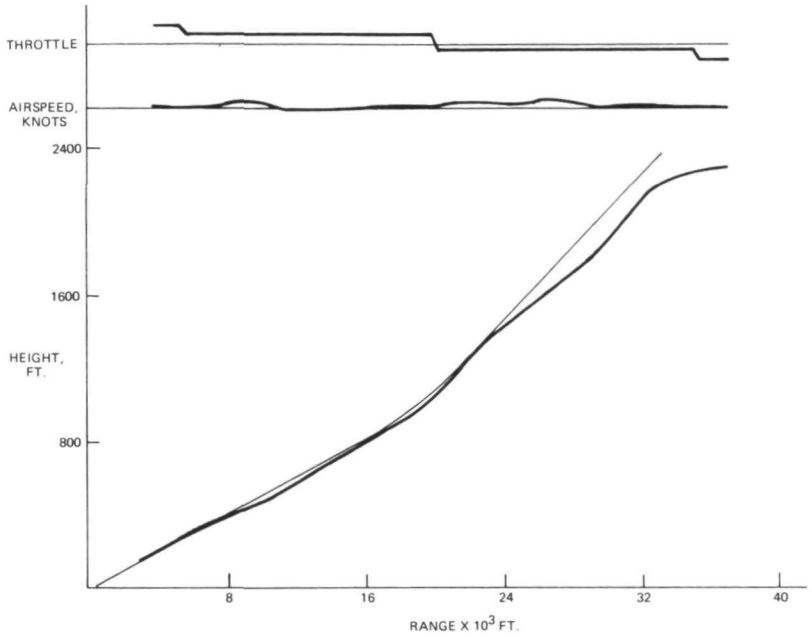

FIGURE 26.–Typical landing approach using graphic display.

tested with a conventional course deviation indicator (CDI) display and compared with the graphic display. Both displays were televised so that they would appear in the same position in the pilot's scan pattern.

The graphic display consists of a 6°/3° profile segmented into capture, transition, and flare segments. It also is stacked vertically for simultaneous display so as to present range-to-go information and aid in scale transitions.

Flight results are presented in the form of kinescope display recordings and vertical profile recordings of 6°/3° approaches. Figures 25 and 26 show typical recordings of flightpath throttle settings and airspeed for approaches with the CDI and graphic displays, respectively.

Application Areas

The graphic display technique can be used in any aviation (civil or military) situation which requires steep (6° or greater) instrument approach profiles. The steeper approach angles could be used in jet noise abatement programs for existing aircraft and future vertical/short takeoff and landing aircraft. The necessary retrofitting of existing ground and aircraft avionic systems, however, would increase operating costs.

Underwater Work

This chapter describes methods that may be used to facilitate human performance in the water. The General Electric Company performed the work described first for the NASA Marshall Space Flight Center (ref. 7) to define techniques and problem areas associated with performing work (maintenance) in a frictionless zero-gravity environment.

RESTRAINTS FOR FORCE APPLICATION

Restraints were varied and accessibility was altered by changing the location and orientation of the force receiver with respect to the subject. The types of restraints applied were—

(1) None
(2) Hand
(3) Waist
(4) Gemini Dutch shoe
(5) Hand and waist
(6) Hand and shoe
(7) Waist and shoe
(8) Hand, waist, and shoe

The test setup is shown in figure 27 and the force-measuring equipment is illustrated in figure 28. The following seven variables were manipulated:

(1) Type of restraint system (eight types)
(2) Receiver angle (15° left, straight ahead, and 45° right)
(3) Receiver distance from a shoulder reference point (38, 48, and 61 cm (15, 19, and 24 in.))
(4) Receiver orientation (local horizontal, 0°, and local vertical, 90°)
(5) Force direction (push/pull, left/right, up/down)
(6) Force type (impulse (1-sec interval) and sustained (4-sec interval))
(7) Suit pressurization method (air or water)

The following conclusions were drawn from these studies:

(1) The hand and shoe restraint combination resulted in the greatest up/down and left/right sustained and impulsive force generating capability.
(2) The hand, waist, and shoe restraint combination and the waist and

550-754 O - 74 - 4

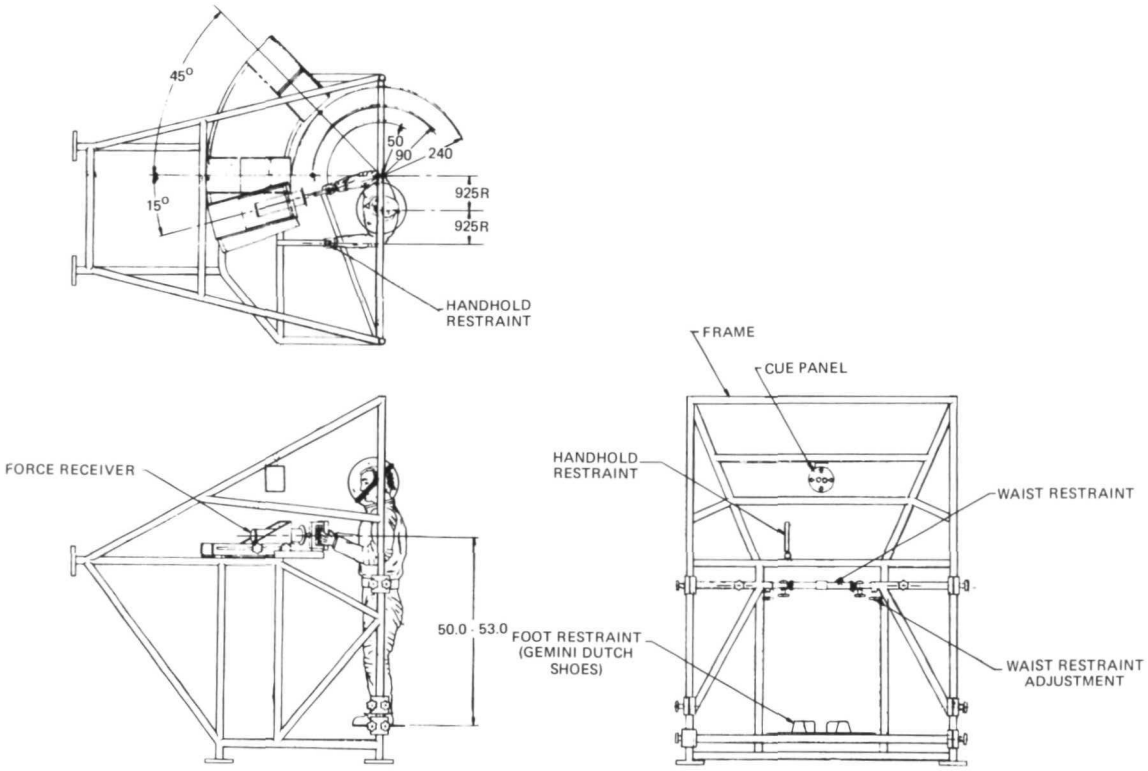

FIGURE 27.–Setup to measure application of force.

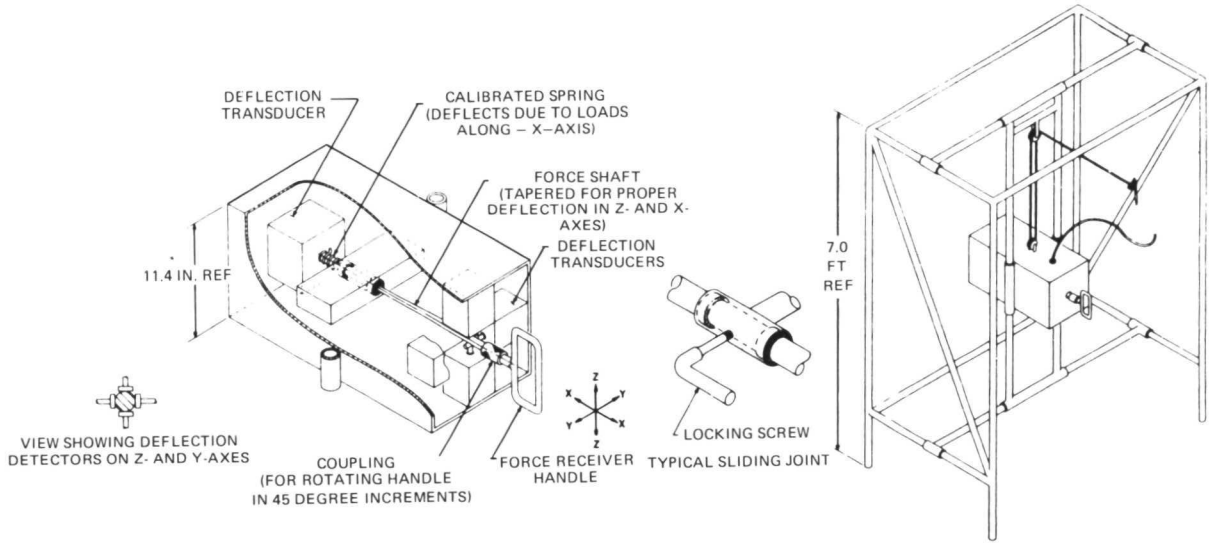

FIGURE 28.–Force measuring equipment.

shoe restraint combination resulted in the greatest push/pull sustained forces.

(3) The waist restraint was the only single-point restraint in which a significant sustained mean push/pull force (above 4.5 kg (10 lb)) could be exerted.

(4) The hand restraint provided the capability for sustaining significant mean forces (above 4.5 kg (10 lb)) in only the left/right directions.

(5) The shoe restraint provided the capability for sustaining significant mean forces (above 4.5 kg (10 lb)) in only the up/down directions.

(6) The mean capability to exert impulsive forces in a no-restraint condition did not differ greatly (1.8 to 6.4 kg (4 to 14 lb) differential range) from the mean capability provided by the single-point restraints (hand, waist, and shoe).

(7) The mean capability to exert impulsive forces did not differ greatly (2.3 to 5.4 kg (5 to 12 lb) differential range) across the multiple-restraint conditions (hand and waist; hand and shoe; waist and shoe; and hand, waist, and shoe).

The capabilities for exerting forces as functions of type of restraint are presented in tables 3 and 4. The data in these tables can be used to design tasks for underwater work when man is the primary source of mechanical power and is not aided by hand tools. The constraints on this application derive from the specifics of the experiment, including limitations in measurements and environment. The tasks must all be accomplished with one hand for these data to apply. If two hands are used, the sustained force would be much higher relative to the impulse force. The subjects were working in relatively warm water. Work in the oceans, except in certain equatorial areas in the Pacific and the Caribbean area in the Atlantic, would be in much colder water; therefore, it is likely that the capability for exerting force would be greatly reduced. It is probable that the Gemini-type suit worn by the subjects restricted their action and that the conventional wetsuit would permit greater force to be exerted. Despite these constraints, these data represent a lower limit of man's capability to exert one-hand force under restraint conditions. Perhaps the best way to view these data are in terms of the relative effectiveness of the different types of constraints.

WATER-COOLED/HEATED SUIT

Webb Associates developed water-cooled/heated spacesuits to cool astronauts during extravehicular activity (EVA) (refs. 8 and 9). The garment consists of a network of small plastic tubes (Tygon vinyl plastic 0.32-cm (1/8-in.) outer diameter by 0.16-cm (1/16-in.) inner diameter). Parallel lines of tubing are joined approximately every 5 cm (2 in.) by small plastic loops so that when the garment is donned, diamond-shaped openings (measuring roughly 5 cm (2 in.) long by 2.5 cm (1 in.) wide) cover the body, as shown in figure 29 (*a*). The tubing closely follows the contours of the arms, legs, and the

TABLE 3.–*Impulse Force as a Function of Force Direction and Type of Restraint*

Restraint	Force, lb					
	Push	Pull	Up	Down	Right	Left
None	35.4	43.2	19.3	22.5	17.5	18.2
Hand	40.9	43.2	21.3	25.8	22.2	29.0
Waist	43.3	46.0	22.7	22.8	21.8	22.2
Shoe	45.8	47.6	27.8	32.7	22.1	23.0
Hand and waist	56.6	50.7	23.3	26.0	25.4	28.0
Hand and shoe	62.4	61.3	30.6	36.6	28.2	34.3
Waist and shoe	58.5	56.8	27.6	30.4	22.8	25.4
Hand, waist, and shoe	69.2	60.9	28.8	32.1	26.7	29.9

TABLE 4.–*Sustained Force as a Function of Force Direction and Type of Restraint*

Restraint	Force, lb					
	Push	Pull	Up	Down	Right	Left
None	0.0	0.2	0.5	1.6	0.1	0.1
Hand	1.3	2.1	4.8	8.6	10.5	16.6
Waist	14.6	22.3	10.4	10.4	12.3	12.1
Shoe	4.1	4.3	17.5	20.8	9.4	8.4
Hand and waist	29.2	30.6	13.6	15.8	15.3	17.4
Hand and shoe	29.7	33.0	18.0	25.6	16.3	20.6
Waist and shoe	35.5	36.5	17.2	19.3	13.6	14.8
Hand, waist, and shoe	42.5	37.6	17.0	21.6	16.1	19.3

trunk. This garment fits almost all body types, and the plastic tubes lie firmly against the skin even when the wearer is active, changing his body contours and angles.

There are five segments to the garment, one for each arm and leg and the adjoining quadrant of the trunk, and one to cover the head and neck. These segments can be seen in figure 29(*b*). All tubes in each segment originate in manifolds that are brought together to form a common inlet. Similarly, all tubes in each segment end in outlet manifolds joined together in a common outlet. The wearer can proportion the total flow by adjusting pinch clamps on each of the five inlet manifolds.

The astronauts' hands, feet, and face, which represent approximately 12 percent of the body surface, were not cooled. The contact area of the cooling

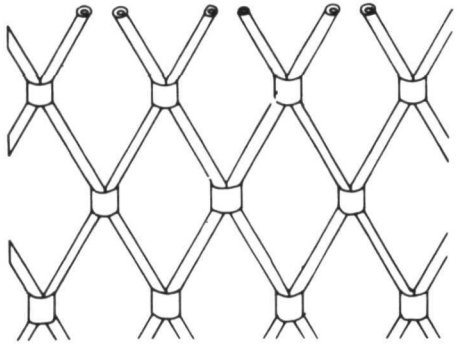

(a)

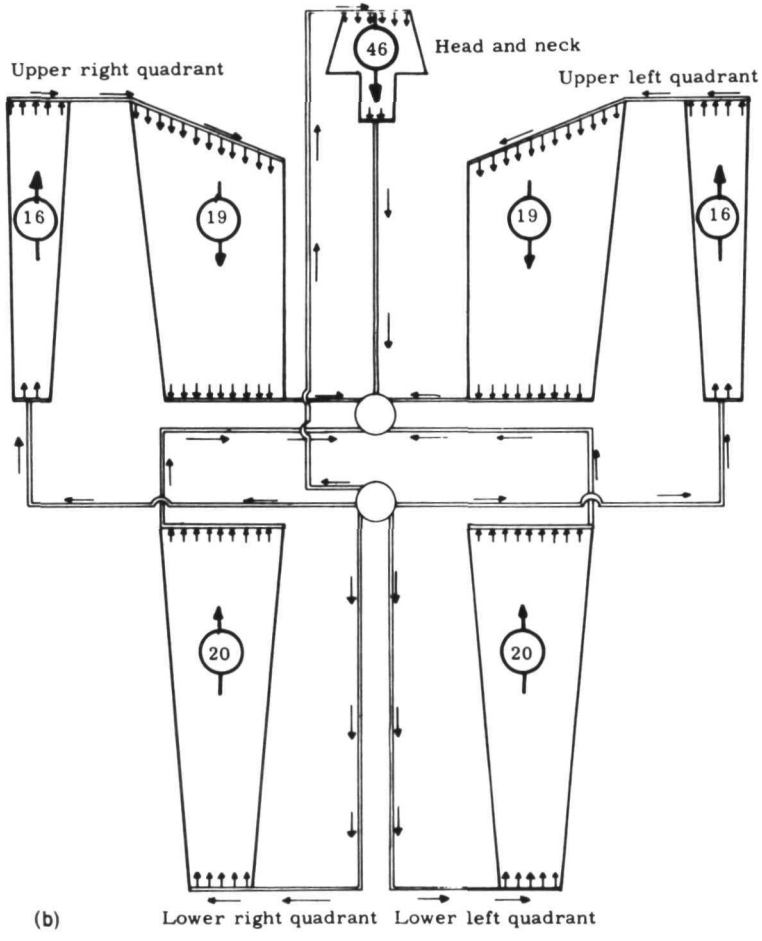

(b)

FIGURE 29.–EVA suit water-cooling tubes. (*a*) Diamond pattern of parallel tubes. (*b*) Schematic of water flow through the water-cooling garment, showing direction of flow and number of tubes in each area.

tubes slightly exceeds 4000 cm^2, representing 22 percent of the surface of a man whose total surface area is 1.8 m^2.

The insulating suit of the next layer is a heavy nylon coverall with flocced-nylon insulating liner resulting in a garment thickness of approximately 0.64 cm (1/4 in.). An air distribution network is located on the innermost surface. It consists of 26 tubes covering the trunk, arms, and legs. Air is delivered to these tubes at a single fitting in the back. It escapes from numerous small holes located along the inner face of each tube and against the skin, which is covered only by the open diamond mesh of the water-cooled undergarment. Figure 30 shows the layers of the clothing assembly.

The next layer is a coverall of 0.051-cm (0.020-in.) vinyl plastic covering the arms, legs, feet, and torso up to the neck. This coverall has a gas-tight zipper along the length of the back.

The hands are covered by plastic-coated fabric gloves and are partially cooled by a loop of the inlet manifold tubing.

The head is covered by a 0.64-cm (1/4-in.) thick neoprene foam skin-diver's helmet, which leaves part of the face exposed.

The outer insulating layer is a jacket and trousers of 0.48-cm (3/16-in.)

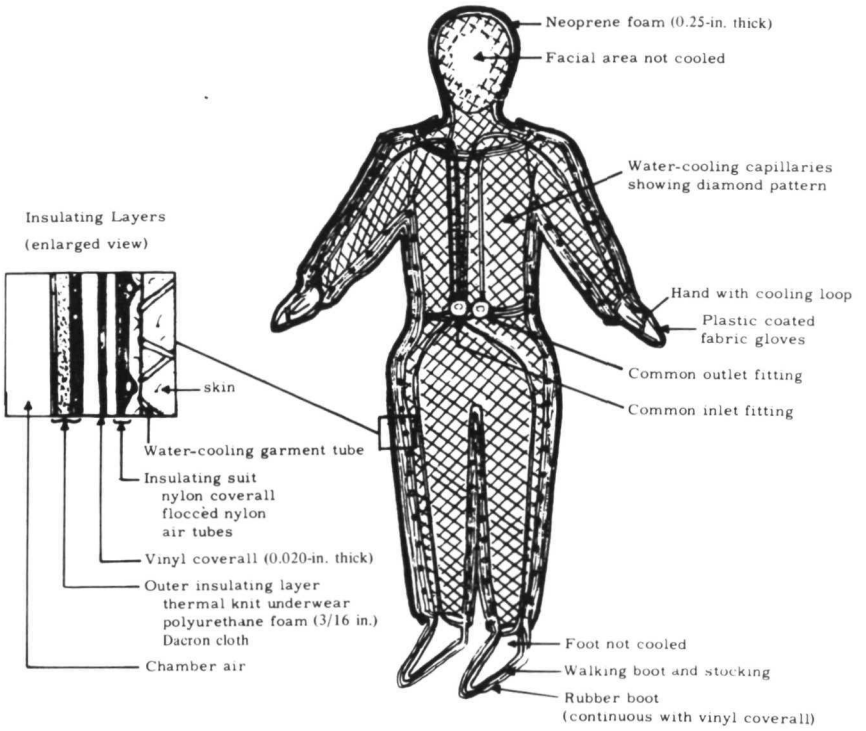

FIGURE 30.–Diagram of clothing layers in the clothing assembly.

polyurethane foam covered on the inside with thermal knit underwear cloth and on the outside with Dacron cloth.

Figure 31 is a typical plot of rectal temperature, skin temperature, body temperature, oxygen consumption, and heat loss during the astronauts' EVA period. The relationships among oxygen consumption, heat production, and heat loss to the water are shown in the figure.

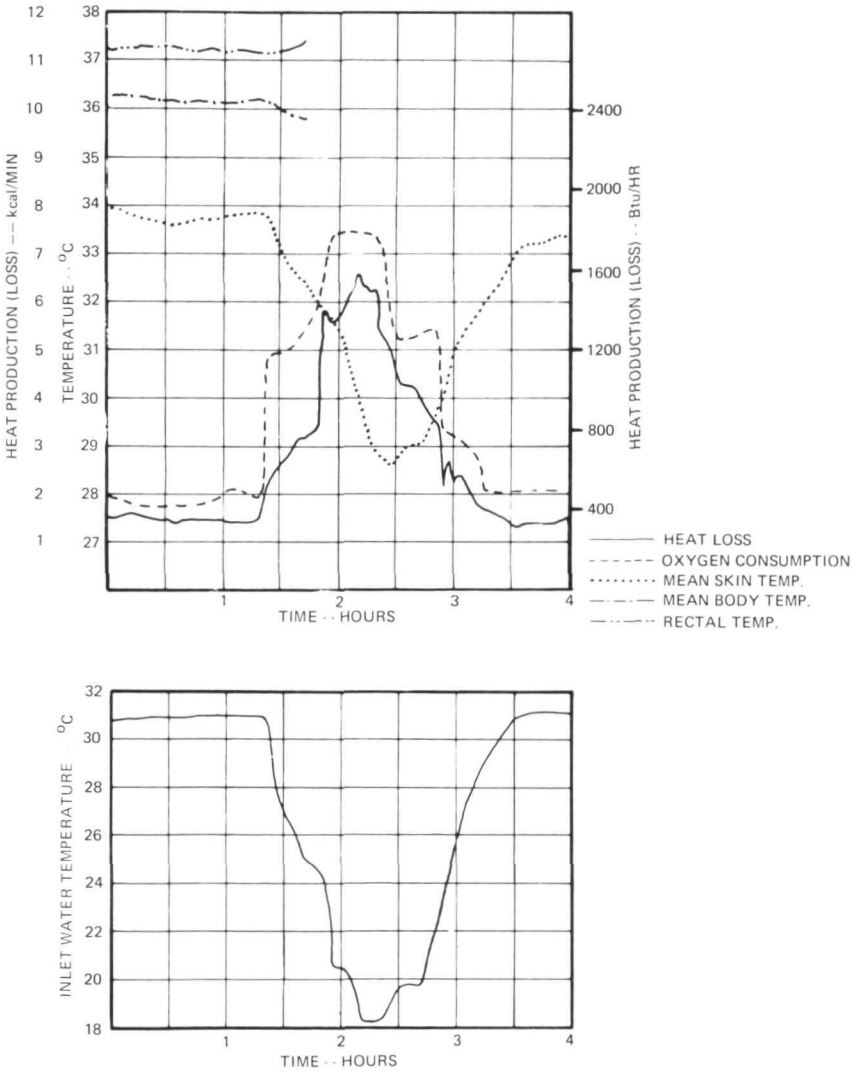

FIGURE 31.–Heat loss during an EVA.

Application Areas

The existing concept can be used whenever man must work for long periods of time in an environment tending to create extreme body temperatures. The length of time he could remain in this situation is a function of the rate of body temperature change. Rescue operations in a mine and underwater work are two opposite extremes. In the former, there could be a rapid accumulation of heat, which, if removed, could result in longer periods of rescue effort. Working underwater results in the loss of heat and the reduction of body temperature. Conventional wetsuits limit work times in cold water to a matter of minutes.

Specific constraints on applications would be a function of the particular application. Properties of the environment will dictate the nature of additional items required, such as protective materials. The main constraint will be the umbilical cord required to supply cool or warm fluids to the suit and to carry used fluids away.

The Suit Control

The control concept as defined by the following equation constitutes the model controller:

$$T_{wi} = T_{wi_0} - \frac{\alpha}{\dot{m}c} H_0 - B(\overline{T}_s - \overline{T}_{s_0}) - \frac{\alpha}{\dot{m}c} H \qquad (2)$$

where

T_{wi} = inlet water temperature
T_{wi_0} = initial resting inlet water temperature
α = proportionality constant for H
H = heat removal rate for any given activity level $= -\tau\dot{H} + \phi$ (RM $+ M$)
τ = the time constant of the response of H
ϕ = the proportionality constant relating H and M
M = resting metabolic rate
RM = the resting heat production rate (resting metabolic rate)
$\dot{m}c$ = mass conductivity of the coolant
H_0 = heat removal rate at rest
B = proportionality constant for $\overline{T}_s$
$\overline{T}_s$ = mean skin temperature for any given activity level
$\overline{T}_{s_0}$ = resting mean skin temperature

The performance characteristics of the suit used to effect cooling had to be known for magnitude scaling of the initial mathematical statement (eq. (2)) so

that the controller could correctly predict T_{wi}. Values for α and B in equation (2) were calculated for the suit to be used. In addition, it was necessary to scale the controller inputs and outputs to be compatible with the voltage control range of the cooler. This scaled expression is given in equation (3):

$$\frac{T_{wi}}{5} = \frac{T_{wi_0}}{5} - \frac{\alpha}{5\dot{m}c}(H - H_0) - \frac{B}{5}(\overline{T}_{cs} - \overline{T}_{cs_0}) \qquad (3)$$

where:

$\overline{T}_{cs}$ = the average of the control skin temperatures

$\overline{T}_{cs_0}$ = the initial average of the control skin temperatures

α = 6.00

B = 0.72

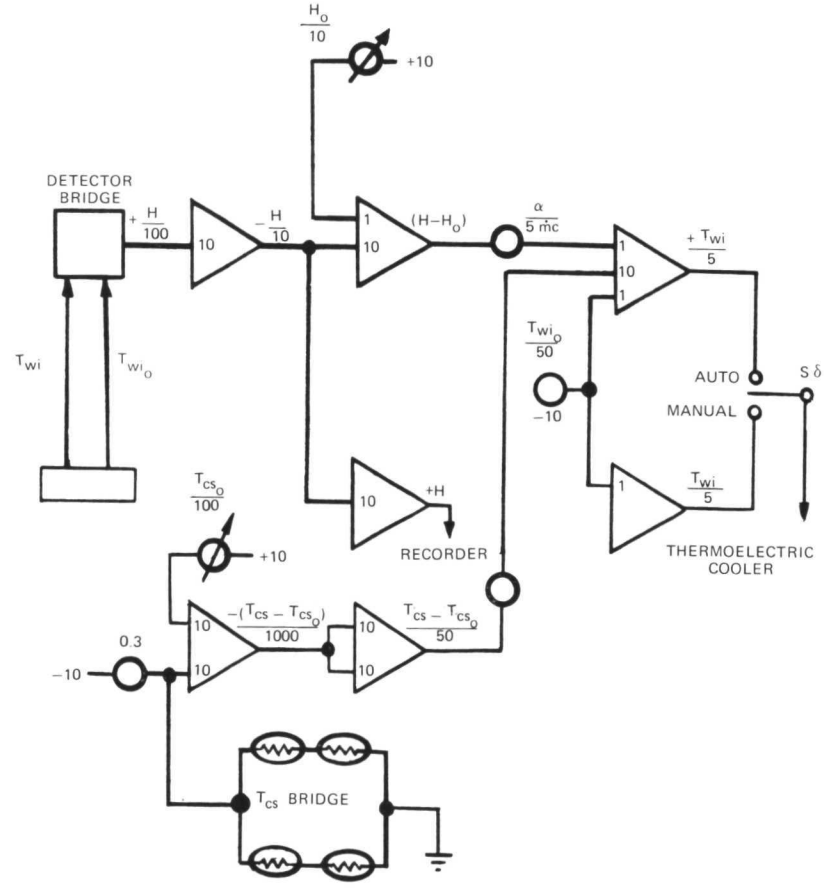

FIGURE 32.–Diagram of ΔT controller.

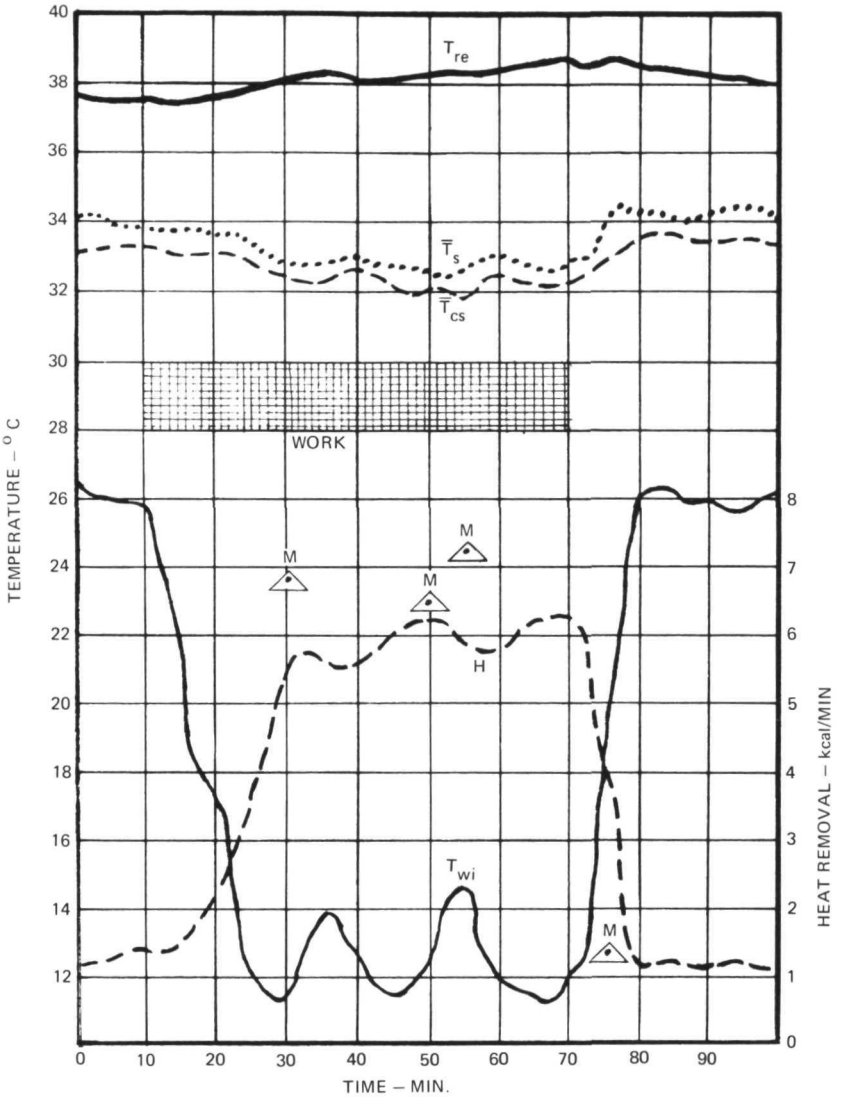

FIGURE 33.–Typical response curves showing relationships among rectal temperature, skin temperature, metabolic rate, heart removal rate, and inlet water temperature.

Figure 32 is a block diagram of the controller equation. Figure 33 is a typical curve showing the relationships among rectal temperature T_{re}, average skin temperature $\overline{T}_s$, average of four control skin temperatures $\overline{T}_{cs}$, measured metabolic rate M, heat removal rate H, and inlet water temperature T_{wi}. The inlet water temperature varies inversely with the generation of heat, which is removed in the water.

CHAPTER 5

Vibration and Impact Research

This chapter describes four techniques that can be used to study the effects of vibrations on human performance.

LANGLEY RESEARCH CENTER COMPLEX COORDINATOR

The Langley Research Center complex coordinator (LRCC) was refined from test equipment first designed at the University of California in 1939 and later designed by the Federal Aviation Agency in 1962. The studies using the LRCC were conducted at the Langley Research Center (ref. 10) to provide an integrated test of signal detection, problem solution, decision, and appropriate motor reaction.

The LRCC is designed to measure human performance. It requires continuous response from both arms and both legs. In addition, the LRCC permits quantitative evaluation of a subject's performance prior to, during, and following normal and programed abnormal conditions. The system consists of an operator's control console, event recorder, subject's display panel and limb controls, and associated cabling. Figure 34 shows the subject's display panel and limb controls, the operator's control console, and the event recorder.

A problem is generated by the programer and appears on the subject's display panel as a series of lights. During a test, manipulation of the limb controls activates the corresponding lights when a problem has been answered correctly. This test and others are described in detail in the section on the subject's display panel and limb controls. The movement of the limb controls is timed and counted by various devices, displayed on the operator's control console, and permanently recorded on the event recorder.

The LRCC can be described as a self-paced, serial reaction, complex coordinator, psychomotor performance test. It is presented to a subject seated in a chair with a display panel set before him. The subject's display panel contains 45 lights, an interval timer, and two red lights that are activated by the interval timer. There are four limb controls for the subject, one for each hand and foot. Each limb control activates any of five lights on the subject's display panel to answer the problem presented.

An operator's control console contains an electromechanical programer, relays, switches, counters, and chronoscopes. From this console, the operator programs and administers the test. An event recorder provides a record of time spent to complete each problem plus each set of problems, and of the number

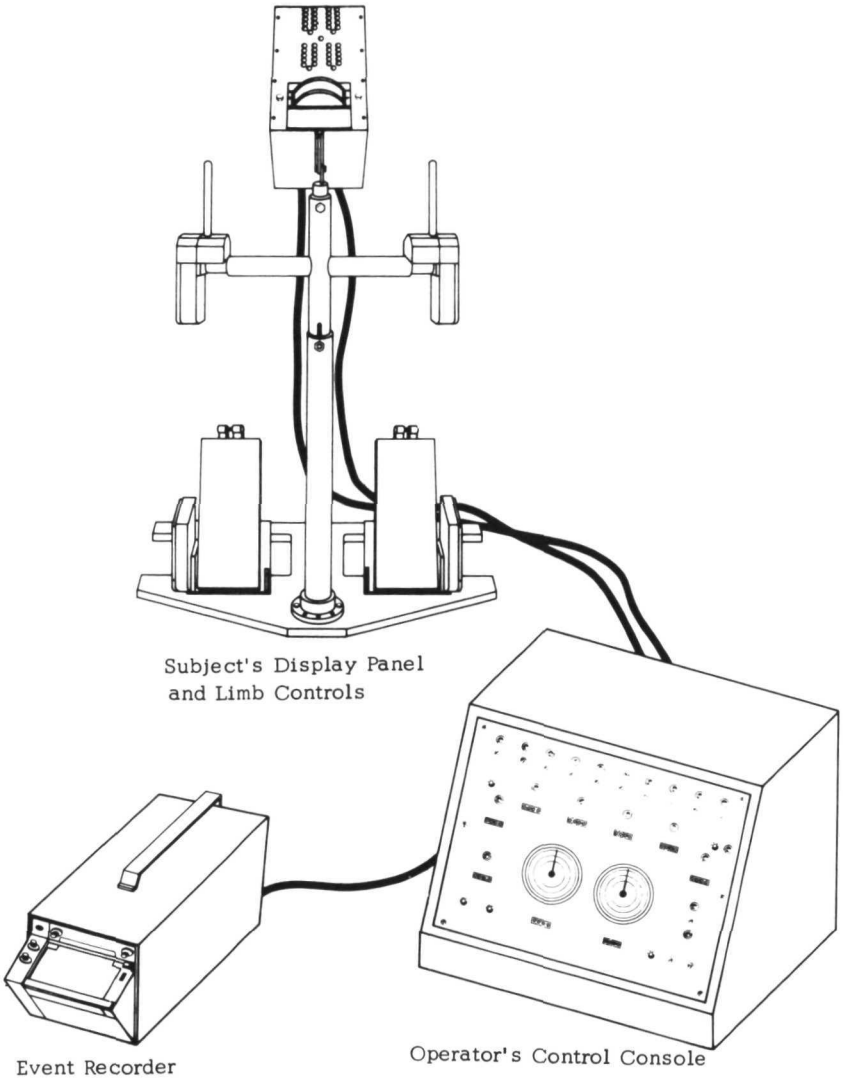

FIGURE 34.–LRCC components.

of times each individual problem is answered or not answered in the preset time.

Application Areas

In the absence of normative data for different populations and age groups, the LRCC is useful primarily as a research tool. It has been used to study the effect of closed life-support systems upon human beings. It was used on the

Tektite I (60-day) and the Benjamin Franklin Gulfstream mission (30 days) to study performance under toxicological, physiological, and psychological stress.

The LRCC was designed primarily for research and can be used in any situation in which a motor response is studied in relation to a visually presented stimulus or in relation to a decision based upon a visually presented stimulus.

One constraint is that there are little or no data available on normative behavior with any one of the five types of problems programed for the LRCC. If such data were available, that is, if the device were standardized for different populations and age groups, it would have far greater utility.

Operator's Control Console

The operator's control console contains the electromechanical programer, chronoscopes, counters, switches, lights, relays, and a power supply. All components, except the programer, are located on the front panel of the console as shown in figure 35.

Programer

The electromechanical programer consists of a drive motor and a drum. The drum contains 60 longitudinal grooves equally spaced about its circumference.

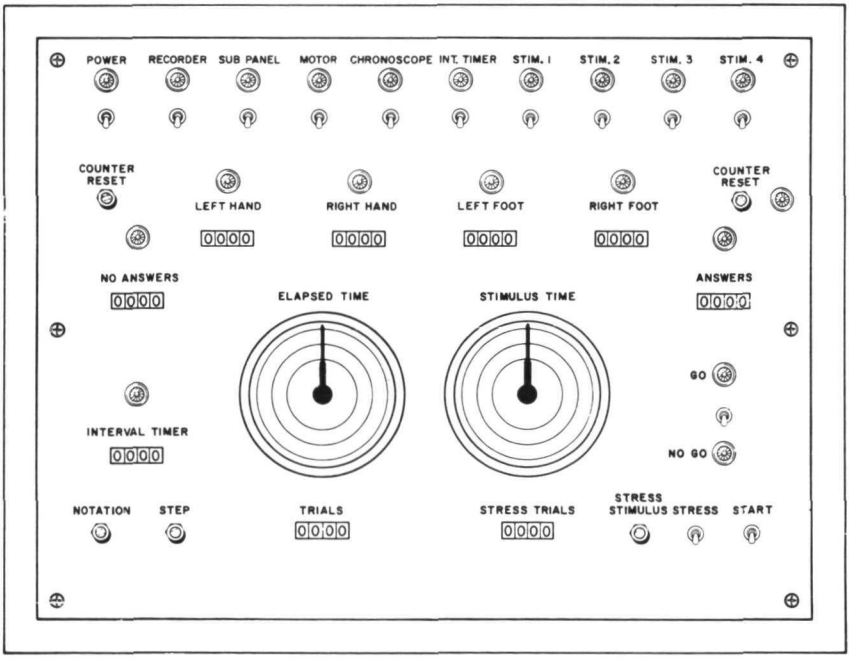

FIGURE 35.–Operator's control console front panel.

Pegs or actuators are placed in these grooves to actuate 57 switches located in positions tangent to the drum. Each row of pegs or actuators in a groove comprises the stored problem and answer. The drum is stepped one problem at a time by a signal generated when the subject makes the correct response and holds the response for a predetermined amount of time. A "step" switch enables the operator to manually step the programer. A "program reset" switch enables the operator to reset the programer if the test has been discontinued. The "program reset light" is activated when the programer drum has been reset. The "go/no go" selector switch selects the length of the test. In the "go" position, the test can be run continuously; in the "no go" position, the test is completed after 50 problems.

The programer motor is controlled by the "motor power" switch. The "motor" light indicates when the "motor power" switch is on.

Chronoscopes

Two chronoscopes located on the front panel of the console are used to indicate elapsed time and stimulus time. The elapsed time chronoscope indicates the duration of a period in which special stresses have been induced into the test by means of a "special stress" switch. The two chronoscopes are readied for operation through the "chronoscope power" switch, which energizes the clutches. The "chronoscope" light is lit once the clutches are energized.

The elapsed time chronoscope operates after the "start" switch has been turned on. The stimulus time chronoscope operates when the "stress" switch is turned on. Both chronoscopes are zeroed when the "counter reset" switch is depressed.

Counters

Various counters located on the front panel of the console present a visual readout of the test results. These counters and their functions are–

(1) *Limb counter*–counts each time a correct response has been made for the limb. There are four counters, one for each limb control. Also, a light above each counter comes on when a correct response has been made.

(2) *Answers counter*–counts each time a correct response has been made for all four limbs. A new problem is not presented until the correct response is held for the time preset on the time delay relay.

(3) *No answers counter*–counts the number of intervals within a trial when no correct response has been made with any limb control.

(4) *Interval timer counter*–counts the number of times the subject fails to complete a problem within the prescribed amount of time.

(5) *Trials counter*–counts the number of problems presented to the subject during the test.

(6) *Stress trials counter*–counts the number of problems presented to the subject while under a special stress.

The "answers," "no answers," and "interval timer" counters have corresponding lights located above each counter and, like the counters, indicate when a correct response has been made. Four "stimulus" switches mounted on the front panel of the console enable the operator to induce four different stimulus actions into the test. A light above each switch comes on when that switch is turned on. The "stimulus 1" switch provides power for the two overtime lights on the display panel. Stimulus switches 2, 3, and 4 are used for locally orientated stimulus actions.

Power Supply

A power supply, located in the operator's control console, is used to convert 115 V ac to 28 V dc. It is controlled by the "power" switch on the front panel of the console.

Subject's Display Panel and Limb Controls

The limb controls, shown in figure 36, consist of four controls: one for each extremity (two hand levers and two spring-loaded foot pedals). The subject manually initiates an electrical response through each respective control to answer the problem presented on the subject's display panel. Each control must be correctly positioned and held for the period of time set by the time delay relay to effect an answer to the problem. The time delay relay setting can be varied from 0 to 0.75 sec. The problem can be self-paced, or the coordinator can be configured to transmit a new problem at a preset time. In the self-pacing configuration, when all of the problem-answer lights are correctly matched and the controls are held stationary for the required length of time, the four limb control, series-connected relays close. This completes the circuit through the time delay relay to the counters and programers and causes the programer to step and transmit a new problem. In the preset time configuration, the drum rotates when the preset time on the interval timer has elapsed, regardless of whether the subject has answered the problem. The interval timer will step the programer at the expiration of the preset time; a new problem will appear and the test will continue.

Each limb control with its respective quadrant of response lights is electrically connected by five magnetic reed switches. These switches are closed independently by moving the respective control, which sweeps a magnet across the switches (see fig. 37). The lever mechanism holding the magnet is spring loaded so that no switch is closed when the control is in the neutral position. The switches are spaced in the limb control so that when the control is moved through its complete arc, each one of the five switches will open and close, thereby illuminating and extinguishing the answer lights throughout 80 percent of the control travel. No switch opening or closure will occur through the additional 20 percent of travel. There is no provision for overshoot at each extreme of control travel.

550-754 O - 74 - 5

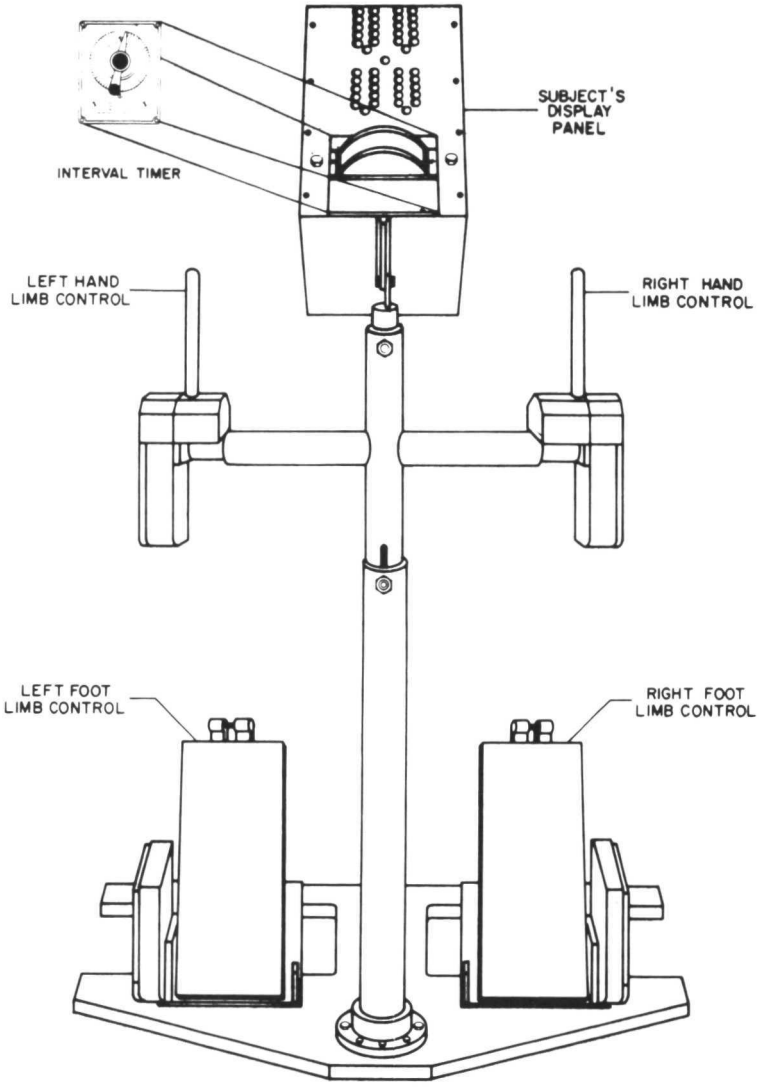

FIGURE 36.–Subject's display panel and limb controls.

Moving the hand controls toward the subject or depressing the foot pedals illuminates and extinguishes the lights in sequence from bottom to top on the subject's display panel. Conversely, retracting the hand controls or releasing the foot pedals illuminates and extinguishes the lights in top to bottom sequence.

The subject's display panel as shown in figure 36 is divided into four quadrants. Each quadrant represents the problem and answer lighting for one limb. The top left quadrant provides problem and answer lighting for the left

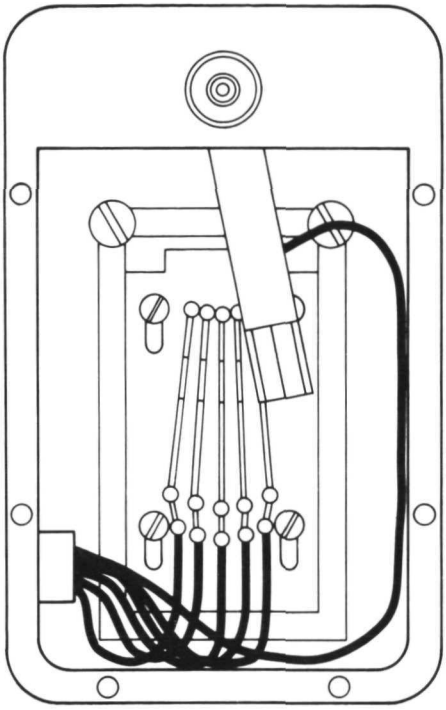

FIGURE 37.–Reed switches and magnet arrangement of limb controls.

hand control, the top right quadrant for the right hand control, the bottom left quadrant for the left foot pedal, and the bottom right quadrant for the right foot pedal. The five colored lights in the left hand column of each quadrant are problem lights energized by the operator's control console. Corresponding lights in the right hand column are answer lights illuminated or extinguished by responses from the limb controls. The white lights located below each quadrant and in the center of the panel are used to inform the subject that mixed problems are being fed into the subject's display panel.

Event Recorder

An integral component of the LRCC is the event recorder (see fig. 38), used to plot the various events of the coordinator. The event recorder has multiple applications and can record any electrical, mechanical, or physiological event that can be represented by an off-on condition. Events are recorded by opening or closing external circuitry connected to the recorder. Should the event be mechanical or physiological in nature, electrical devices must be used to convert the event to electrical impulses. Electrical energy is supplied to the recorder from the coordinator and external sources. The coordinator "recorder power" switch energizes the recorder electromagnets. Actuation of the "notation" switch marks the chart paper to indicate the beginning of the test. The chart drive and heating circuitry are energized from external sources.

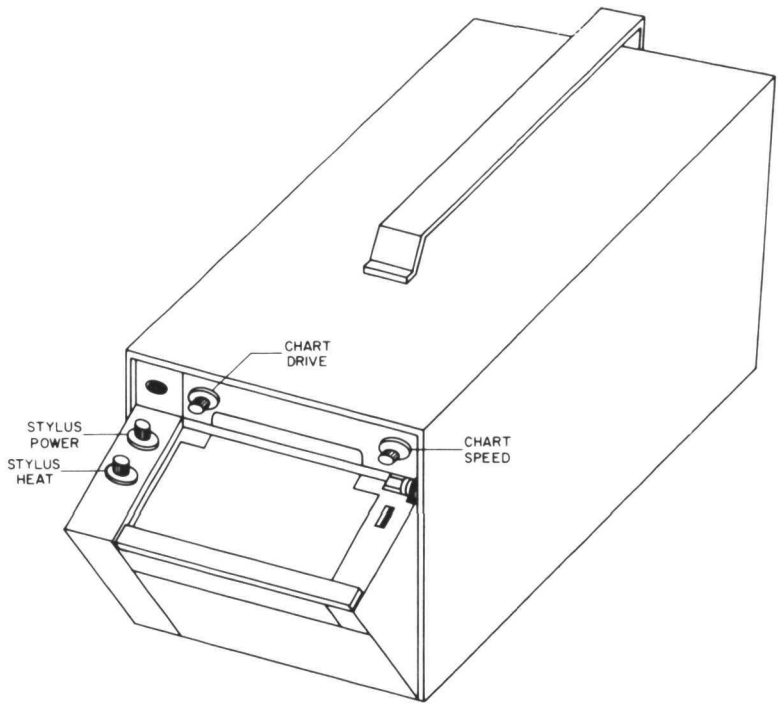

Twenty functions may be recorded on the recorder chart. An explanation of what each writing pen records is shown below:

PEN	FUNCTION	PEN	FUNCTION
1	Time Mark	11	Right foot
2	Program drum revolutions	12	Stimulus #1
3	Program drum steps	13	Stimulus #2
4	Error-Interval Timer	14	Stimulus #3
5	Notation	15	Stimulus #4
6	Special Stimulus	16	Interval timer On-Off
7	Problem answered	17	Not used
8	Left hand	18	Not used
9	Right hand	19	No answer
10	Left foot	20	Time mark

FIGURE 38.–Event recorder.

PASSENGER RIDE QUALITY APPARATUS

A passenger ride quality apparatus (PRQA) is under development at the NASA Langley Research Center. Environmental factors such as vibration, noise, and temperature are important considerations in the design of transportation systems because such factors may adversely affect passenger acceptability of the system. Future transportation systems such as short takeoff and landing aircraft and high-speed ground vehicles are expected to

experience larger vibration amplitudes than those encountered in currently operating systems. The question arises as to whether the passenger will accept these levels and, if not, how much reduction in vibration level will be needed to achieve acceptability. To answer these questions, the relationship between vibration and passenger comfort must be understood. The PRQA has been developed to study this relationship.

The PRQA is shown in figure 39. The passenger cabin is bolted to the table of the motion-base system in one of two positions 90° apart. The hydraulic actuators and restraints are indicated. The supports, one below each corner of the motion-base table, are used to support the table and cabin when not in use. The reaction mass is made of steel-reinforced concrete and weighs approximately 50 000 kg (100 000 lb). This PRQA is the only simulator capable of multidegree-of-freedom motion using a close simulation of a transportation system at vibration frequencies up to 30 Hz.

Three hydraulic servocontrolled actuators are used to control the vertical motion. The actuators are located such that one is on the roll axis. By forcing the other two actuators with a phase difference of 180°, the motion-base table is forced to rotate.

A fourth actuator used for obtaining lateral motion is connected from the underside of the center of the table to a vertical extension of the reaction mass. The electronic servocontrols are compensated such that correction signals are directed to any actuators that are not directly controlling the motion. For

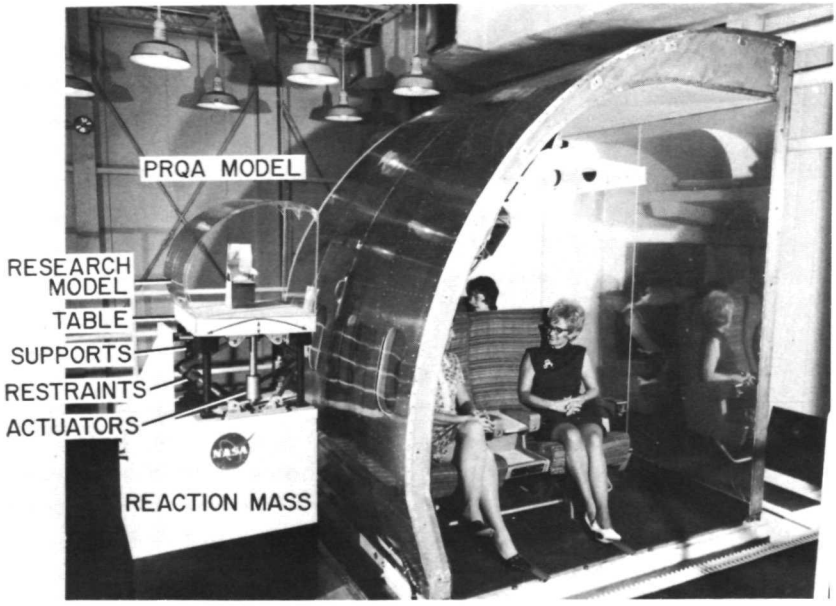

FIGURE 39.–Interior view of the PRQA and a model of the PRQA.

example, for side-to-side motion of the table, the vertical actuators must extend to keep the table moving in only one plane. All four actuators are mounted on ball joints to allow side, vertical, and rolling motions of the table. Other motions are restrained.

The distinctive operating feature of the PRQA is its ability to reproduce three degrees of freedom of the ride recorded from an actual vehicle. Furthermore, it can do it in single or multiple degrees of freedom under control of the operator. The three motions are heave (vertical), lateral (sideways), and roll. The amplitude and phase relationships are infinitely variable between axes.

The performance of the PRQA is limited by its actuators and controls. Curves showing its capabilities are given in figure 40.

An indication of the reproducibility of the PRQA is shown in figure 41. Signals proportional to the accelerations measured on the floor of a bus were used as input to the PRQA. These signals were integrated twice to obtain control signals for the actuators. The resulting motions on the floor of the PRQA were measured using the same portable vibration measuring/recording system used to obtain the bus measurements. From the figure, it is seen that accelerations measured on the floor of the PRQA passenger compartment closely resemble those measured on the floor of the bus. When a sinusoidal input representing either displacement or acceleration was used, the reproducibility was excellent.

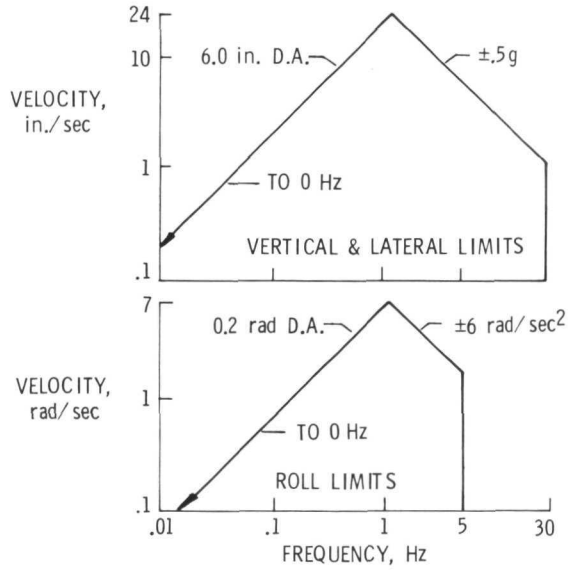

FIGURE 40.—Displacement, velocity, and acceleration capabilities of the PRQA.

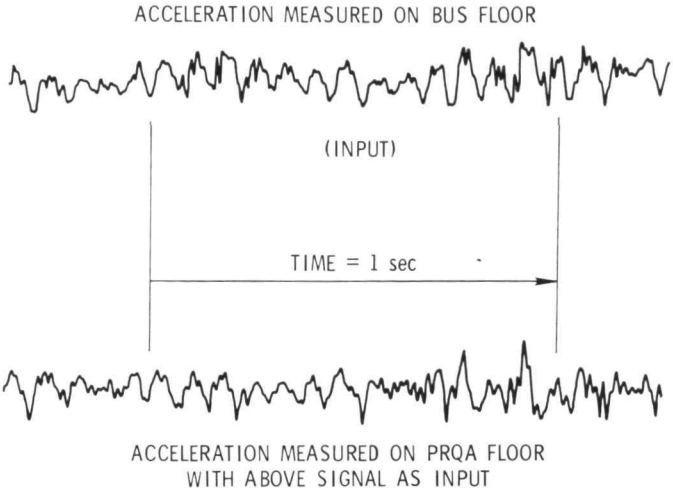

FIGURE 41.–Comparison of PRQA response to input.

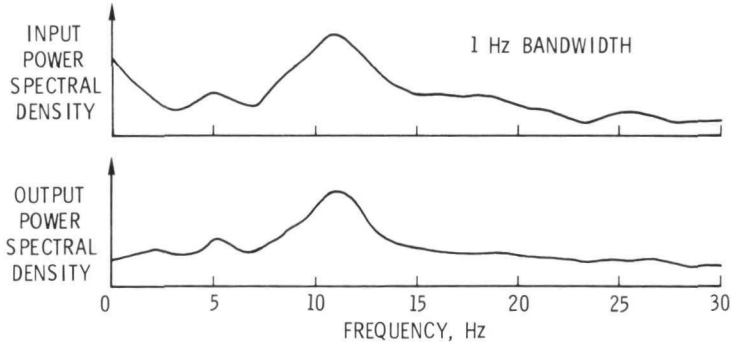

FIGURE 42.–Comparison of PSD of input and output of the PRQA.

Another indication of the PRQA reproducibility is shown in figure 42, again using the acceleration measurements obtained during the previously mentioned bus ride. The upper curve in figure 42 shows the power spectral density (PSD) of the accelerations measured on the floor of the bus. The data used for this PSD encompass the 1-sec interval of data shown at the top of figure 41. The lower curve in figure 42 shows the PSD of the response measured on the floor of the PRQA compartment for the same time period as the upper curve. With the exception of the responses below 2 Hz, excellent agreement exists between input and output.

The PRQA could be used to study the effects of ride comfort factors to accumulate a number of types of data:

(1) Threshold data for each comfort factor

(2) Threshold data for interacting comfort factors
(3) Tolerance limits for comfort factors
(4) Tolerance limits for interacting comfort factors
(5) Human reactions to specific vehicle design characteristics
(6) Scales of tolerance data for the several ride comfort factors separately and in interaction

These types of information would be useful in designing vehicles to maximize ride comfort and acceptance by the public.

In addition, if the PRQA could be standardized for different populations and age groups in context with specific values of the ride comfort factors, the device could be useful in selecting personnel for specific employment. It could be helpful also in diagnosing specific disease processes relative to the inner ear.

Aside from the degrees of freedom for motion, there are relatively few constraints on the application of the PRQA.

ACTIVE VIBRATION ISOLATOR

An active vibration isolator (AVI) developed at the NASA Langley Research Center is an automatic controller specifically designed for vibration protection of systems that experience changes in steady load and/or accelerations. The AVI was designed to perform three functions simultaneously: isolate a flexible structure or payload from disturbances such as vibrations, alternate the response of a flexible structure to transient disturbances, and maintain the equilibrium position of a payload within predetermined limits over a wide range of steady loads and accelerations.

Figure 43 is a schematic of an AVI improved from earlier versions. It has sensing elements to measure the dynamic response of the flexible payload and position of an actuator, electrical control networks to compare the signals of the sensing elements with preset standards and to provide an output to the actuator; and an actuator that applies a force to the payload so as to null the response of the payload as well as to maintain a fixed equilibrium position.

The acceleration $\ddot{x}$ of the flexible payload is measured by a servo accelerometer, and the signal is compared with a desired or command acceleration signal $\ddot{x}_c$ (which for this application is set equal to 0). The error signal, $\ddot{x}_e$, is then sent to the acceleration control network for compensation. The output of the acceleration control network is amplified, and the resulting signal is used to drive the servo valve. The actuator responds to the servo valve command and moves the piston to null the response of the payload. A linear potentiometer attached to the actuator piston measures the piston position. The difference between the measured position Y and the command position Y_c is the error signal Y_e, which is fed to a secondary control loop. This loop restricts the isolator to move about a predetermined, fixed position.

Payloads to be isolated can be discrete or distributed systems. Sensing elements can be selected to respond to position, velocity, or acceleration, or to

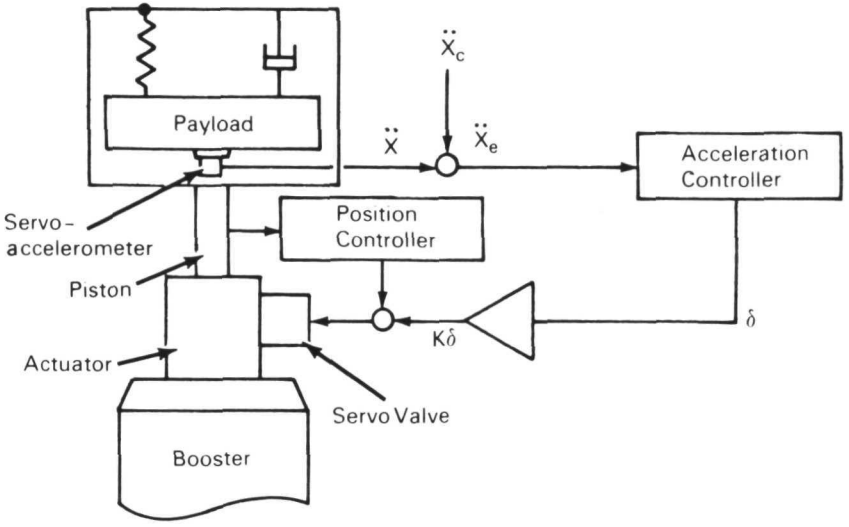

FIGURE 43.–AVI schematic.

combinations of these variables. The actuator may be hydraulic, pneumatic, or electromechanical.

An electrohydraulic AVI system for an XH-51 helicopter has been developed for the NASA Langley Research Center and the USAARMDL, Langley directorate, by Barry Wright Corp. The system was designed to isolate either the cabin or the pilot's seat of a high-performance, hingeless rotor helicopter. Vibration tests on the installed system were conducted at Langley Research Center and vehicle responses compared with and without isolation. The ultimate objective of the program is to subjectively evaluate pilot reactions during flight-test to cabin isolation and to compare these reactions with those obtained during the less expensive seat isolation (fig. 44).

Two systems were developed: a cabin isolator and a pilot's seat isolator. The cabin is actively isolated using a hydraulic servoactuator operated by a hydraulic power supply and a control electronics package mounted inside the cabin. For the seat isolation system, the original pilot seat was modified to be supported by an actuator using the same hydraulic and control circuitry as in the cabin isolator. Both systems were designed to fit into the available space with minimum vehicle modification.

The system design was subject to the following specifications:

(1) At least 90 percent reduction of isolated-mass vertical vibrations at the blade passage frequency and at one or two additional frequencies as necessary and feasible
(2) Insensitivity to rotor speed variation up to ± 10 percent
(3) Maximum vertical dynamic deflections of ± 0.63 cm (±¼ in.)

FIGURE 44.–AVI installed in helicopter.

(4) Zero static deflection during maneuver accelerations up to 2½ *g*
(5) Fail-safe and flight-qualified design

Loads to be isolated were 600 kg (1320 lb) for the cabin and 175 kg (385 lb) for the seat out of a total flight mass of approximately 1910 kg (4200 lb).

Servocontrol system design concepts were developed and checked out using a simple lumped-mass analog computer model. One pitch and four vertical degrees of freedom were included. Masses and moment arms were chosen to yield approximate dynamic characteristics of the real vehicle. This model exhibited cabin-vertical/fuselage-pitch coupled resonance at about 14.5 Hz, necessitating the design of an isolation system that provided a high degree of isolation at rotor input frequencies but which remained essentially rigid at this resonance. Simultaneously, the system had to provide isolation over a bandwidth equal to ±10 percent of the primary input frequencies (e.g., 16.2 to 19.8 Hz for the 18-Hz input to compensate for rotor speed variation). A notch system (one that isolates over very narrow frequency bands only) was used. The notches would track (i.e., automatically change their nominal center frequency) in order to compensate for rotor speed variation. Two notches were used, one at 18 Hz and one that could be set at either 36 or 6 Hz by means of a minor electronics change.

A simplified block diagram of the isolator control system developed to

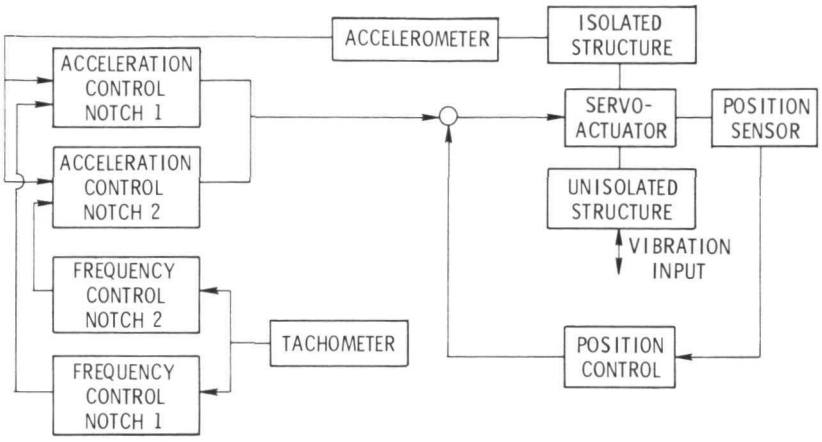

FIGURE 45.–Block diagram of AVI system.

meet the design requirements is shown in figure 45. The system consists of a hydraulic servoactuator that is, in turn, controlled by position and acceleration feedback. The position loop has an upper frequency cutoff of 3 Hz, which enables it to maintain a preset static position of the actuator but minimizes interference with the acceleration control at higher frequencies. The acceleration loop uses quadratic feedback control, which has very high gain when the accelerometer input frequency equals the notch frequency and low gain at other frequencies.

The frequency control systems shown in the block diagram of figure 45 contain two basic control operations. One is a frequency tracking control that varies the notch center frequency as the rotor tachometer frequency varies about the preset notch frequency. The other is a phase-lock control that compensates for tachometer inaccuracy. This system senses the frequency difference by comparing phase between the incoming accelerometer signal and the notch frequency and changes the notch frequency as needed. The phase-lock system was designed to be operational over a range of ±3 percent of the tachometer signal.

Two types of tests were conducted: discrete frequency and continuous sweep. Also, acceleration data were recorded from the isolator control accelerometer and from accelerometers mounted on the vehicle structure. The entire vehicle response when an isolator was in operation differed from that which occurred with no isolation. To include the effects of vehicle dynamics, all data will be presented in terms of ratios of output acceleration to shaker mass acceleration (referred to as transfer functions) and in terms of ratios of isolated to nonisolated transfer functions (referred to as isolator performance).

A series of evaluation tests was conducted on the cabin isolator installed in the vehicle in which constant shaker-acceleration, discrete-frequency steps were

input to the vehicle. For this series of tests, three fixed notches were studied: 6, 18, and 36 Hz. Figure 46 shows isolator performance for these tests as monitored at the isolator control accelerometer. More than 90-percent isolation was obtained at all notch frequencies. The majority of the laboratory test data was obtained in controlled, continuous-sweep tests using 18- and 36-Hz notches only. Isolator performance was measured on the cabin floor at the cabin center of gravity rather than at the control accelerometer to obtain more realistic performance information. The transfer function of the cabin is compared for the 18- and 36-Hz tracking notch modes and the nonisolation mode in figure 47. With no isolation, a rather large amplification occurs at 18.6 Hz. This is thought to be due to a cabin/fuselage relative pitch resonance, although instrumentation was insufficient to define it exactly. This type mode was not included in the analytical model. With the isolator in operation, however, a significant reduction in vibration occurs across the tracking band from approximately 17 to 19.5 Hz, and the amplification peak is completely eliminated. A peak occurs at each end of the tracking band as the tracking tachometer signal is manually switched in and out of operation. This represents an abnormal condition because in a helicopter the frequency varies about the nominal. Although the isolation system was switched in at 16 Hz, it did not start operating until a frequency of 17 Hz was reached; it continued to provide some isolation at a frequency 1 Hz greater than that occurring when it was switched out. The frequency sweep rate was a nominal 1/4 decade per minute or about 1 Hz every 2 sec.

The 18-Hz tracking notch provided about 75 percent vibration reduction at 18 Hz in this test and 93 percent at the 18.6-Hz peak. The 36-Hz notch, which

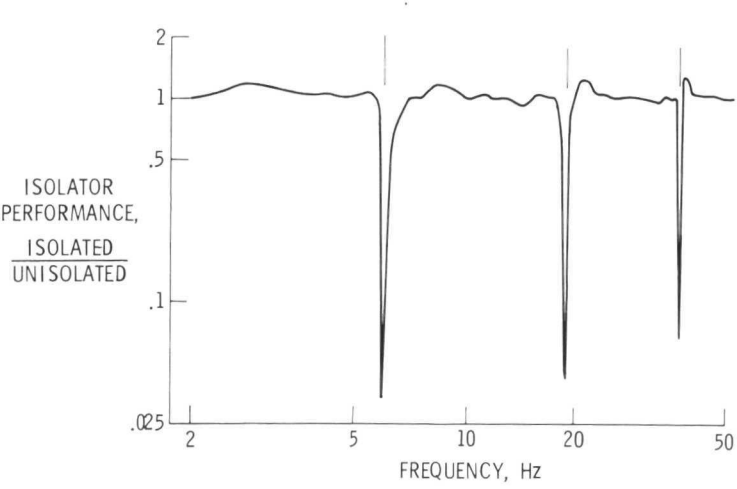

FIGURE 46.–Cabin isolator performance in discrete-frequency tests.

was tracking from 32 to 40 Hz, provided only 37 percent reduction at best, at about 34 Hz, and increased the vibration by a factor of 3 over the unisolated case at about 38 Hz. This was the best performance provided by the 36-Hz notch in the continuous-sweep tests. The fixed notch resulted in the same vibration as the nonisolated case at 36 Hz, and the phase-locked notch could not be stabilized.

Isolator performance for the various modes of operation in the sweep tests is compared for the 18-Hz notch in figure 48. The best performance, 93 percent reduction, is obtained with the tracking notch, whereas the phase-locked and fixed notches provide 80 and 72 percent reduction, respectively. However, peak reduction in all cases occurs at 18.6 Hz, the amplification peak of figure 47. At 18 Hz, the system is just becoming effective, whereas it had provided over 90 percent reduction in discrete-frequency tests. In comparing results from the continuous-sweep tests with the discrete-frequency tests, it appears that if a notch-type active isolation system must work at some finite sweep rate, as it may in a helicopter, continuous-sweep tests must be conducted to evaluate its true performance.

Performance of the seat isolation system in the helicopter was evaluated in discrete-frequency step tests similar to those conducted on the cabin for three fixed-notch frequencies: 6, 18, and 36 Hz. Results are presented in figure 49, where isolator performance, as measured by the control accelerometer, is shown as a function of frequency. Better than 93 percent isolation is obtained

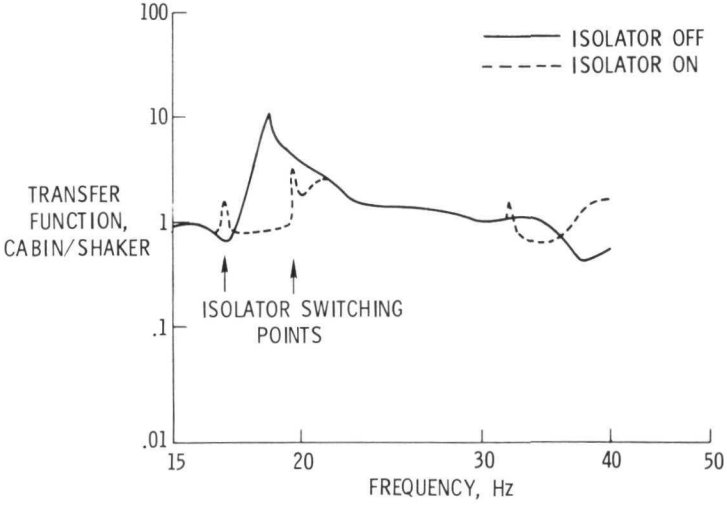

FIGURE 47.–Comparison of isolated and unisolated cabin transfer functions for 18- and 36-Hz tracking notches in continuous-sweep tests.

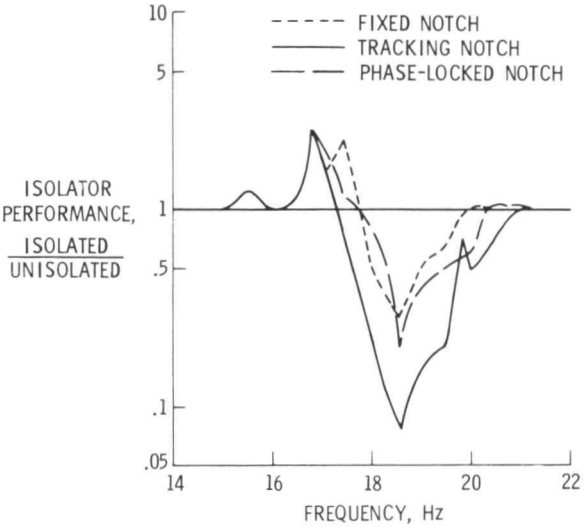

FIGURE 48.–Cabin isolator performance for three different operational modes in continuous-sweep tests.

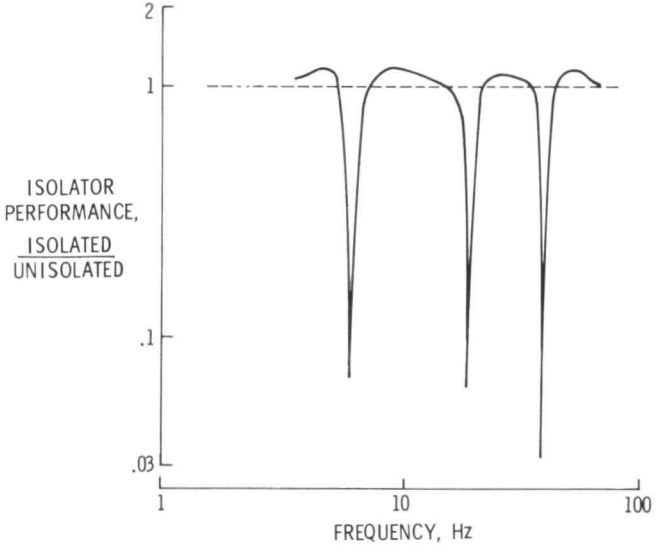

FIGURE 49.–Seat isolator performance for fixed-notch operational mode in discrete-frequency tests.

at 6 and 18 Hz and almost 98 percent was obtained at 36 Hz. Slight amplification occurs before and after each notch.

As in the cabin tests, the seat was not completely free of all vibration because of lateral and longitudinal vibrations caused by nonvertical inputs at the floor. Also, the offset center of gravity of the isolated mass resulted in a rocking motion about the seat attachment points.

Continuous-sweep tests were conducted on the seat in the vehicle to evaluate notch frequency tracking controls. Only the isolation notches at 18 and 36 Hz were evaluated. The acceleration transfer function of the seat at the actuator attachment point is shown in figure 50 for the tracking notch isolation and nonisolation modes of operation. In the 18-Hz tracking (from 16 to 20 Hz) isolation mode, the amplification peak is reduced by about 84 percent, not as much as for cabin isolation. Across the bandwidth, average reduction is about 80 percent. In the 36-Hz tracking notch mode, the isolator provided better than 90 percent isolation over most of the band from 32 to 40 Hz.

A comparison of isolator performance for the three isolation modes at 18 Hz is shown in figure 51. Unlike the cabin data, the best isolation at 18 Hz is exhibited by the fixed notch. The phase-locked and tracking notches increase the bandwidth at the expense of some isolator effectiveness. Although no data are shown, the fixed notch performed well at 36 Hz, providing a peak isolation effectiveness of 95 percent. This indicates that the seat system is somewhat less sensitive to tracking rate than the cabin system, possibly because of the smaller

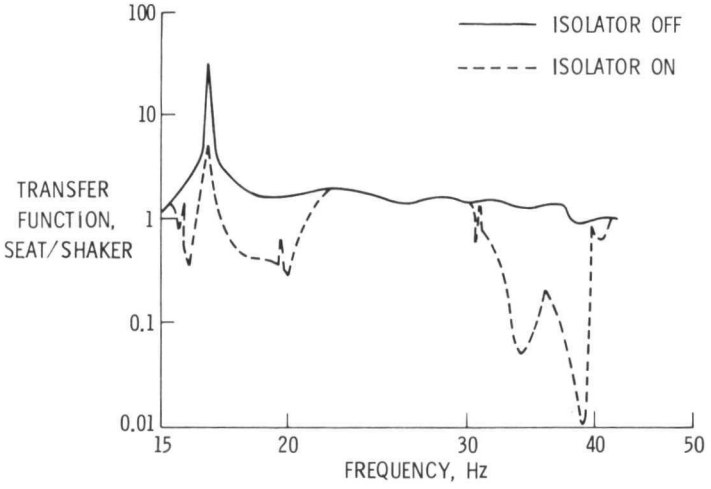

FIGURE 50.–Comparison of isolated and unisolated seat transfer functions for 18- and 36-Hz tracking notches in continuous-sweep tests.

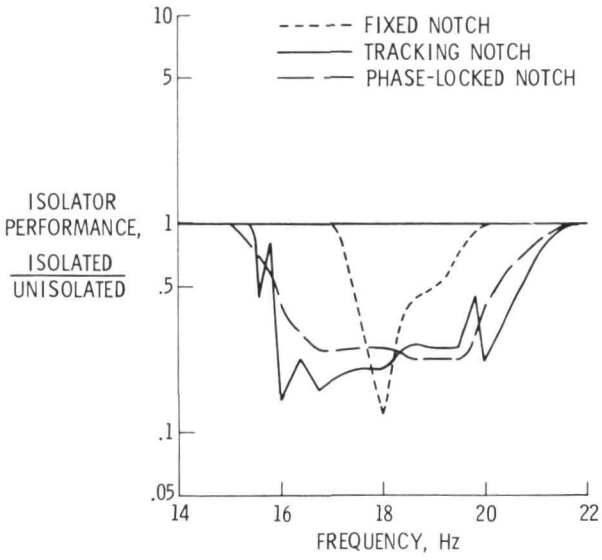

FIGURE 51.–Seat isolator performance for three different operational modes in continuous-sweep tests.

actuator size. As in the cabin tests, the 36-Hz phase-locked notch could not be stabilized with the seat mounted in the helicopter.

Narrowband active isolation systems capable of isolating either the pilot's seat or the entire cabin of a full-scale helicopter were tested. These tests were conducted in the laboratory on the systems mounted in the helicopter. The following conclusions and recommendations resulted:

(1) Active isolation techniques can effectively reduce helicopter cabin response to rotor inputs even near resonances. Narrowband isolation systems that track input frequency provide good isolation for a varying rotor speed environment.

(2) Active vibration isolation of a large portion of a structure can significantly change the vibration characteristics of the unisolated portion. Development of any such active vibration isolation system should include elastic response studies of the entire vehicle.

(3) AVI performance can be seriously degraded by isolated structure flexibility. The use of multiple actuators or multiple control accelerometers located over the isolated structure with electronic compensation for the structure should be investigated to overcome this difficulty.

(4) Continuous-sweep tests must be used to adequately describe the performance of an active isolation system that must operate in a changing frequency environment (ref. 11).

AVI's could have application in a number of vehicles in which it is desirable to protect the operator from vibration effects. Such vehicles include trains, helicopters, fixed-wing aircraft, buses, automobiles, and large earthmoving vehicles. It should be recognized that the AVI does not remove all vibrations; however, all vibrations are reduced and the major jarring vibrations are eliminated.

The major constraint on the application of the AVI is cost. Therefore, two major conditions must exist to justify the cost of an AVI, such as the one devised for the XH-51 helicopter. The first condition is the existence of a relatively expensive vehicle. The second is the availability of a highly paid operator who possesses relatively great skill and who could work over a longer period of time if he did not have his innards severely shaken by vibration.

SHOCK-ABSORBING FOAM

Temper foam is a polyurethane-silicone plastic material developed as an energy-absorbing cushion material by Dynamic Systems, Inc., for NASA Ames Research Center (ref. 12). Beside the use made of it at Ames Research Center, it is now being manufactured and sold by Dynamic Systems, Inc.

This flexible urethane has viscous and elastic properties that give it unique temperature sensitivity as well as compression rate sensitivity. It absorbs energy, taking sudden impact without shock or bounce. It is a fluid elastic that can cushion to a comfortable flow-fitting support. Upon impact, hard, high-pressure points yield to safe, uniform, low-pressure resistance.

Temper foam can be molded easily while maintaining stiff properties and recovers fully after 90 percent sustained compression. It behaves like a rigid foam at low temperatures and like an elastic foam at high temperatures. Temper foam physical property data are—

(1) Density: 80 kg/m^3 (5 lb/ft^3)
(2) Cell structure: mixed open and closed
(3) Natural color: white
(4) Energy absorption: 0.2 to 0.7 J/m^3 (2 to 8 ft-lb/in^3)
(5) Compression at 14 kN/m^2 (2 psi): 25 percent in 70 sec at 21° C (70° F)
(6) Viscous sensitivity range: 10° to 32° C (50° to 90° F)
(7) Maximum service temperature: 150° C (300° F)
(8) Flammability: self-extinguishing

The foam was formulated for use in seat cushions in common room temperature environments. Local body heat and the foam's temperature sensitivity combine to produce cushion flow to a fitted uniform support. Such support reduces fatigue, absorbs vibration, and prevents soreness over long periods. Figures 52 to 54 present impact compression response, static compression time, and stiffness, respectively.

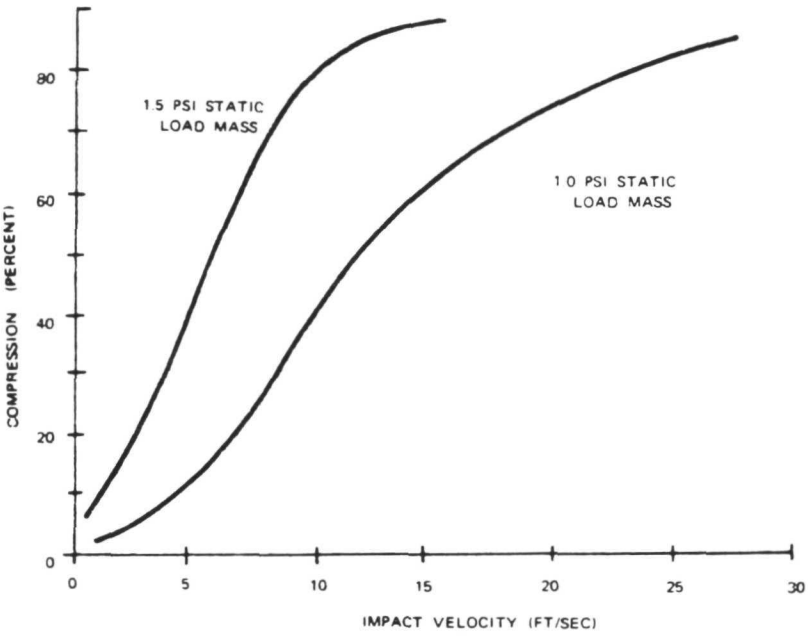

FIGURE 52.–Temper foam impact compression response.

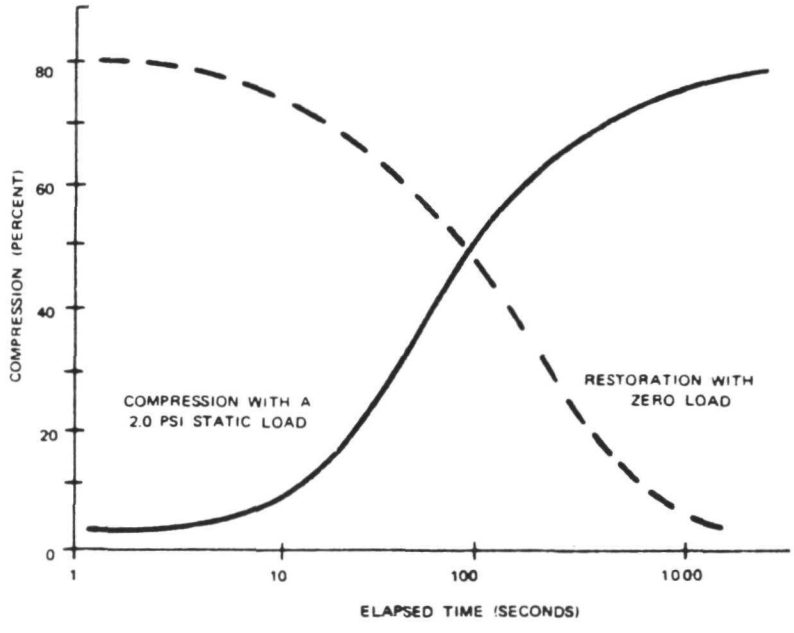

FIGURE 53.–Temper foam static compression time.

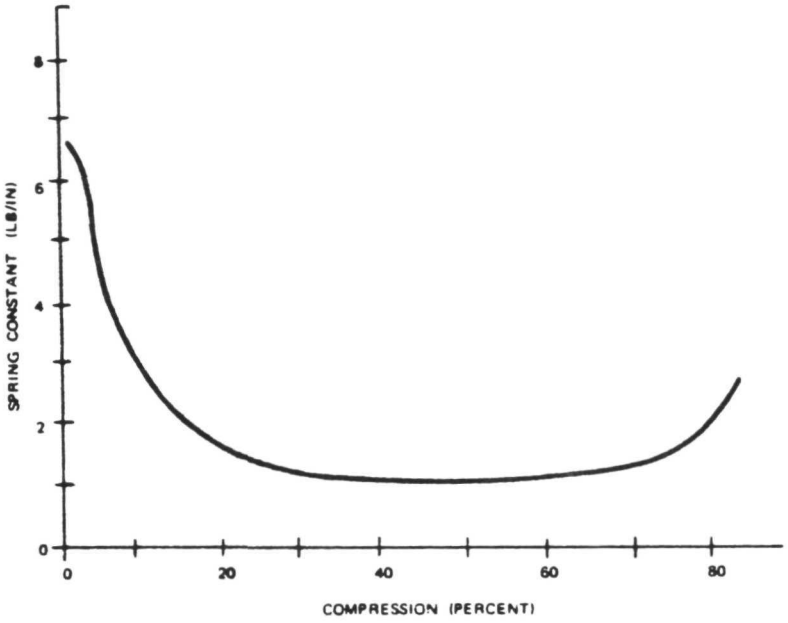

FIGURE 54.–Temper foam stiffness.

Temper foam can be used wherever a cushion effect is desired. It has already been used in office seats, vehicle seats, orthopedic pads, prosthetic pads, safety pads, exercise pads, and sport cushions. It has additional possible applications for special packaging, burn pads, aircraft pilot seats, and contouring molded ribs. Temper foam could be used also in items such as splints, shoe insert pads, arch supports, sports protective pads, and helmets.

Constraints on the application of temper foam are primarily the energy absorption range, viscous sensitivity range, compression rate, and maximum service temperatures. All of these values were listed under physical property data. The other constraint is the size of the sheet or block normally manufactured. Standard thickness is in 0.64-cm (1/4-in.) intervals, up to 5 cm (2 in.). Maximum thickness is 30 cm (12 in.). Standard dimensions are 43 by 48 cm (17 by 19 in.) and 61 by 61 cm (24 by 24 in.). Larger sizes and thicknesses must be specially ordered.

Vision Testing

Two vision testing devices have been devised that could facilitate the testing of human vision by automating it and by relieving the monotony of present refraction procedures.

AUTOMATED VISUAL SENSITIVITY TESTER

The automated visual sensitivity tester (AVST) was designed and developed at the NASA Ames Research Center (ref. 13) to investigate changes in visual functioning in a variety of aerospace stress environments to allow early diagnosis of visual problems. The AVST makes possible a self-administered test for several visual dysfunctions. Primary design objectives were adequate sensitivity to changes in visual performance, sufficient comprehensiveness to detect the possibilities of change in visual functioning, and adequate diagnostic value (that is, ability to detect a dysfunction and indicate the extent of its development).

Each vision test is filmed on an 8-mm film cassette, which is then inserted into the AVST. Prerecorded verbal instructions (now available in English and Spanish) are also included on each film cassette for test administration standardization so that the patient, to administer the test, need only turn on the unit. This method of visual stimulus presentation effectively controls for such important test parameters as stimulus and background brightness, stimulus speed, and randomization.

Figure 55 is a schematic cutaway of the AVST. The latest version of the AVST is shown in figure 56. It includes a cover, control panel, chin rest, forehead rest, and response button. Figure 57 is a rear view of the AVST with the fiberglass case removed to show the three fixation projectors (cylindrical tubes at upper left), three spare projection lamps (at right), and structural members added to increase rigidity. The projection screen is behind the circular mask.

Application Areas

The AVST can be used whenever it is desired to determine visual sensitivity or to map a blind spot (scotomata detection) of a subject. These situations include–

(1) Visual screening of subjects to detect selected visual dysfunctions and changes in the size, shape, or location of the blind spot

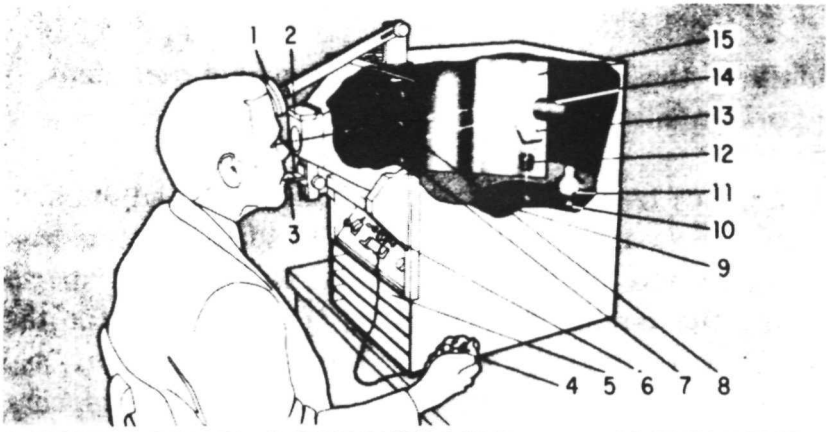

1. FOREHEAD SUPPORT
2. VIEWING LENS AND FILTER HOLDER
3. IMPRESSION WAX MOUTHPIECE
4. SUBJECT RESPONSE SWITCH
5. STORAGE FOR 8 FILM CARTRIDGES
6. FIXATION SELECT SWITCH
7. FIXATION CROSS PROJECTED ON SCREEN
8. PHOTO CELLS
9. FILM CARTRIDGE
10. FIRST MIRROR
11. LAMP
12. LENS
13. SECOND MIRROR
14. FIXATION PROJECTORS
15. THIRD MIRROR

FIGURE 55.–Schematic cutaway drawing of the AVST.

FIGURE 56.–Latest version of the AVST.

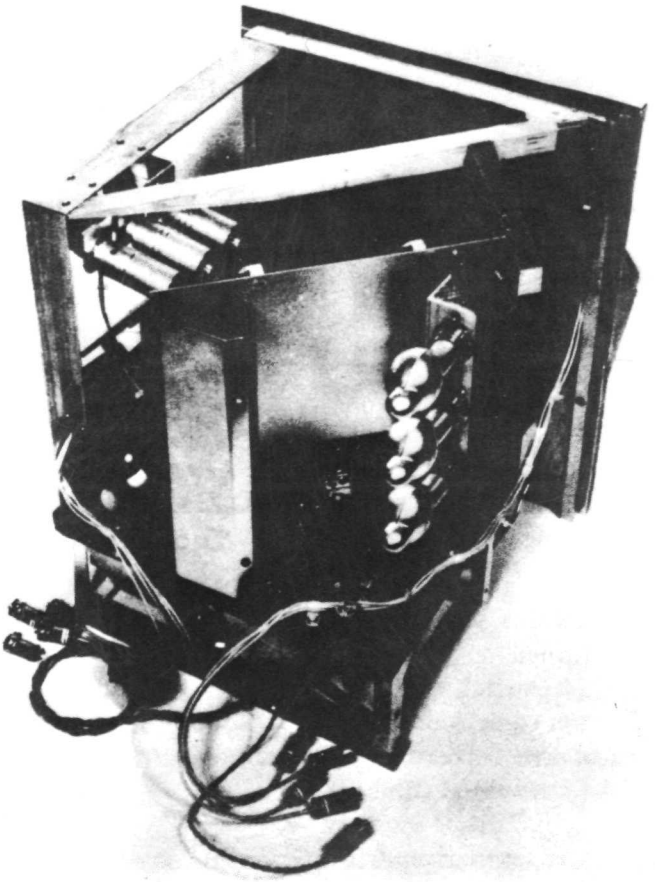

FIGURE 57.–Rear view of the AVST.

(2) A diagnostic testing pool for specific diseases
(3) Demonstration of visual capacities
(4) A research tool for making specific visual or blind spot measurements

The existing limitation to two tests (determining visual sensitivity loss and measuring blind spots) is being remedied. Efforts are presently underway to provide a test of muscle balance and color perception. Other visual tests are planned for the future.

The only constraint on the use of AVST is that the subject must understand the language spoken on the test film cassette (English or Spanish) and be able to press a response button.

Components

Cabinet and Interior Framework Construction

The removable outer case of the AVST is made of 0.40-cm (0.15-in.) thick laminated fiberglass. Although the case provides some structural rigidity, the existing framework was strengthened by adding aluminum channel.

Viewing Screen and Photocell Assembly

The standard Fairchild Mark IV S viewing screen is used. An aluminum mask on the observer's side of the screen produces a 60°-arc-diameter field of view. The eight photocells are located outside this field of view on the observer's side.

Clairex CL905L photocells are used. Each frame of the stimulus films contains an image of the moving, white (stimulus) spot of light as well as small, fixed spots of light that are appropriately coded to indicate test spot position and movement direction on each of the 12 meridians and are used for driving the response plotter.

Miscellaneous Interior Details

Three visual fixation projectors are used to project 10-min-arc bar length red crosses upon the viewing screen. Each projector consists of a 6.3-V (no. 44) lamp, opal glass diffuser, photographic negative of a cross, focusable achromat lens, and a red no. 24 Wratten (Kodak) filter. Lamp luminance is controlled by adjustable resistors.

Response Plotter

A two-pen Honeywell Model 540 XXY' recorder is used to record both the stimulus and response. It was modified so that the pens could be dropped independently onto the graph paper. The lower pen remains connected to the original solenoid; the upper pen control bar scale is tied by a roller and arm to a new solenoid and bar running across the top rear of the plotter. Green ink is used in the stimulus pen and red ink in the response pen. The plotter is operated in accordance with the manufacturer's instructions. The two pens are offset from each other during use to facilitate interpretation of the data. The medical practitioner simply compares the two ink plots, noting when and where the patient does not respond when the visual stimulus is presented. The patient's response time may also be analyzed from the record's line length if necessary.

Electronic Control Unit

The primary function of the electronic control unit is to drive the response plotter pens in accordance with the position of the viewing screen image. This is done by projecting eight small spots of light from each film frame through the screen and onto eight photocells.

The design of this control unit makes it possible to operate the response plotter in each of three modes:

(1) Automatically from screen images that operate the photocells
(2) Manually from the front face of the control unit
(3) From an external device, such as a digital computer or other preprogramable device

The front panel control provides two control functions. When the "auto-manual" switch is in the "manual" position, the 12 front panel switches and the "out/in," "run-reset," and "run/hold" switches are operational. This provides for local control of pen travel for calibration purposes. Initial calibration of pen travel is achieved by depressing the "cal" button (located on the right hand side of the depression on top of the electronic control unit) and adjusting the X, Y, Y' sensitivity controls on the plotter until both pens are at the desired maximum radial paper location. The "rate" control, located within the depression in the top, is used to equate the pen's angular velocity to the screen stimulus velocity.

In the "auto" position, the functions are automatically controlled by externally generated control signals from the viewing screen photocells. The eight lights on the front of the panel display the ongoing programed information from each of the eight photocells.

THE OPTOMETER

An optometer (ref. 14) was developed at the NASA Ames Research Center by the Stanford Research Institute to investigate the human visual accommodation response.

Figure 58 shows the optometer. The major components of the optometer are illustrated in figure 59. In the top center of figure 59, the subject is looking through the aperture of a focus stimulator. The focus stimulator provides for a controlled focus stimulus to the eye while the optometer continuously tracks the focus of the eye. The optometer is shown in the center and lower left of figure 59. Its principle of operation is based on simple optics. If two tiny apertures are placed in front of a lens, an object at infinity (not a requirement) will be imaged at the focal plane of the lens. At any other plane two images will be formed, each provided by the narrow beams admitted by the small apertures. Defocus, then, instead of resulting in a blur circle (for a point), results in two separate images. The distance between the two images depends upon the amount of defocus, and their relative displacement from the optic axis indicates the direction, or the sign, of the defocus. Furthermore, if a single aperture is moved up and down across the face of the lens, defocus direction will be determined by either in-phase or out-of-phase movement of the image. This defocus principle, known as the Scheiner defocus analysis, is incorporated into the optometer. However, because the lens of interest is the eye lens, the

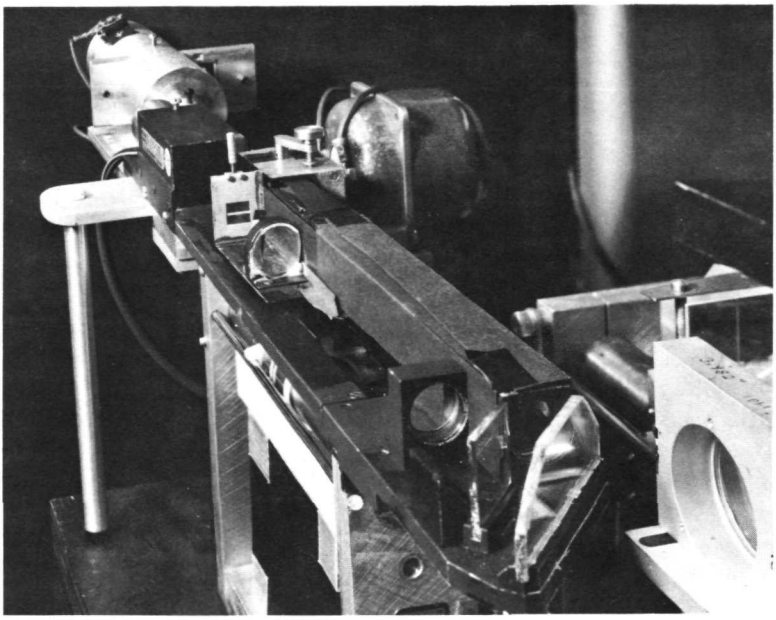

FIGURE 58.–The optometer.

aperture is projected upon the lens from a distance. Also, the point object is replaced by a vertically oriented rectangular aperture, the retinally reflected image of which is focused on a split field photosensor. A dc error signal is generated from the photosensor output of appropriate direction and sign to drive the optometer servo and null the image motion. In the null position, the optometer maintains the same relative focus as that being maintained by the eye it is measuring (relative because the eye views white light and the optometer is operating on infrared).

Light from the checkerboard target enters the aperture of the focus stimulator, and an image is formed by the first lens. This image is the object for the last lens, and the distance from that lens depends upon the distance of the target from the input aperture, which is constant, and the position of the moving prism, which is experimentally varied. In most previous applications of the Badal optometer principle, an actual object is placed in the vicinity of a lens' focal plane. The dioptric power required to focus the object at the other lens' focal plane is a linear function of the object's axial displacement from the focal plane. Moving the object closer to the lens from the focal plane requires positive accommodation. For instance, an object 5 cm from a lens of 10-cm focal length will require 5 diopters of accommodation. The limit for this lens is 10 diopters.

When the moving prism approaches the stationary prism, the image of the target moves toward the last lens, and the subject must accommodate to keep

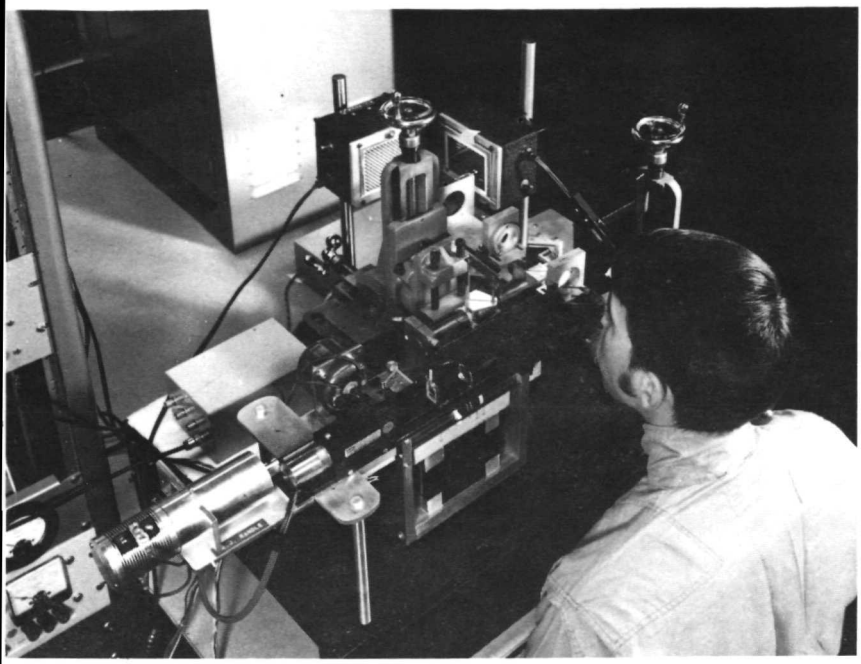

FIGURE 59.–The optometer and the focus stimulator.

it in clear focus. The result is exactly as in the Badal optometer, but here a variety of target stimuli can be used without changing the servo requirements that provide focus changes in this system through the servoed prism movement.

The aperture is brought to focus in the entrance pupil plane of the subject's eye. This is accomplished as follows: the last lens receives collimated light; the aperture is placed at the focal plane of the first lens, which does the collimating; the eye is placed at the focal plane of the last lens.

An important application of the optometer was in its use at Ames Research Center as a device for training pilots to control their visual focus voluntarily. It has been demonstrated that when viewing in empty or targetless visual fields, visual focus settles at about 1 meter from the eye; the observer is unaware that his focus is not at the distance it should be for effective out-of-the-cockpit scanning. This reflex phenomenon is known as "empty field myopia" and can seriously affect the pilot's visual performance.

Because the optometer is a continuous automatic nulling device, its output could be used to modulate a tone and the pilot could have a continuous auditory signal indicating where he was focused even when there were no targets in the visual field. This auditory feedback was used, then, to train subjects to maintain infinity (distance) focus even when targets were removed from the field. The subjects learned to feel and be aware of where they were focused even after the tone feedback was removed. Thus they now could

maintain a visual search "mode" and be focused for distant targets when they appeared in the empty visual field.

The optometer has also been used in a study of the circadian rhythm of accommodation and in a study of the speed of accommodation in response to step and sine wave targets. It will have many future uses in aerospace research.

The optometer could be used in clinical settings as a diagnostic or screening device and to determine patient's refractive error. The optometer can be used also to evaluate the response to visual pathology treatment and the efficacy of the therapeutic technique.

The basic drawback in using the optometer is that there are no standards for its application during routine examinations. Lengthy studies would have to be conducted to establish norms of visual functioning. The equipment must be standardized over a large stratified sample of the population.

Tools

This chapter describes eight tools selected from a much larger list that were developed for use in outer space in zero-gravity conditions. The selection criteria were that each tool be easy to use in a test situation and require no great skill (ref. 15). All of these tools except the handheld electron beam gun can be used underwater. They were designed for space application; however, the problems of performing work at zero gravity are similar to those of working underwater, in confined places, on a high tower, or on a work platform.

KUPU LATCH

The KUPU latch shown in figure 60 was designed to provide a quick-connect and quick-disconnect attachment point for restraint devices and tethers. It also served as a quickly placed fastener for in-space assembly.

The latch is inserted into a hole just slightly larger than the diameter of the bolt mechanism. Once it has been inserted past the locking levers, these levers spring outward and prevent the latch from being extracted. To secure the latch, the finger lever nut can be rotated into position by a user wearing gloves. The latch can then serve as an attachment point for a snap ring, a tiedown ring, or a handheld attachment. Loosening the finger lever nut releases the latch. When the release plunger is pressed, the locking levers retract within the bolt and the bolt can be removed from the hole. The retainer ring is permanently installed to prevent the nut and bolt from ever disengaging.

The KUPU latch permits one-man assembly and tiedown. It is designed to minimize the number of loose parts. The nut and bolt form a single unit and are not separated during use, thereby eliminating the usual difficulty of mating a nut and bolt assembly; one-handed placement and removal is possible. The latch does not require the use of any hand tools, but does require a precut hole.

COAXIAL CABLE CUTTER

The 15-cm (6-in.) long coaxial cable cutter shown in figure 61 was developed to cut and strip coaxial cable quickly and accurately. It has sharp blades positioned to cut the shielding and insulation at the right distance from the cable end as well as at precisely the right depth. The tool is held in one hand, and the coaxial cable is inserted into the guide-spacer tube with the other

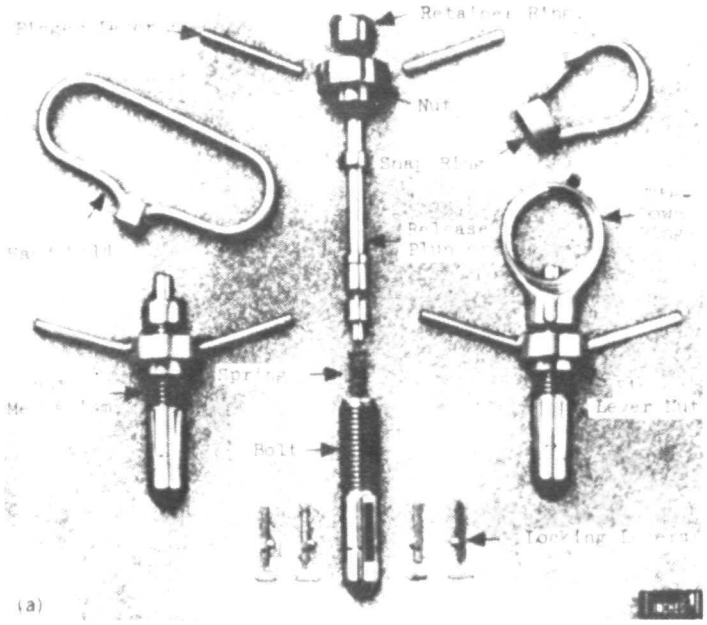

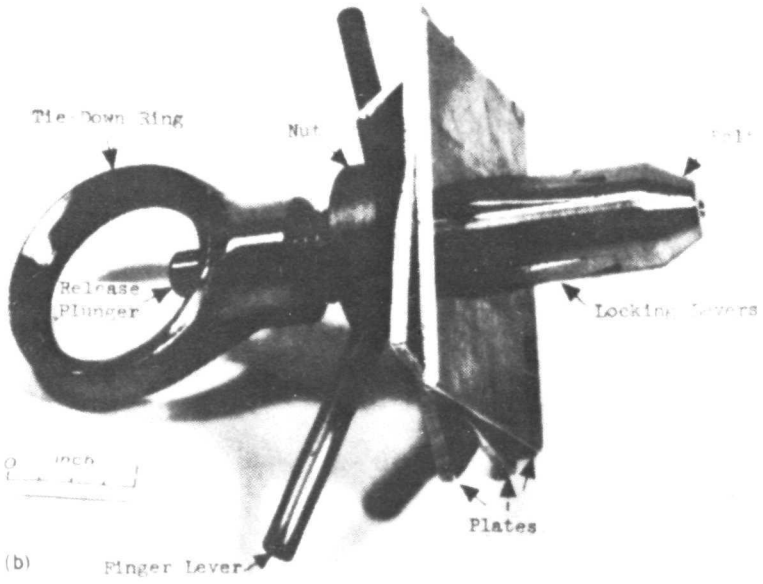

FIGURE 60.–KUPU latch. (*a*) Components. (*b*) In operation joining three plates.

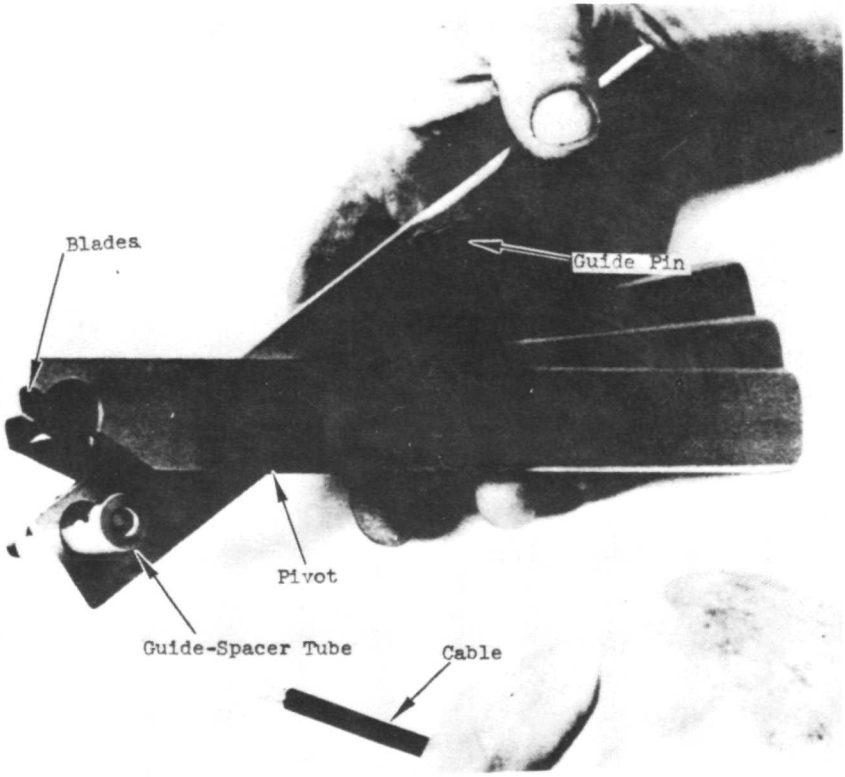

FIGURE 61.–Coaxial cable cutter.

hand. When both handles are squeezed together, the coaxial cable is cut and stripped. This high-speed connector assembly operation requires little skill. Having proven its usefulness, the cutter is now in commercial manufacture.

BOEING TORQUE CANCELING TOOL

The Boeing torque canceling tool shown in figure 62 was designed as a ratcheting, zero-reaction socket wrench. It is a simple ratchet wrench with two handles. A user operates the tool by placing a hand on each handle and alternately pushing the handles toward each other and then pulling them apart the way the handles on a pair of scissors are operated. Thus, reaction forces on the operator from the tool are opposed and tend to cancel one another. The motion of the handles is transferred into a rotation of the socket drive by means of a ratchet mechanism. This mechanism does not have a reversing switch. To reverse the direction of socket motion, the socket is removed from one end of the socket drive and placed on the other end, which protrudes from the other side of the tool. Reaction torques on the tool from the fastener are transmitted back to the worksite by an accessory bar on the tool, which can be

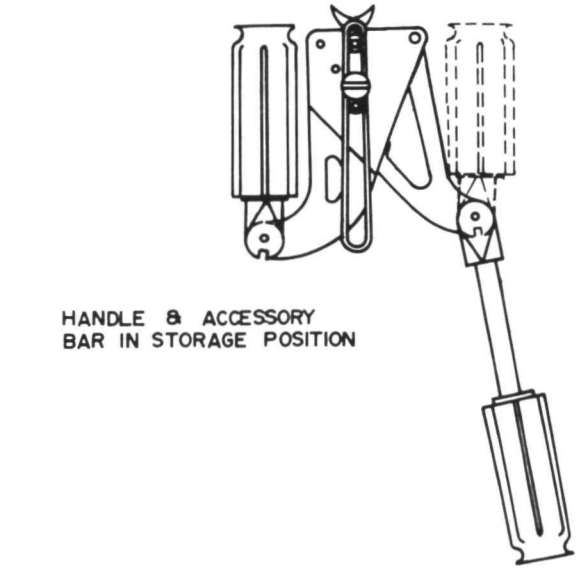

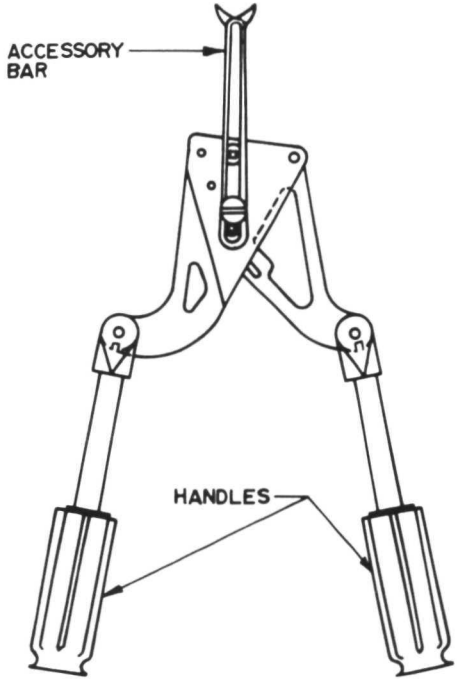

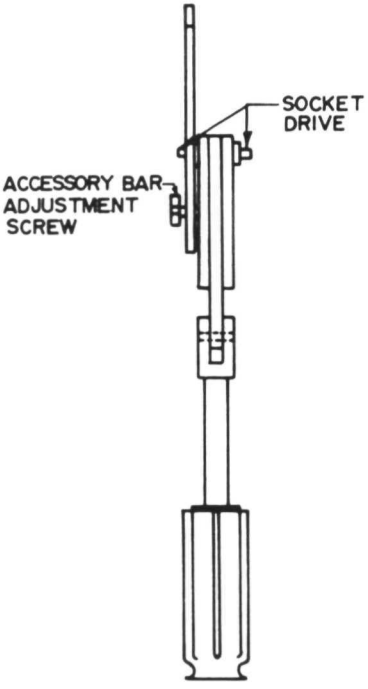

FIGURE 62.–Boeing torque canceling tool.

extended to come into physical contact with a protrusion from the worksite. When not in use, the tool may be stored in minimal space. The accessory bar is retracted and the handles fold.

Both hands are required to operate the tool, and a nearby protrusion is needed to cancel reaction torques

APOLLO TORQUE WRENCH

The 16-cm (6¼-in.) long Apollo torque wrench shown in figure 63 was designed to limit the amount of torque that is applied to remove or replace threaded fasteners. It also can serve as a crank for operating the astrosextant

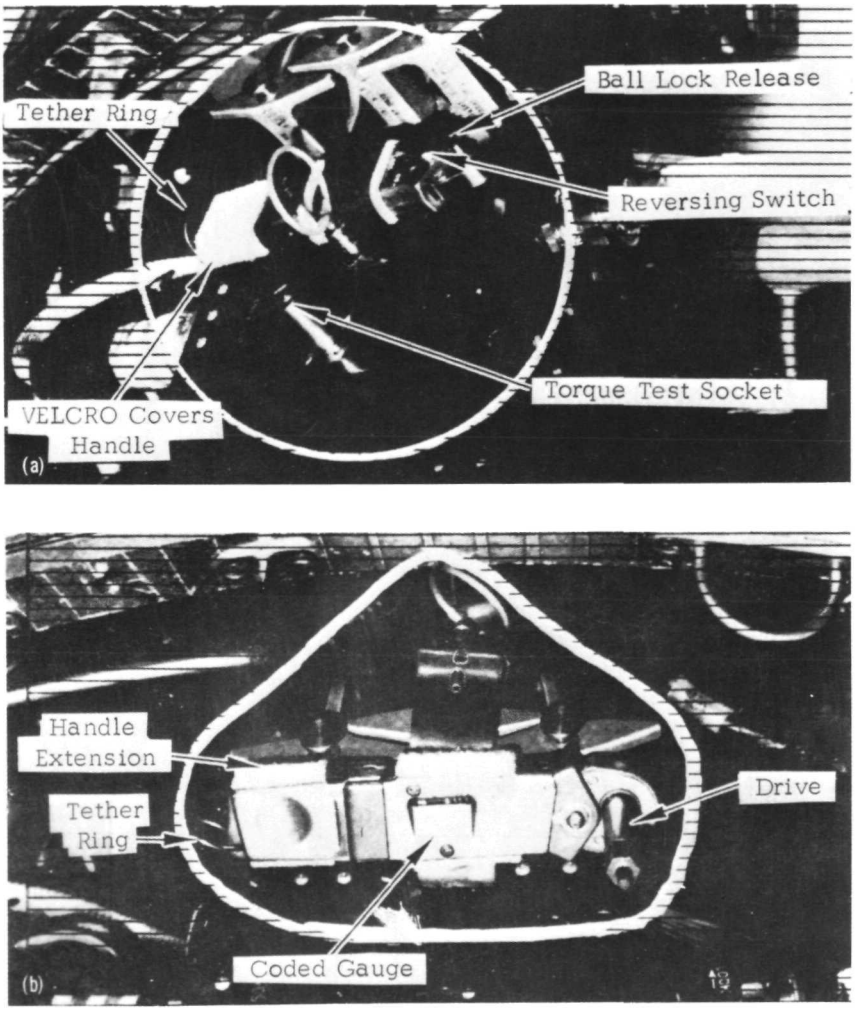

FIGURE 63.–Apollo torque wrench. (*a*). Top view. (*b*) Bottom view.

and to activate various mechanisms that require an Allen hexagonal wrench or a screwdriver.

This tool is basically a ratchet wrench designed to "break free" when a preset value of torque is exceeded. The torque value is established by pulling back the handle extension and rotating it in unit turns of 180°. As the handle is rotated, a white marker moves up a coded gage in the front of the wrench; rotation of the handle is stopped when the code for 5.65, 11.3, 17.0 or 22.6 m-N (50, 100, 150, or 200 in.-lb) is reached. If the handle extension is pulled back farther past a detent, it can be turned up to be used as a crank knob. The drive end consists of 1.11- and 0.40-cm (7/16- and 5/32-in.) male hexagonal wrench heads with a ball lock for extension attachments. The ball lock is controlled by the ball lock release button, which is pressed by the user's thumb when an attachment is inserted or removed. The ratchet direction of the wrench is controlled by a ratchet lever at the back of the tool.

The Apollo torque wrench with a hand and wrist tether was used by an astronaut during the Gemini 12 flight to exert a torque greater than 11.3 m-N (100 in.-lb).

PLIERS-WRENCH (PLENCH)

The pliers-wrench (PLENCH) shown in figure 64 was designed as a ratcheting zero-reaction socket wrench for space use. Repeated squeezing of the pliers-like grips causes the device to ratchet, as in a ratchet wrench. Thus, the fastener can advance or withdraw without the operator having to exert a torque motion or any push force. An adjustable reaction pin can abut against some protrusion from the ship or engage in a hole in the ship's structure to transmit the external reaction torque associated with tightening a bolt to the ship. Qualitative assessments of this tool's utility were made on an air-bearing platform; the tool performed satisfactorily.

The plench is powered and operated with one hand, but there must be a protrusion or hole in the ship's structure near the working area for the reaction pin to counteract the reactive forces.

SEMIREMOTE SPUNFIT WRENCH

The semiremote Space Union and Fitting (spunfit) wrench shown in figure 65 was designed for turning hydraulic fittings located deep in the structure of a vehicle.

The head of the semiremote wrench locks onto the fitting. Gripping and turning jaws, located in the head, are actuated by a flexible cable connected to scissorslike handles. When operated, the scissor motion of the handle causes gripping dogs in the tool head to turn the female tube fitting and hold stationary the male tube-to-tube connector.

The head of the tool can be made small enough to slip into very small quarters. After locking the tool on a fitting, the user can work in various

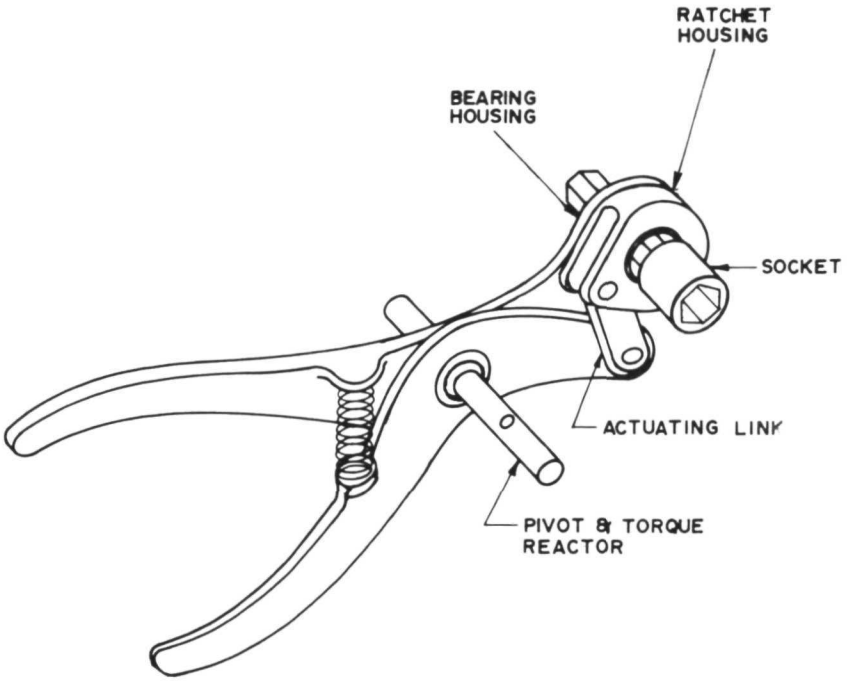

FIGURE 64.–Pliers-wrench (PLENCH).

positions, loosening or tightening fittings with no reactions on himself or the spacecraft.

TUBE-SWAGING DEVICE

The tube-swaging device shown in figure 66 was designed to join a sleeve on two sections of tubing (constructed of titanium, aluminum, stainless steel, or copper), providing a leakproof, lightweight, strong connection. It was designed for use with liquid systems; however, it is believed that it could be used also with gas systems.

First, either one or two circular grooves are rolled into the ends of each section of tubing, using a cutoff tool with a roller instead of the usual cutting wheel. Then a sleeve slightly softer than the tubing is placed over the end of one tube. The top of the tube-swaging device is opened and closed over the tube and sleeve so that an annular ring cavity in the tool fits over the section of sleeve covering one of the grooves in the tube. A 22-caliber blank cartridge is fired into this cavity to increase the pressure on the surface of the sleeve inside the tool (to approximately 8.3×10^7 N/m^2 (12 000 psi) in the case of aluminum tubing). The sleeve deforms and swages into the receiving groove, creating a sealed area. If there is another groove on the tube, the sleeve is swaged into it, too. Next, the second tube is placed into the other end of the

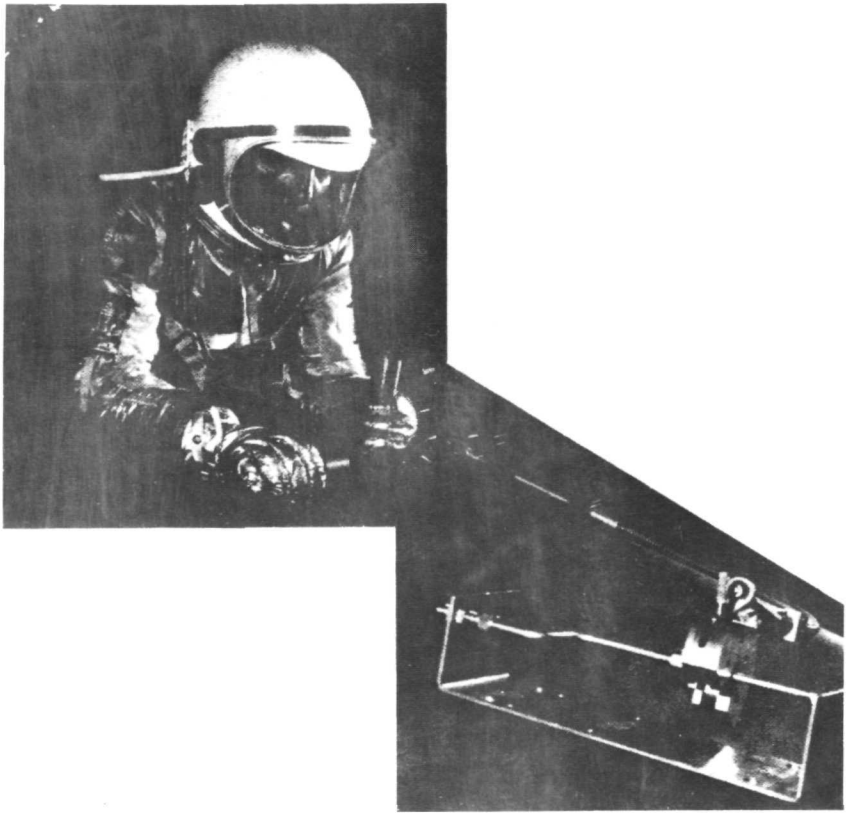

FIGURE 65.–Semiremote spunfit wrench.

sleeve and the above procedures are repeated. For applications requiring lower ultimate pressure couplings, grooves need not be rolled into the tubes. In this case, the sleeve is pressed into the tube so that depressions formed in the tube and sleeve interlock and form a seal.

Laboratory tests have been performed on no-groove, one-groove, and two-groove fittings in 0.95-cm (3/8-in.) o.d. wall 6061-T6 aluminum tubing. The sleeves were 1.11-cm (7/16-in.) o.d. wall 6061-0 aluminum. Results with the no-groove fittings were poor because the tubes tended to collapse slightly when swaged, which led to hydrostatic leaks at 2.17×10^6 N/m^2 (300 psig) or less. The tube samples with grooved fittings withstood hydrostatic pressures of 1.4×10^7 N/m^2 (2000 psig) without leaks. The sharp edges of the grooves bite into the sleeve, producing a tightly sealed joint. With pressures greater than this the sleeves, made of softer metal than the tubing, appeared to yield. A sleeve also would yield when a hydrostatic pressure of 2.17×10^6 N/m^2 (300 psig) and a torque in excess of 8.5 m-N (75 in.-lb) were transmitted through the fittings.

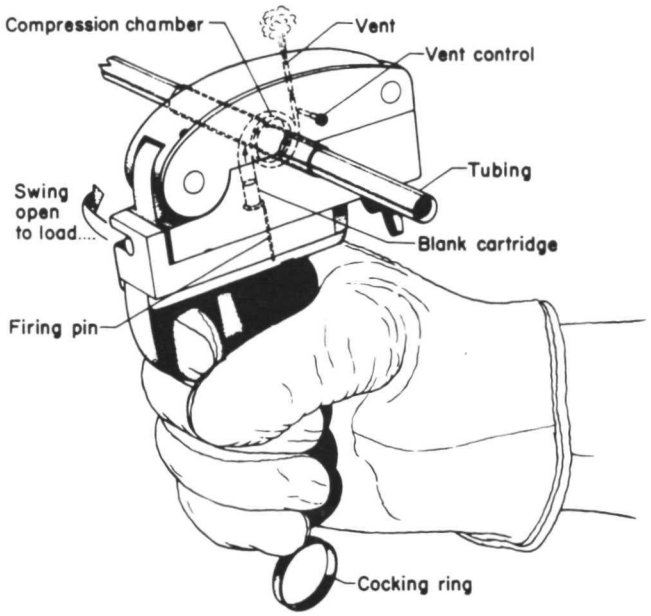

FIGURE 66.–Tube-swaging device.

Because the sleeve used in the swaging process is made of the same metal as the tubing, problems arising from differences in thermal and galvanic properties are eliminated. This is of particular importance when the tubing must carry highly reactive material such as hydrogen peroxide. Another advantage of the device is that the quality of the seal can be determined, in a simple and reliable manner, by examining the depression in the sleeve.

HANDHELD ELECTRON BEAM GUN

The prototype handheld electron beam gun shown in figure 67 was designed to explore the possibility of using the electron beam concept to develop a simple portable welder. This gun was designed to operate with an external power supply. A heated cathode emits electrons that are accelerated by a bias cup and anode system. These electrons are focused on the workpiece by a magnetic lens. The workpiece is heated to a weld temperature by absorption of the kinetic energy of the bombarding electrons. A warning light indicates when the power is on. The handle has a safety "on-off" switch and an "operating" switch for activating the tool.

Two types of vapor radiation shields were developed for use with this tool. Both automatically hold the gun at the correct distance from the workpiece, and both have leaded glass windows to allow the user to observe the welding process. The shields reduce emission of splattering material, electrostatic

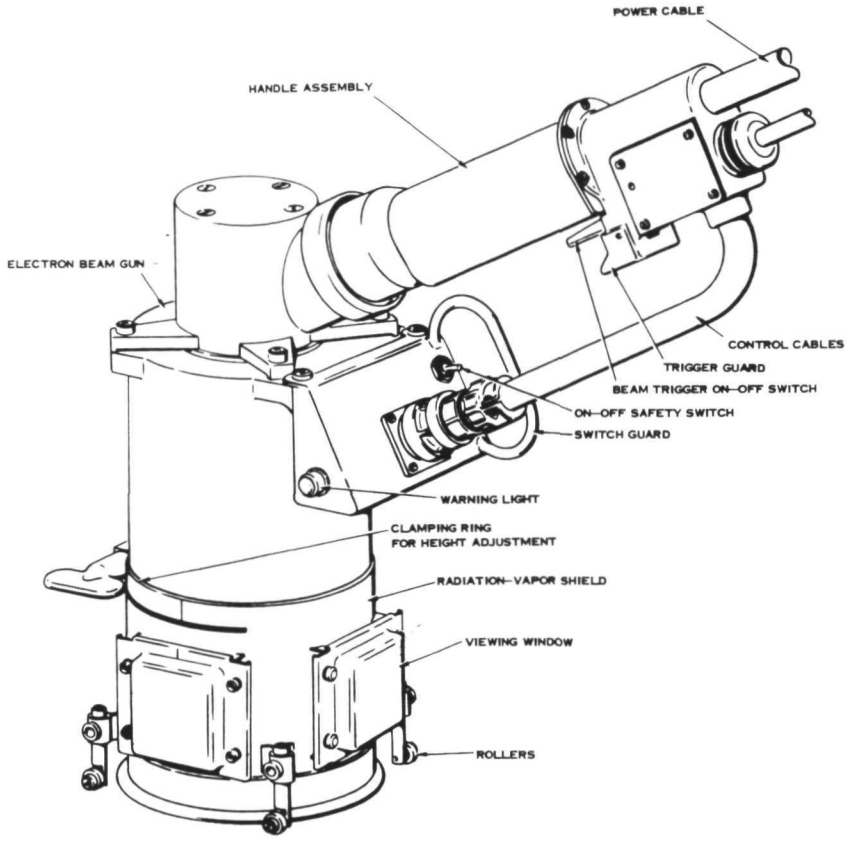

FIGURE 67.–Handheld electron beam welder.

charging, and radiation. One shield is cylindrical and rolls on bearings. The direction of travel and rate of speed are controlled by hand and auxiliary tracks that can be used to help guide the gun. The other shield, an open-bottomed, box-shaped shell, is placed over the work surface and remains fixed in position as the gun runs down a track on the top of the shield.

In man-rated chamber tests performed at 3.46×10^{-3} N/m^2 (5.02×10^{-7} psi), the gun worked well. It was established that satisfactory butt welds can be made in aluminum, titanium, and stainless steel of material thickness up to 0.318 cm (0.125 in.) at a rate of 0.635 cm/sec (15 in./min).

The grid cup, cathode insulator, and filament mounting pieces comprise one subassembly that is removable as a unit to permit bench-type servicing. Tool specifications are as follows:

Cable length	15.3 m (50 ft)
Diameter	8.9 cm (3.5 in.)

Length	25.4 cm (10 in.)
Mass	4.54 kg (10 lb)
Accelerating voltage	20 kV
Current	150 mA

The external power supply must provide 150 mA at 20 kV for an electron beam accelerating voltage and current and 25 A at 20 V for the filament heating, the warning light, the magnetic lens, and the bias on the bias cup.

A workpiece fixture assembly was used with the electron beam gun for producing the first series of welds in a man-rated vacuum chamber. The assembly provided a mount for the metal plates to be welded, tracks to guide the gun, and further shielding for the operator from workpiece emissions.

Human Factors Engineering Consultants

An alternative to reading the literature is obtaining assistance from a human factors engineering expert. The names of practicing professionals can be obtained from the Human Factors Society, 1134 Montana Avenue, Santa Monica, California (213) 394-1811. This society has chapters throughout the country.

Companies with specific problems may also consult NASA. For example, you may wish to know whether protective clothing is available for firemen who have to enter a burning building in which there is a type of toxic gas. Such an inquiry could be addressed to any of the six regional dissemination centers established by NASA:

Aerospace Research Applications Center [1]
Indiana University Foundation
Bloomington, Ind. 47405
Phone (812) 337-7970

Knowledge Availability Systems Center
University of Pittsburgh
Pittsburgh, Pa. 15213
Phone (412) 621-3500, ext. 6352

Technology Application Center
University of New Mexico
Box 185
Albuquerque, N.M. 87106
Phone (505) 277-3118

New England Research Application Center
University of Connecticut
Storrs, Conn. 06268
Phone (203) 429-6616

North Carolina Science & Technology Research Center
Post Office Box 11235
Research Triangle Park, N.C. 27709
Phone (919) 834-7357 or 549-8291

[1] The Aerospace Research Applications Center specializes in human factors engineering data.

Western Research Applications Center
University of Southern California
Los Angeles, Calif. 90007
Phone (213) 746-6133

References

1. Chapanis, Alphonse: Man-Machine Engineering. Wadsworth Pub. Co., Inc., 1965.
2. Fitzwater, M.; Corichill, D.; Jackson, E.; Halvorson, P.; and Sepper, W.: Physiological Monitoring Technique Using Unattached Sensors. NASA CR-86048, Mar. 1968.
3. Conway, Bruce A.: Development of Skylab Experiment T-013 Crew/Vehicle Disturbances. NASA TN D-6584, Jan. 1972.
4. Anon.: Experiment Operations Handbook. (NAS8-24000), Dec. 1970.
5. Hatfield, Jack J.: A Programmable Display Synthesizing System for Man-Machine Communications Research. Paper presented at Nat. Symp. Inform. Display, 7th (Boston), Oct. 1966.
6. Elkins, Henry C., and Hatfield, Jack J.: Televised Graphic Displays for Step Approach to Landing Research. Paper presented at Nat. Symp. Inform. Display, 11th (New York), May 1970.
7. Anon.: Study for the Collection of Human Engineering Data for Maintenance and Repair of Advanced Space Systems. NASA CR-61649, Dec. 1967.
8. Webb, Paul; and Annis, James A.: Bio-Thermal Responses to Varied Work Programs in Men Kept Thermally Neutral by Water Cooled Clothing. NASA CR-739, Apr. 1967.
9. Troutman, Samuel J., Jr.; and Webb, Paul: Automatic Control of Water Cooled Suits From Differential Temperature Measurements. NASA CR-86244, Aug. 1969.
10. Anon.: LRC Complex Coordinator. NASA Brief TB70-10619 (TSP), undated.
11. Hanks, Brantley R., and Snyder, William J.: Ground Tests of an Active Vibration Isolation System for a Full-Scale Helicopter. Paper presented at Shock Vibr. Symp., 43d, Dec. 1972.
12. Anon.: Temper Foam. Dynamic Systems, Inc. (Leiuster, N.C.), undated.
13. Haines, Richard F.; Fitzgerald, James W.; and Rositano, Salvador A.: Development of an Automated Visual Sensitivity Tester. NASA TN D-6190, Mar. 1971.
14. Randle, Robert J.: Volitional Control of Visual Accommodation. Adaptation and Acclimatisation in Aerospace Medicine, conf. proc. 82, Advisory Group for Aerospace Research and Development (Paris), 1971.
15. Johnson, Lawrence B.; Sander, Eric; and Lebow, Stanley: NASA List of Potential Space Tools and Equipment. NASA CR-1760, May 1971.

Sources of Further Information

Anon.: Infinity Display Optical Unit ("Pancake Window"). Farrand Optical Co., Inc. (New York), Nov. 1969. (N70-19901)

Clevenson, Sherman A.; and Leatherwood, Jack D.: On the Development of Passenger Vibration Ride Acceptance Criteria. Paper presented at Shock Vibr. Symp., 43d, Dec. 1972.

DeGreene, Kenyon B. (ed.): Systems Psychology. McGraw-Hill Book Co., Inc., 1970.

Fogel, Lawrence J.: Biotechnology: Concepts and Applications. Prentice-Hall, Inc., 1969.

Grandjean, Etienne: Fitting the Task to the Man: An Ergonomic Approach. Taylor and Francis, 1969.

Harris, Douglas H.: Human Factors in Quality Assurance. Wiley-Interscience, 1969.

Hopkinson, Ralph G.: The Ergonomics of Lighting. MacDonald and Co., 1970.

Howell, William Carl: Engineering Psychology: Current Perspectives in Research, 1971.

Johnson, Edwin G.; and Corliss, William R.: Human Factors Applications in Teleoperator Design and Operation. Wiley-Interscience, 1971.

Meister, David: Human Factors: Theory and Practice. Wiley-Interscience, 1971.

Morgan, Clifford T. (ed.): Human Engineering Guides to Equipment Design. McGraw-Hill Book Co., Inc., 1963.

Murrell, K. F. H.: Human Performance in Industry. Reinhold Pub. Corp., 1965.

Anon.: Databook for Human Factors Engineers; Vols. I and II, NASA CR 114271 and CR 114272 (NAS2-5298).

NATIONAL AERONAUTICS AND SPACE ADMINISTRATION
WASHINGTON, D.C. 20546

OFFICIAL BUSINESS
PENALTY FOR PRIVATE USE $300

SPECIAL FOURTH CLASS MAIL
Book

POSTAGE AND FEES PAID
NATIONAL AERONAUTICS AND
SPACE ADMINISTRATION
NASA-451

U.S.MAIL

POSTMASTER: If Undeliverable (Section 158
Postal Manual) Do Not Return

"The aeronautical and space activities of the United States shall be conducted so as to contribute . . . to the expansion of human knowledge of phenomena in the atmosphere and space. The Administration shall provide for the widest practicable and appropriate dissemination of information concerning its activities and the results thereof."

—NATIONAL AERONAUTICS AND SPACE ACT OF 1958

NASA TECHNOLOGY UTILIZATION PUBLICATIONS

These describe science or technology derived from NASA's activities that may be of particular interest in commercial and other non-aerospace applications. Publications include:

TECH BRIEFS: Single-page descriptions of individual innovations, devices, methods, or concepts.

TECHNOLOGY SURVEYS: Selected surveys of NASA contributions to entire areas of technology.

OTHER TU PUBLICATIONS: These include handbooks, reports, notes, conference proceedings, special studies, and selected bibliographies.

Details on the availability of these publications may be obtained from:

National Aeronautics and Space Administration
Code KT
Washington, D.C. 20546

Technology Utilization publications are part of NASA's formal series of scientific and technical publications. Others include Technical Reports, Technical Notes, Technical Memorandums, Contractor Reports, Technical Translations, and Special Publications.

Details on their availability may be obtained from:

National Aeronautics and Space Administration
Code KS
Washington, D.C. 20546

NATIONAL AERONAUTICS AND SPACE ADMINISTRATION

Washington, D.C. 20546